

การพัฒนาโครงเลี้ยงเซลล์ชนิดใหม่จากเจลาติน ไคโตโอลิโกแซคคาไรด์ และผงกระดูก  
เพื่อใช้ในงานวิศวกรรมเนื้อเยื่อกระดูก

นายสุภากร จิตติเศรษฐ์

วิทยานิพนธ์นี้เป็นส่วนหนึ่งของการศึกษาตามหลักสูตรปริญญาวิทยาศาสตรดุษฎีบัณฑิต

สาขาวิชาวิศวกรรมชีวเวช (สหสาขาวิชา)

คณะวิศวกรรมศาสตร์ จุฬาลงกรณ์มหาวิทยาลัย

ปีการศึกษา 2554

ลิขสิทธิ์ของจุฬาลงกรณ์มหาวิทยาลัย

บทคัดย่อและแฟ้มข้อมูลฉบับเต็มของวิทยานิพนธ์ตั้งแต่ปีการศึกษา 2554 ที่ให้บริการในคลังปัญญาจุฬาฯ (CUIR)

เป็นแฟ้มข้อมูลของนิสิตเจ้าของวิทยานิพนธ์ที่ส่งผ่านทางบัณฑิตวิทยาลัย

The abstract and full text of theses from the academic year 2011 in Chulalongkorn University Intellectual Repository (CUIR)

are the thesis authors' files submitted through the Graduate School.

DEVELOPMENT OF THE NOVEL SCAFFOLDS FROM GELATIN, CHITOLIGOSACCHARIDE  
AND DEMINERALIZED BONE MATRIX FOR BONE TISSUE ENGINEERING APPLICATION

Mr. Thakoon Thitiset

A Dissertation Submitted in Partial Fulfillment of the Requirements  
for the Degree of Doctor of Philosophy Program in Biomedical Engineering  
(Interdisciplinary Program)

Faculty of Engineering  
Chulalongkorn University

Academic Year 2011

Copyright of Chulalongkorn University



ฐาภรณ์ วุฒิศาสตร์ : การพัฒนาโครงเลี้ยงเซลล์ชนิดใหม่จากเจลาติน ไคโตโอลิโกแซคคาไรด์ และผงกระดูกเพื่อใช้งานวิศวกรรมเนื้อเยื่อกระดูก. (DEVELOPMENT OF THE NOVEL SCAFFOLDS FROM GELATIN, CHITOLIGOSACCHARIDE, AND DEMINERALIZED BONE MATRIX FOR BONE TISSUE ENGINEERING APPLICATION) อ.ที่ปรึกษาวิทยานิพนธ์หลัก: รศ.ดร.นพ. ลีพิศักดิ์ หรรษาเวก, อ.ที่ปรึกษาวิทยานิพนธ์ร่วม: รศ.ดร. ศิริพร ดำรงค์ศักดิ์กุล, 144 หน้า.

งานวิจัยนี้มีวัตถุประสงค์เพื่อที่จะศึกษาการเปลี่ยนแปลงเป็นเซลล์ต้นกำเนิดเนื้อเยื่อประสานของเซลล์ประจุมุมุมที่แยกได้จากเยื่อหุ้มกระดูกของมนุษย์ โดยพบว่าเซลล์ดังกล่าวมีการแสดงออกของตัวบ่งชี้ผิวเซลล์ที่จำเพาะต่อเซลล์ต้นกำเนิดเนื้อเยื่อประสาน แต่ไม่พบการแสดงออกของตัวบ่งชี้ผิวเซลล์ที่จำเพาะต่อเซลล์ต้นกำเนิดเม็ดเลือด เซลล์ชนิดดังกล่าวสามารถถูกชักนำให้เปลี่ยนแปลงเป็นเซลล์กระดูก เซลล์กระดูกอ่อน และเซลล์ไขมันด้วยการพิสูจน์การแสดงออกของยีนและการย้อมจำเพาะทางพยาธิวิทยา จากนั้นทำการศึกษาอิทธิพลของขนาดอนุภาคของกระดูกที่ใช้ในการผสมกับคอลลาเจนเพื่อใช้ในการขึ้นรูปโครงเลี้ยงเซลล์สามมิติที่มีต่อสมบัติทางกายภาพของโครงเลี้ยงเซลล์ และกิจกรรมของเซลล์ต้นกำเนิดเนื้อเยื่อประสาน เช่น การยึดเกาะและการแบ่งตัวเพิ่มจำนวนบนโครงเลี้ยงเซลล์ โดยพบว่าเซลล์มีแนวโน้มในการยึดเกาะและเพิ่มจำนวนบนโครงเลี้ยงเซลล์ผสมผงกระดูกและคอลลาเจนได้ดีกว่าโครงเลี้ยงเซลล์คอลลาเจนเพียงอย่างเดียว นอกจากนี้ยังพบว่าขนาดอนุภาคของผงกระดูกในช่วง 250-500 ไมครอน ส่งเสริมการเปลี่ยนแปลงของเซลล์ต้นกำเนิดเนื้อเยื่อประสานไปเป็นเซลล์กระดูกได้ดีที่สุดเมื่อเปรียบเทียบกับขนาดอนุภาคที่เล็กกว่า เพื่อพัฒนาโครงเลี้ยงเซลล์กระดูกที่มีประสิทธิภาพในการชักนำการสร้างกระดูกใหม่ ผงกระดูกขนาดอนุภาคในช่วง 250-500 ไมครอนถูกนำไปผสมกับเจลาตินและไคโตโอลิโกแซคคาไรด์ เปรียบเทียบกับโครงเลี้ยงเซลล์ผสมจากเจลาตินและไคโตโอลิโกแซคคาไรด์และโครงเลี้ยงเซลล์เจลาติน จากการศึกษาพบว่าชนิดของวัสดุไม่มีผลต่อสมบัติทางกายภาพที่แตกต่างกัน ในขณะที่โครงเลี้ยงเซลล์จากผงกระดูกผสมเจลาตินและไคโตโอลิโกแซคคาไรด์ส่งเสริมการเปลี่ยนแปลงของเซลล์ต้นกำเนิดเนื้อเยื่อประสานไปเป็นเซลล์กระดูกได้ดีที่สุด จากการศึกษาประสิทธิภาพของโครงเลี้ยงเซลล์ต่อการสร้างเนื้อเยื่อกระดูกในสัตว์ทดลอง โดยทำการฝังโครงเลี้ยงเซลล์เจลาติน โครงเลี้ยงเซลล์เจลาตินผสมไคโตโอลิโกแซคคาไรด์ และโครงเลี้ยงเซลล์ผสมเจลาตินและไคโตโอลิโกแซคคาไรด์ ลงใต้ผิวหนังของหนูวิสตาร์เพศผู้ พบการสร้างคอลลาเจนใหม่และกลุ่มเซลล์กระดูกใหม่ตั้งแต่สัปดาห์ที่สอง และเมื่อติดตามผลการทดลองในสัปดาห์ที่แปดพบว่ามีการรวมตัวของเซลล์กระดูกใหม่มากขึ้นในบริเวณที่กว้างขึ้น เมื่อเปรียบเทียบกับชนิดของโครงเลี้ยงเซลล์จากผงกระดูกผสมเจลาตินและไคโตโอลิโกแซคคาไรด์มีศักยภาพในการส่งเสริมการเปลี่ยนแปลงเป็นเซลล์กระดูกได้ชัดเจนกว่าโครงเลี้ยงเซลล์อีกสองชนิด

สาขาวิชา วิศวกรรมชีวเวช .....ลายมือชื่อนิสิต.....  
 ปีการศึกษา 2554 .....ลายมือชื่อ อ.ที่ปรึกษาวิทยานิพนธ์หลัก.....  
 .....ลายมือชื่อ อ.ที่ปรึกษาวิทยานิพนธ์ร่วม.....

# # 5087766921 : MAJOR BIOMEDICAL ENGINEERING

KEYWORDS : GELATIN / CHITOLIGOSACCHARIDE / DEMINERALIZED BONE MATRIX / PERIOSTEAL-DERIVED STEM CELLS / BONE TISSUE ENGINEERING

THAKOON THITISET: DEVELOPMENT OF THE NOVEL SCAFFOLDS FROM GELATIN, CHITOLIGOSACCHARIDE, AND DEMENERALIZED BONE MATRIX FOR BONE TISSUE ENGINEERING APPLICATION.

ADVISOR: ASSOC. PROF. SITTISAK HONSAWEK, M.D., Ph.D.,

CO-ADVISOR: ASSOC. PROF. SIRIPORN DAMRONGSAKKUL, Ph.D.,

144 pp.

This research aimed to study the differentiation of mesenchymal stem cells (MSCs) isolated from human periosteal primary cells. The study found that periosteum-derived cells expressed MSC surface markers but did not express hematopoietic cell surface markers. They could be induced to osteoblasts, chondroblasts, and adipoblasts as indicating by the expression of bone, cartilage, and fat cell indicator genes and specific histological staining. After that, the influences of particle size of demineralized bone (D) that was use to blend with collagen in order to fabricate three dimensional scaffolds were studied. The physical properties and biological properties of the scaffolds were evaluated. The results demonstrated that MSCs could attach and proliferate on collagen/demineralized bone powder scaffold better than on pure collagen scaffold. Furthermore, collagen scaffolds blended with D at the particle size of 250-500  $\mu\text{m}$  had excellent osteoblastic differentiation when compared to the ones with smaller D. The D having the size of 250-500  $\mu\text{m}$  was further blended with gelatin and chitooligosaccharide (GCD) to form novel scaffold compared to gelatin/chitooligosaccharide (GC) scaffold, and pure gelatin (G) scaffold. It was found that biomaterial type did not affect their physical properties. Also, GCD scaffold could best promote osteoblastic differentiation. Finally, for *in vivo* study, all scaffolds were implanted in subcutaneous of male Wistar rats. After 2-weeks implantation, new collagen and new osteoid formation was found. After 8-weeks implantation, more bone formation was noticed. Comparing the potential of biocompatibility and osteoinductivity, GCD scaffold exhibited remarkably higher osteogenic differentiation potential than the other two scaffolds.

Field of Study : Biomedical Engineering Student's Signature .....

Academic Year : 2011 Advisor's Signature .....

Co-advisor's Signature .....

## ACKNOWLEDGEMENTS

My dissertation is completed with the aid and support of many people. Firstly, I would like to thank my advisor, Associate Professor Dr. Sittisak Honsawek, who advised and supported me from the beginning to the final stage of this research. Also, his insights and experiences that have been shared advocate my wider vision towards the topic. Secondly, I am truly thankful my co-advisor, Associate Professor Siriporn Damrongsakkul, for her assistance, continuous encouragement, and kind contribution on staying and doing my research. Next, I would like to appreciatively thank Assistant Professor Tanom Bunaprasert for his helpful suggestions and discussion for my project. I also would like to thank Associate Professor Dr. Voranuch Tanakit, Department of Pathology, Faculty of Medicine, for very good consult about definite analysis for bone formation. Furthermore, I appreciate to thank Associate Professor Mana Sriyuthasak for his invaluable instruction during the whole period of my study, including Assistant Professor Sorada Kanokpanont for her kindness suggestions to my dissertation.

In addition, I would like to thank Associate Professor Sutthiluck Pathumraj, and Assistant Professor Wilairat Leraanantsaksiri for their contribution as the chairman and the dissertation committee, whose comments were constructively informative. The most important person who I have to thank is Dr. Juthamas Ratanavaraporn for her kind attentions, supports and suggestions in techniques for my research.

The financial support from the 90<sup>th</sup> anniversary of Chulalongkorn University Fund (Ratchadaphiseksomphot Endowment Fund), Office of the Higher Education Commission (CHE), and National Nanotechnology Center (NANOTEC) were highly acknowledged.

I would like to thank the staffs of Department of Biochemistry, Chula Medical Research Center (Chula-MRC), Faculty of Medicine, for advice and providing the experimental instruments. Besides, I am especially thanks to Dr. Supranee Buranapraditkun for helping FACS analysis. Furthermore, I am pleased to extend my grateful thanks to all Master and Ph.D. students of the Bone Biology research laboratory, Medical Material Laboratory Unit (TE group), and i-Tissue Laboratory for their helps, encouragement, and friendship during my study at Chulalongkorn University.

Finally, I would like to express my sincere thanks to my family for their love, understanding and affectionate encouragement.

# CONTENTS

	<b>PAGE</b>
<b>ABSTRACT (IN THAI)</b> .....	iv
<b>ABSTRACT (IN ENGLISH)</b> .....	v
<b>ACKNOWLEDGEMENTS</b> .....	vi
<b>CONTENTS</b> .....	vii
<b>LIST OF TABLES</b> .....	xii
<b>LIST OF FIGURES</b> .....	xiii
<b>LIST OF ABBREVIATIONS</b> .....	xvi
<b>CHAPTER</b>	
<b>I. INTRODUCTION</b> .....	1
1. Background .....	1
2. Objectives.....	6
3. Scope of research .....	6
<b>II. LITERATURE REVIEWS</b> .....	9
1. Anatomy and physiology of the bone .....	9
1.1 Bone function .....	9
1.2 Bone structures and mechanics .....	9
1.3 Cellular organization .....	11
1.4 Bone formation.....	11
1.5 Fracture healing .....	12
2. Bone tissue engineering .....	13
2.1 Osteoconduction: matrix-based strategies.....	14
2.2 Osteogenesis: cell-based strategies.....	15
2.3 Osteoinduction: growth factor-based strategies .....	16
3. Biomaterials .....	16
3.1 Demineralized bone powder.....	17
3.2 Collagen.....	19
3.3 Gelatin .....	24
3.4 Chitosan.....	28
3.5 Chitooligosaccharide .....	31

	<b>PAGE</b>
<b>CHAPTER</b>	
4. Mesenchymal stem cells.....	32
4.1 Sources of mesenchymal stem cells .....	32
4.2 Phenotypic characteristics of mesenchymal stem cells .....	33
4.3 Growth and differentiation of mesenchymal stem cells .....	34
5. Fabrication technique of the scaffolds .....	36
5.1 Freeze drying technique .....	37
5.2 Cross-linking technique.....	38
6. Related researches .....	39
<b>III. MATERIALS &amp; METHODS</b> .....	<b>46</b>
1. Raw materials, chemical and reagents .....	46
2. Experimental procedures.....	50
<b>Part I:</b> Characterization of periosteum-derived cells as mesenchymal stem cells .....	53
2.1 Isolation and cultivation of mesenchymal stem cells .....	53
2.2 Analysis of the specific cell surface of periosteum-derived (PD) cells.....	53
2.3 <i>In vitro</i> functional characterizations of PD cells .....	54
2.3.1 Osteogenic differentiation study of PD cells .....	54
2.3.2 Chondrogenic differentiation study of PD cells.....	54
2.3.3 Adipogenic differentiation study of PD cells.....	55
<b>Part II:</b> Osteogenic characterization of collagen and various particle size of demineralized bone powder .....	56
2.4 Preparation of demineralized bone powder .....	56
2.5 Fabrication of demineralized bone blended collagen scaffolds .....	57
2.6 Physical and chemical characterization of the scaffolds .....	58
2.6.1 Morphology observation of the scaffolds .....	58
2.6.2 Mechanical test of the scaffolds.....	58
2.6.3 Swelling ability of the scaffolds .....	58



<b>CHAPTER</b>	<b>PAGE</b>
2.7 <i>In vitro</i> biological characterizations of PD cells onto the collagen and various particle size of demineralized bone powder scaffolds.....	59
2.7.1 <i>In vitro</i> cell culture of PD cells .....	59
2.7.2 <i>In vitro</i> osteogenic differentiation of PD cells .....	60
2.7.3 The observation of cultured cells in the scaffolds .....	61
2.7.4 Elemental analysis of cultured cells in the scaffolds .....	61
<b>Part III: Gelatin/chitooligosaccharide/demineralized bone powder scaffolds for bone tissue engineering .....</b>	<b>62</b>
2.8 Fabrication of the gelatin, chitooligosaccharide, and demineralized bone scaffolds ....	62
2.9 Physical and chemical characterization of the gelatin, chitooligosaccharide, and demineralized bone scaffolds .....	63
2.9.1 Morphological observation of the scaffolds .....	63
2.9.2 Mechanical test of the scaffolds.....	63
2.9.3 Swelling ability of the scaffolds.....	63
2.10 <i>In vitro</i> biological characterizations of PD cells onto the gelatin/ chitooligosaccharide/demineralized bone powder scaffolds .....	64
2.10.1 <i>In vitro</i> cell culture of the scaffolds with PD cells.....	64
2.10.2 <i>In vitro</i> osteogenic differentiation of the scaffolds with PD cells .....	64
2.10.3 The observation of PD cells cultured on scaffolds .....	64
2.10.4 Elemental analysis of PD cells cultured on scaffolds .....	64
2.10.5 Study of biological properties of the scaffolds in animal model .....	65
2.11 Statistical analysis.....	66
<b>IV. RESULTS.....</b>	<b>67</b>
<b>Part I: Mesenchymal stem cells for bone tissue engineering.....</b>	<b>67</b>
1. Characteristics of PD cells .....	67
2. Cell surface marker characteristics of PD cells.....	69
3. <i>In vitro</i> osteogenic, chondrogenic, and adipogenic differentiation of PD cells .....	71
4. Summary .....	78
<b>Part II: Osteogenic characterization of collagen/demineralized bone powder scaffolds.....</b>	<b>79</b>
5. Characteristic of the demineralized bone powder .....	79
6. Morphology of collagen and collagen/demineralized bone powder scaffolds .....	79

<b>CHAPTER</b>	<b>PAGE</b>
7. Compressive modulus of the scaffolds .....	82
8. Swelling property of the scaffolds .....	82
9. FT-IR analysis of the scaffolds .....	84
10. Biological characterization of the scaffolds .....	86
10.1 Initial attachment and cell proliferation of PD cells cultured collagen and demineralized bone powder scaffolds .....	86
10.2 <i>In vitro</i> osteogenic differentiation test .....	86
10.3 Morphology of PD cells cultured collagen and demineralized bone powder scaffolds .....	91
11. Summary .....	91
<b>Part III: Gelatin/chitooligosaccharide/demineralized bone powder scaffolds for bone tissue engineering .....</b>	<b>93</b>
12. Physical characterization of the scaffolds .....	93
13. Biological characterization of the scaffolds .....	97
13.1 Cell proliferation of PD cells cultured o the scaffolds.....	97
13.2 Osteogenic differentiation test .....	99
14. Summary .....	109
15. Osteogenic differentiation potential of gelatin, chitooligosaccharide, and demineralized bone powder scaffolds in animal model .....	110
16. Summary .....	115
<b>V. DISCUSSIONS .....</b>	<b>118</b>
1. Discussions.....	118
Part I: Mesenchymal stem cells for bone tissue engineering .....	118
Part II: Osteogenic characterization of collagen/demineralized bone powder scaffolds .....	120
Part III: Gelatin/chitooligosaccharide/demineralized bone powder scaffolds for bone tissue engineering .....	123
2. Conclusions .....	125
3. Recommendations .....	126
References.....	127

<b>CHAPTER</b>	<b>PAGE</b>
Appendices .....	138
Appendix A: PCR primer sequences .....	139
Appendix B: Standard curve for MTT assay .....	140
Appendix C: Standard curve for DNA assay .....	141
Appendix D: Standard curve for <i>p</i> -nitrophenyl phosphate assay .....	142
Appendix E: Standard curve for O-cresolphthalein assay .....	143
Biography.....	144

## LIST OF TABLES

<b>TABLE</b>	<b>PAGE</b>
2.1 The superfamily of BMPs.....	18
2.2 Chain composition and body distribution of collagen types .....	20
2.3 Amino acid composition of bovine collagen $\alpha$ -chains .....	23
2.4 Typical specifications for gelatin .....	25
2.5 Amino acid compositions of gelatin .....	27
2.6 Type of mesenchymal stem cell surface markers .....	33
4.1 Element analyses on PD cell surface after cultured on scaffolds .....	90
4.2 Physical characterization of the different scaffolds from gelatin, chitooligosaccharide, and demineralized bone powder .....	94
4.3 Weight percentage of elemental analyses on PD cells surface after 28 days cultured in osteogenic medium compared with non-cell seeding condition .....	108

## LIST OF FIGURES

<b>FIGURE</b>	<b>PAGE</b>
1.1 Application of biocomposited materials for bone substitution .....	5
2.1 Gross anatomy and histology of bone .....	10
2.2 Fracture healing process .....	12
2.3 Parameters required for cartilage repair regeneration .....	13
2.4 Molecular structure of collagen .....	22
2.5 Preparation processes for acidic and basic gelatins from collagen .....	25
2.6 Structure of the gelatin .....	26
2.7 Structure of chitin and chitosan .....	28
2.8 The chitosan produced from deacetylation of chitin.....	29
2.9 The structure of chitooligosaccharide .....	31
2.10 The MSCs capacity to differentiate into tissues of mesodermal origins .....	32
2.11 Schematic model for differentiation of a mesenchymal stem cell into tissue specific cells by specific transcription factors .....	35
3.1 Implanted sites of Wistar rat .....	66
3.2 The group and the number of Wistar rat used to evaluate <i>in vivo</i> osteogenic responses .....	66
4.1 Periosteum-derived cells from primary outgrowth technique .....	68
4.2 FACS histogram of periosteum-derived cells performed specific antibody staining .....	70
4.3 Specific chemical staining of cultured periosteum-derived cells for osteogenic differentiation .....	72
4.4 Specific chemical staining of cultured periosteum-derived cells for chondrogenic differentiation at day 21 .....	74
4.5 Specific chemical staining of cultured periosteum-derived cells for adipogenic differentiation at 28 days .....	76
4.6 A typical result of gel-electrophoresis of PCR products to evaluate the expression of MSC-specific genes in control medium and conditioned medium .....	77
4.7 The particle size of DBP in different ranges .....	80
4.8 Pure collagen scaffold and demineralized bone blended collagen scaffolds at different blending ratios .....	81

<b>FIGURE</b>	<b>PAGE</b>
4.9 The pore morphology of the pure collagen scaffold and various demineralized bone blended collagen scaffolds .....	81
4.10 The average compressive modulus of pure collagen scaffold and collagen scaffold blended various size of demineralized bone powder in dry and wet conditions .....	83
4.11 The average swelling ability ratio of pure collagen scaffold and collagen scaffold blended various size of demineralized bone powder .....	83
4.12 FT-IR spectra of the different scaffolds .....	85
4.13 Number of PD cells attached and proliferated on the COL scaffold and the COL/DBP scaffolds .....	87
4.14 ALP activity of PD cells cultured on COL/DBP scaffolds in osteogenic medium .....	87
4.15 Increased calcium level from the PD cells cultured on the COL/DBP scaffolds at different blending ratios for various times in osteogenic medium .....	88
4.16 The morphology of PD cells after cultured with scaffolds in control medium .....	90
4.17 The pore morphology of the gelatin/chitooligosaccharide/demineralized bone powder scaffolds .....	92
4.18 The pore morphology of the gelatin/chitooligosaccharide/demineralized bone powder scaffolds .....	95
4.19 Compressive modulus of G, GC, and GCD scaffolds .....	96
4.20 Number of PD cells attached and proliferated on G, GC, and GCD scaffolds from 6 h to 7 days .....	98
4.21 ALP activity of PD cells cultured on G, GC, and GCD scaffolds under osteogenic medium from 3 days to 14 days .....	100
4.22 Calcium content of PD cells cultured on G, GC, and GCD scaffolds under osteogenic medium from 6h to 28 days .....	101
4.23 A typical result of gel-electrophoresis of PCR products to evaluate the expression of PD cells cultured with combination of G, GC, and GCD scaffolds .....	103
4.24 Morphology of PD cells cultured under proliferating medium for 7 days on the combination scaffolds from gelatin, chitooligosaccharide, and demineralized bone powder .....	104
4.25 Morphology of periosteum-derived cells cultured under osteogenic medium for 28 days on the combination scaffolds from gelatin, chitooligosaccharide, and demineralized bone powder .....	105

<b>FIGURE</b>	<b>PAGE</b>
4.26 Surface element of PD cells cultured on G, GC, and GCD scaffolds under osteogenic medium for 28 days, analyzed by EDX .....	107
4.27 Deposited calcium of scaffolds after implantation in Wistar rats .....	111
4.28 H&E histological sections of subcutaneously implanted G, GC, and GCD scaffolds in Wistar rat at 4 weeks post implantation .....	112
4.29 H&E histological sections of subcutaneously implanted G, GC, and GCD scaffolds in Wistar rat at 8 weeks post implantation .....	113
4.30 Histomorphometric analysis of H&E of subcutaneously implanted G, GC, and GCD scaffolds in Wistar rat after 4 weeks and 8 weeks of implantation .....	114
4.31 von Kossa histological sections of subcutaneously implanted G, GC, and GCD scaffolds in Wistar rat at 8 weeks post implantation .....	115
4.32 Histomorphometric analysis of von Kossa of subcutaneously implanted G, GC, and GCD scaffolds in Wistar rat after 4 weeks and 8 weeks of implantation .....	116

## LIST OF ABBREVIATIONS

$\alpha$ -MEM	alpha minimum essential medium
ALP	alkaline phosphatase
BMPs	bone morphogenetic proteins
bp	base pairs
BSA	bovine serum albumin
OC	degree celsius
CD	cluster of differentiation
COL	collagen
COS	chitooligosaccharide
D	demineralized bone
DD	degree of deacetylation
DMEM	Dulbecco's modified Eagle medium
DMSO	dimethyl sulfoxide
DNA	deoxyribonucleic acid
ECM	extracellular matrix
EDTA	ethylene diamine tetra-acetic acid
EDX	energy-dispersive X-ray spectroscopy
<i>et al.</i>	et alii (latin), and others
FBS	fetal bovine serum
FT-IR	fourier transform-infrared spectroscopy
G	gelatin
GAG	glycosaminoglycans
GAPDH	glyceraldehyde-3-phosphate dehydrogenase
h	hour
HCl	hydrochloric acid
H&E	hematoxylin and eosin
IR	infrared
L929	mouse fibroblast cells
MSC	mesenchymal stem cell
MTT	3-(4,5-dimethylthiazol-2-yl)-2,5-diphenyltetrazolium bromide
MW	molecular weight



NaCl	sodium chloride
NaOH	sodium hydroxide
M	molar
mg	miligram
min	minute
ml	mililiter (10 <sup>-3</sup> litre)
mm	milimeter
mM	milimolar
mol	mole
mRNA	messenger RNA
OD	optical density
OM	osteogenic medium
PBS	phosphate buffer saline
PD	periosteum-derived cells
pI	isoelectric point
pNP	para-nitrophenol
pNPP	para-nitrophenyl phosphate
RGD	one letter code for Arg-Gly-Asp
RNA	ribonucleic acid
rpm	revolution per minute
RT-PCR	reverse transcription-polymerase chain reaction
Runx2	runt-related transcription factor 2
SEM	scanning electron microscope
S.D.	standard deviation
SDS	sodium dodecyl sulfate
sGAG	sulfated glycosaminoglycans
TGF- $\beta$	transforming growth factor- $\beta$
UV	ultraviolet
v/v	volume by volume
w/v	weight by volume
3D	three-dimensional

# CHAPTER I

## INTRODUCTION

### 1. Background

It is estimated that approximately 1.5 million bone grafting operations are performed annually in the United States. Bone grafting markets generated revenues of \$517 million in 2001 that are expected to reach \$1,837 million by 2008 (Einhorn et al., 2003). Bone grafts are performed to enhance healing of spine fusions and fractures and to regenerate bone in osseous defects and malformations. Approximately 60 percent of the bone grafting operations use autografts; 30 percent use allogenic products (including demineralized bone powder); and 10 percent use synthetic materials, such as calcium phosphate-based ceramics, collagen or fibrin polymers, and various combinations. Although there are recognized deficiencies associated with each option, rational surgical applications and maximizing materials' therapeutic properties will minimize product deficiency and patient risk (Frost and Sullivan, 2008).

Tissue engineering is an interdisciplinary science that integrates basic principles of biomedical sciences, medicines, material sciences, and engineering in order to construct living tissues from their cellular components. A major perspective of tissue engineering is the medical application of such tissues for replacement of congenital defected, impaired, injured, or otherwise damaged human tissues (Anthony and Lanza, 2001; Tabata, 2003). Bone tissue engineering is developed in order to heal bone loss due to trauma or disease without the limitations and drawbacks of current clinical autografting and allografting treatments (Einhorn et al., 2003). One aspect of tissue engineering is concerned with the formation of three dimensional (3D) tissue substitutes by culturing cells on natural biomaterial scaffolds such as demineralized bone powder or collagen matrix. After implantation into patients, such engineered devices may help to create or restore the lost tissues or organ functions. The three essential components for tissue engineering are cellular components, growth and differentiation factors and scaffolds or matrices. The engineered bone can be studied into their osteoinductivities and properties *in vitro* (Cao et al., 2005).

Bone tissue engineering has been developed for the treatment of bone defect using osteoconductive materials, osteogenic cells and osteoinductive molecules. The osteoconductive material provides mechanical support for cell attachment and vascular ingrowth. However, it serves as a delivery vehicle for implanted growth factors and cells. Collagens are widely used as materials due to their appropriate biological characteristics. Scaffolds used in bone tissue engineering are designed to mimic natural tissues consisting of cells and an integrated vascular system for oxygen and nutrient supply. In general, an ideal scaffold should be biocompatible and biodegradable with a controllable degradation rate. It should be highly interconnected porosity, with an appropriate pore size and alignment to facilitate oxygen, nutrient and waste transfer. A suitable mechanical property of the scaffold is required to maintain a defined three-dimensional structure for the regenerating tissue and to withstand contractile force exerted by tissue formation. The scaffold should be able to provide the appropriate chemical signals to guide tissue growth and prevent immune rejection. In addition, it should have appropriate size and shape to match the target tissue (Cao et al., 2005; Mistry and Mikos, 2005; Nedović and Willaert, 2005).

Biomaterial is a key component of tissue engineering for medical application. Among various types of biomaterials, collagen is mainly found in extracellular matrix (ECM) of bone and is one of the most dominant materials in tissue engineering applications. Collagen scaffolds have been widely used due to a number of beneficial properties such as excellent biocompatibility, haemostatic effect, low antigenicity, and great tensile strength. (O'Brien et al., 2004; O'Brien et al., 2005). In addition, collagen scaffolds have been reported to promote cell attachment and growth. Collagen contains basic residues such as lysine and arginine and specific cell adhesion molecules such as arginine-glycine-aspartate (RGD) residues. The RGD residues actively induce cellular adhesion by binding to integrin receptors. This interaction plays an important role in cell growth and differentiation including overall regulation of cell function (Quirk et al., 2001).

Demineralized bone powder (DBP) is well known as biomaterial utilized for tissue engineering. Andrades (2001) has demonstrated that DBP was combined with osteoprogenitors and then implanted into animals. They found that it could support and induce new bone formation *in vivo*. Moreover, they showed that DBP could trigger osteoinductivity both *in vitro* and *in vivo*. The osteoinductivity of the DBP may result from their components including collagenous proteins and noncollagenous proteins (such as basic fibroblast growth factor (bFGF), transforming growth factor- $\beta$  (TGF- $\beta$ ), vascular endothelial

growth factor (VEGF), insulin-like growth factor (IGF), especially bone morphogenetic proteins (BMPs)). The DBP stand for potential candidates for bone tissue repair because of their close relation in structure and function with autologous bone. In general, DBP derived from cortical and cancellous bone have been utilized largely for clinical repair of bone injuries in orthopedic, periodontal, and cranio-maxillofacial application. DBP acts as a potential biomaterial for use in tissue engineering because of their ability to support and induce osteogenesis of matrix-incorporated osteoprogenitors (Honsawek et al., 2010). From the study of Kohles (2000), they combined DBP with collagen used for implantation of the baboon's periodontal defects for 3 months. The results indicated that combinations of demineralized, freeze-dried bone allograft (DFDBA) and collagen provided a better fill response than collagen matrix. Moreover, the mass ratio of combinations with 60/40 collagen to DBP resulted in the largest defect fill response.

Collagen is an acceptable biomaterial use for tissue engineering. Its structure consists of amino acids mainly glycine, proline and hydroxyproline that is biocompatible, biodegradable, non-immunogenic. Collagen molecule also contains RGD-like sequence that promotes cell adhesion and migration (Mistry and Mikos, 2005). However, it has some limitation because collagen is expensive and only dissolves in acid condition. In contrast, gelatin derived from hydrolytic degradation of collagen has been of interest because it is much cheaper and easier to obtain into the solution than collagen.

Gelatin is biocompatible, non-immunogenic and non-antigenic (Zhao et al., 2006). Moreover, gelatin contains RGD-like residues that promote cell adhesion, migration and proliferation (Huang et al., 2005). Previous studies demonstrated that gelatin could be used as a base material substituting a large portion of collagen to produce scaffolds without affecting the biological properties (Ratanavaraporn et al., 2006). Therefore, gelatin is selected as a base material to fabricate the scaffolds instead of collagen in this study on bone tissue engineering.

Chitosan is a glycosaminoglycan (GAG) analog due to its similarity of molecular structure to natural GAG (Zhao et al., 2006). Chitosan, the deacetylated derivative of chitin, is an amino polysaccharide consisting of  $\beta$ -(1, 4)-2-acetamido-2-deoxy-D-glucose and  $\beta$ -(1, 4)-2-amino-2-deoxy-D-glucose units. It has attractive biological properties such as anti-microbial, anti-tumor, and haemostatic (Madhally and Matthew, 1999). In addition, chitosan is reported to accelerate wound healing and enhance bone formation (Park et al., 2005). Depending on source and preparation process, the molecular weight of chitosan can be varied in a wide range. Recent study has shown that low molecular weight chitosan is highly

effective to promote the proliferation of mouse fibroblasts compared to high molecular weight chitosan (Tangsadthakun, et al., 2007). It was reported that low molecular weight chitosan was more effective to promote the proliferation of mouse fibroblasts.

Chitooligosaccharide (COS) is one of the very low molecular weight water-soluble chitosan that can be obtained from various methods such as enzymatic, acid and free radical hydrolysis (Chang et al., 2001). Recently, polysaccharides like chitosan and its derivative have become of increasing interest in the field of tissue engineering as shown in Figure 1.1 (Greenwald, et al., 2001). From the study of Rattanavaraporn (2009), they developed the scaffolds from gelatin (G) and COS via freeze drying technique. They found that G/COS scaffolds promoted cell attachment and proliferation as good as pure gelatin scaffold. Importantly, G/COS scaffolds enhance osteogenic differentiation of MSCs when compared to pure gelatin scaffold. Particularly, G/COS scaffold in the blending ratio of 70/30 was found to enhance osteogenic differentiation of bone marrow-derived stem cells (Rattanavaraporn et al., 2009).

Apart from scaffold-based strategy, stem cell is another key factor for bone tissue engineering. Mesenchymal stem cells (MSCs) are promising cell sources for bone regeneration, which are capable of differentiation into a variety of specialized mesenchymal tissues, including bone, tendon, cartilage, muscle, ligament, fat and bone marrow. Stem cells have usually been seeded on scaffolds, cultured *in vitro* and then implanted to observe bone formation *in vivo*. It is believed that stem cells can differentiate into osteoblasts and chondroblasts which can then accelerate bone repair. In this study, the periosteum-derived MSCs are employed in term of *in vitro* proliferation and osteogenic differentiation on the scaffolds (Maniatopoulos et al., 1988; Pittenger, et al., 1999; Krampera et al., 2006).

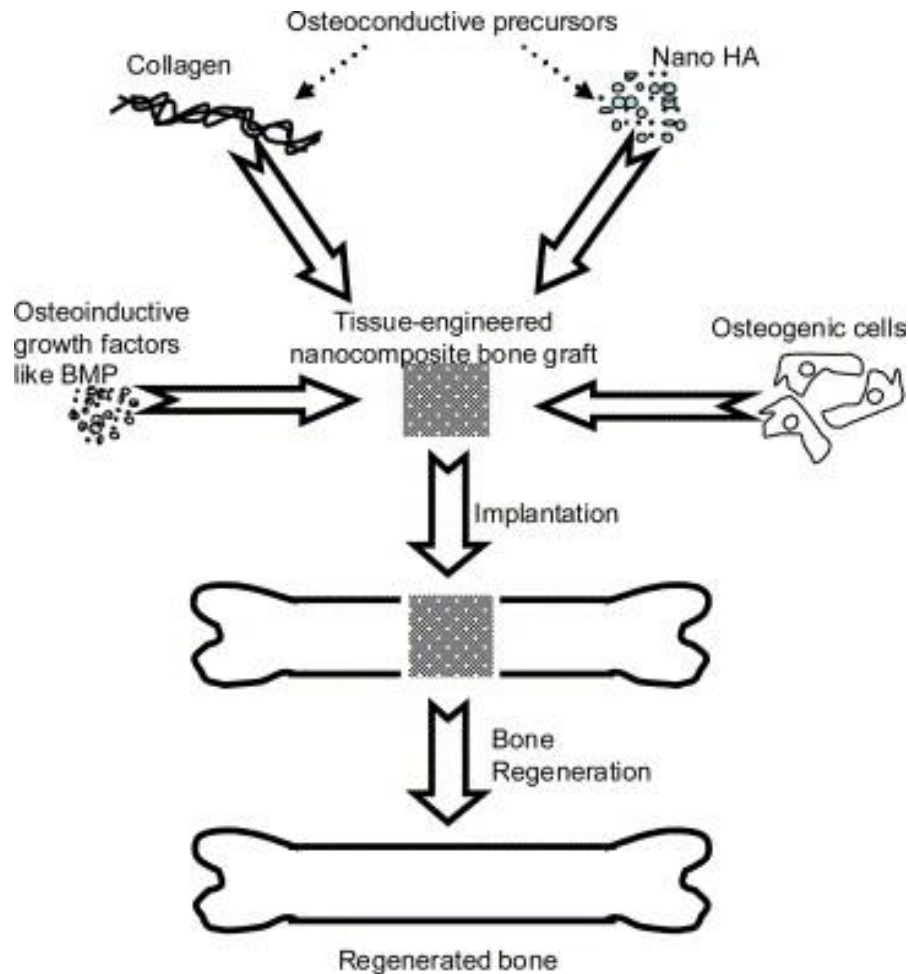


**Figure 1.1** Application of biocomposited materials for bone substitution .

(Murugan and Ramakrishna, 2005)

The aim of this research is to develop new scaffolds from natural biomaterials containing gelatin, chitooligosaccharide, and demineralized bone powder (DBP) for bone tissue engineering application. Although DBP contains BMPs and osteoinductive proteins, DBP may be difficult to fabricate into the three dimensional structure. Furthermore, the gelatin and the chitooligosaccharide are alternative biomaterials used for tissue engineering that enhance osteoblastic differentiation of bone marrow stromal cells. Therefore, this research is aimed to study gelatin and chitosan combined with DBP to fabricate into three dimensional scaffolds used for bone tissue engineering. The DBP may enhance osteoinductivity, strength, and biodegradation time. This study investigated the properties of the scaffolds both *in vitro* and *in vivo*. These scaffolds are expected to be used as alternative biomaterial for bone tissue engineering.

## 2. Objectives

1. To investigate the characteristics of mesenchymal stem cells (MSCs) isolated from periosteal cells.
2. To study the influences of particle size of demineralized bone in collagen scaffold on cell behavior, and osteogenic differentiation of MSCs.
3. To develop the novel scaffolds from the combination of gelatin, chitooligosaccharide, and demineralized bone in order to investigate their osteogenic potential for bone tissue engineering in *in vitro* and *in vivo*.

## 3. Scope of research

### **Part I: Characterization of mesenchymal stem cells for bone tissue engineering**

1. Isolation and cultivation of mesenchymal stem cells from human periosteum
2. Analysis of specific cell surface of MSCs
3. *In vitro* functional characterizations of MSCs
  - 3.1 Osteogenic differentiation study of MSCs
  - 3.2 Chondrogenic differentiation study of MSCs
  - 3.3 Adipogenic differentiation study of MSCs

### **Part II: Osteogenic characterization of collagen and various particle size of demineralized bone powder**

1. Preparation of the demineralized bone powder
2. Fabrication of collagen and various size demineralized bone powder scaffolds
3. Physical and chemical characterization of collagen and various size demineralized bone powder scaffolds
  - 3.1 Morphology observation of the scaffolds
  - 3.2 Mechanical testing of the scaffolds
  - 3.3 Swelling ability of the scaffolds

4. *In vitro* biological characterizations of MSCs onto the collagen/demineralized bone powder scaffolds
  - 4.1 *In vitro* cell culture of MSCs with collagen/demineralized bone powder scaffolds
    - 4.1.1 Initial cell attachment of MSCs with scaffolds
    - 4.1.2 Cell proliferation of MSCs with scaffolds
  - 4.2 *In vitro* osteogenic differentiation of MSCs with the collagen/demineralized bone powder scaffolds
    - 4.2.1 Alkaline phosphatase (ALP) activity assay of MSCs with scaffolds
    - 4.2.2 Calcium determination assay of MSCs with scaffolds
    - 4.2.3 Surface elemental analysis of MSCs with scaffolds
    - 4.2.4 The observation of cultured MSCs with scaffolds

**Part III: Gelatin/chitooligosaccharide/demineralized bone powder scaffolds for bone tissue engineering**

1. Fabrication of the gelatin/chitooligosaccharide/demineralized bone powder scaffolds
2. Physical and chemical characterization of the gelatin/chitooligosaccharide/demineralized bone powder scaffolds
  - 2.1 Morphological observation of the scaffolds
  - 2.2 Mechanical test of the scaffolds
  - 2.3 Swelling ability of the scaffolds
3. *In vitro* biological characterizations of the gelatin/chitooligosaccharide/demineralized bone powder scaffolds with MSCs
  - 3.1 Initial cell attachment of MSCs with the scaffolds
  - 3.2 Cell proliferation of MSCs with the scaffolds



4. *In vitro* osteogenic characterization of the gelatin/chitooligosaccharide/demineralized bone powder scaffolds with MSCs
  - 4.1 Alkaline phosphatase (ALP) activity assay of MSCs with the scaffolds
  - 4.2 Calcium determination assay of MSCs with the scaffolds
  - 4.3 Surface elemental analysis of MSCs with the scaffolds
  - 4.4 The observation of cultured MSCs with the scaffolds
5. *In vivo* osteogenic potential of the gelatin/chitooligosaccharide/demineralized bone powder scaffolds in Wistar rat model
  - 5.1 Implantation method
  - 5.2 Explantation method
  - 5.3 New bone formation evaluation of the implant
  - 5.4 Mineralization evaluation of the implant

# CHAPTER II

## LITERATURE REVIEWS

### 1. Anatomy and Physiology of the Bone

#### 1.1 Bone Functions

The function of bone is to protect vital organs of the body and provide the frame for motion of the musculoskeletal system. Both the material properties of bone and the structure of whole bones contribute to exceptional stiffness and strength that yield the ability to withstand physiological loads without breaking. In addition, bone is a reservoir for many essential minerals, such as calcium and phosphate, and plays an important role in the regulation of ion concentration in extracellular fluid. Bone marrow contains mesenchymal or marrow-derived stem cells (MSCs), which are pluripotent cells capable of differentiation into bone, cartilage, tendon, muscle, dermis, and fat tissues. Also, hematopoietic cells that produce the red and white blood cells are found in marrow.

#### 1.2 Bone structures and mechanics

Typically, the adult skeleton contains 80% compact bone and 20% spongy (cancellous) bone as shown in Figure 2.1. Compact bone is a hard dense part surrounding the marrow cavity. Compact bone is only 10% porous, allowing room for only a small number of cells and blood vessels. The structural unit of compact bone is the cylindrical shaped osteon, which is composed of concentric layers of bone called lamella. Blood vessels run through Haversian canals located at the center of each osteon while nutrient diffusion is further conducted by canaliculi, which are microscale canals within bone. Osteons are aligned in the longitudinal direction of bone which shows strength values are 79-151 MPa in tension and 131-224 MPa in compression. The moduli range from 17-20 GPa for both tension and compression. Spongy and porous trabecular bone is found in ribs, spine, and the ends of long bones. Spongy bone, which may be as much as 50-90% porous, is an interconnected network of small trabecular bone aligned in the direction of loading stress. The porous volume contains vasculature and bone marrow, which provide little mechanical support compared to compact bone. The strength and moduli of spongy bone vary with density, reported

approximately 5-10 MPa in tension and 50-100 MPa in compression (Yaszemski et al., 1996).

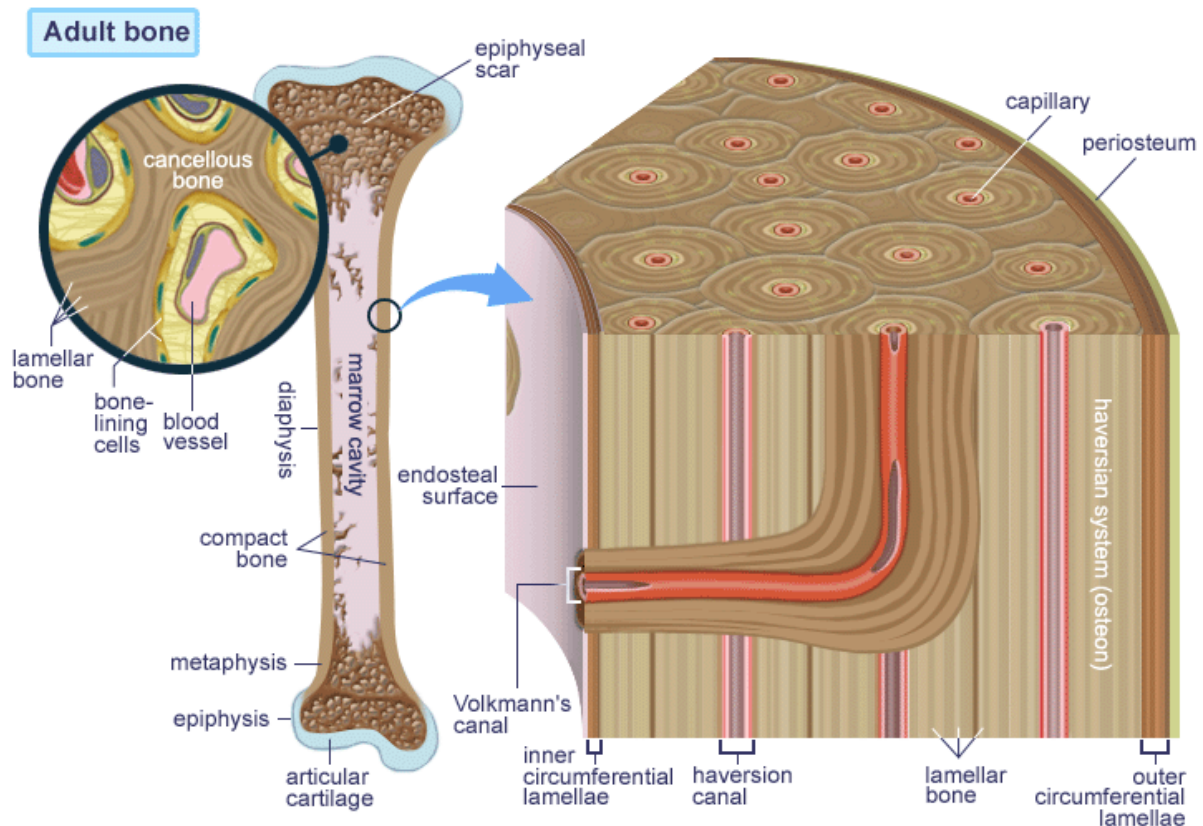


**Figure 2.1** Gross anatomy and histology of bone (Keaveny et al., 1999)

Bone is composed of roughly 60% inorganic mineral, 30% organic material, and 10% water. Calcium phosphate crystals, primary hydroxyapatite (HA), comprise the inorganic phase while collagen mostly comprises the organic phase. Collagen molecules align into triple helices that bundle into fibrils which then bundle into collagen fibers. HA crystals are small plates 2-3 nm thick and 10 nm in length and width that precipitate onto the collagen fibers. Rigid HA crystals provide compressive strength to the composite, while collagen fibers, capable of energy dissipation, impart tensile properties to bone (Mistry and Mikos, 2005).

### **1.3 Cellular organization**

There are three types of cells living in the inorganic-organic composite structure of bone. Osteoblasts, derived from MSCs, secrete collagenous proteins that form the organic matrix of bone, called osteoid. Mature osteoblasts surrounded by osteoid stop secreting the matrix and become osteocytes, which are important in signal transduction of mechanical stimuli. The third cell type, osteoclasts, are derived from hematopoietic cells of the marrow and secrete acids and proteolytic enzymes which dissolve mineral salts and digest the organic matrix of bone. In response to various chemical, biological and mechanical factors, osteoblasts and osteoclasts turn over frequently in a balanced manner so that bone tissue is constantly remodeled (Keaveny et al., 1999; Mistry and Mikos, 2005).

Five stages describing the bone remodeling process are quiescence, activation, resorption, reversal, and formation. The process begins with the quiescence stage in which inactive cells are present on the surface of bone. Normally, free bone surfaces are more than 80% in this stage. The activation phase arises when biochemical or physical signals attract mononuclear monocytes and macrophages to the remodeling site and promote differentiation into osteoclasts. Resorption from the osteoclasts is to break down the organic and inorganic components of the bone to form a cavity. During reversal, osteoclasts leave the site and mononuclear macrophage-like cells secrete a cement-like substance on the surface. In the final phase, formation, osteoblasts fill the cavity with bone matrix and form new osteons. This begins with the rapid deposition of collagen in densely packed columns, followed by mineralization. As these processes complete, the surface returns to its quiescent stage (Mistry and Mikos, 2005).

### **1.4 Bone formation**

Process of bone formation within a fracture or implanted bone graft begins with differentiation of MSC progenitors into chondrocytes, or cartilage-forming cells. These cells form a cartilaginous matrix. MSCs originating in the bone marrow migrate, differentiate, and proliferate in the matrix. These cells are prone to stimulate bone formation rather than cartilage and subsequently construct passage ways for vascularization while continuing to build bone. Osteocytes and randomly oriented collagen fibrils form the bulk of the weak material were known as immature woven bone. Remodeling of woven bone into mature, lamellar bone is a slow process that yields a more organized tissue of distinct mechanical strength (Mistry and Mikos, 2005).

### 1.5 Fracture Healing

Fracture healing is composed of three biological stages which are inflammation, repair, and remodeling. The initial acute inflammatory response entails the formation of a hematoma at the site of damaged blood vessels (Figure 2.2). Neutrophils and macrophages arrive and ingest the cellular debris of necrosis while releasing growth factors and cytokines. These biochemical signals induce the migration and differentiation of MSCs from surrounding bone, bone marrow, and periosteum. Capillary growth and fibroblast activity create fibrovascular granulation tissues at the injury site. As MSCs accumulate and differentiate into osteoblasts. The relatively short inflammatory phase is followed by the repair phase, which begins as osteoblasts rapidly lay down new osteoid to form woven bone at the injury site. Gradually, the third phase of healing, remodeling, and reshapes recognizes collagen fibers forming mechanically strong lamellar bone. Through the remodeling phase may take up to a full year for severe fractures, it returns bone to its original, pre-fracture strength. However, if the body's response to bone injury does not provide enough active cells, or if a defect is too large for the body's natural healing response, non-union can occur at the fracture site (Keaveny et al., 1999; Mistry and Mikos, 2005).

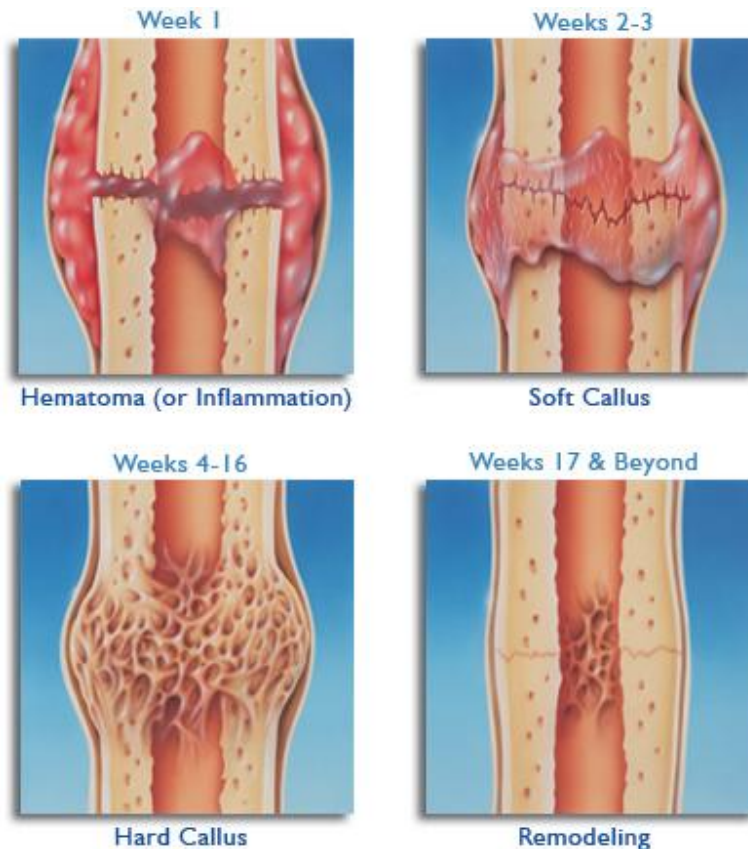


**Figure 2.2** Fracture healing process (Mizuno and Glowacki, 1996)

## 2. Bone tissue engineering

Natural healing of severe fractures results in non-union of injured bone. Therefore, medical treatments such as autograft and allograft are required. However, these substitutes have many associated problems including donor site morbidity and immune responses. Thus, treatment using the bone tissue engineering has being developed through the use of cells, scaffolds, and bioactive growth factors. This technology could lead to natural, mechanically sound bone at the site of injury and also eliminate the use of permanent material that may impede the natural growth of bone (Mistry and Mikos, 2005; Nedović and Willaert, 2005).

Basically, tissue engineering strategies consist of three general categories: (1) matrix-based strategies, (2) cell-based strategies, and (3) growth factor-based strategies. In the field of bone tissue engineering, these strategies require interaction between osteoinductive, osteogenic and osteoconductive substances. A material that supports bone growth on itself demonstrates osteoconductivity. An osteoconductive scaffold may provide mechanical support, sites for cell attachment and vascular ingrowth, and a delivery vehicle for implanted growth factors and cells. Osteogenic components include cells capable of bone production such as osteoprogenitor cells or differentiated osteoblasts. Osteoinductive factors include bioactive chemicals such as growth factors that induce recruitment, differentiation, and proliferation of the proper cell types at an injury site (Bruder and Fox, 1999).

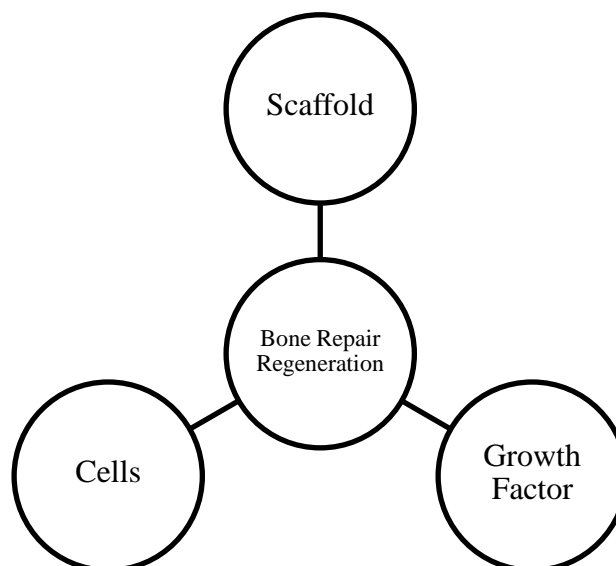


**Figure 2.3** Parameters required for cartilage repair regeneration using a combinatorial approach (Barron and Pandit, 2003)

### **2.1 Osteoconduction: matrix-based strategies** (Bruder and Fox, 1999; Mistry and Mikos, 2005)

A scaffold biomaterial is essential for filling a critical-sized defect and acts as a carrier for cells and/or growth factors to heal the defect. For successful regeneration of bone tissue at a defect, a potential bone tissue engineering scaffold must exhibit the following properties:

- (1) Provide temporary mechanical strength to the affected area.
- (2) Act as a substrate for osteoid deposition and growth.
- (3) Contain a porous architecture to allow for vascularization and bone ingrowth.
- (4) Encourage bone cell migration into a defect and enhance cell activity for regeneration and repair.
- (5) Degrade in a controlled manner to facilitate bone development in the defect.
- (6) Degrade into non-toxic products that can safely be removed by the body.
- (7) Not cause a significant inflammatory response.
- (8) Be capable of sterilization without loss of bioactivity.

Mechanical properties of the scaffold should match with the target tissue to provide structural stability to an injury site. In this case, the chosen biomaterial must be strong enough to support the physiological load of the body without absorbing the mechanical stimuli required for natural growth in the affected area. It is also essential that biomaterials allow gradual load transfer to developing tissue for proper healing to occur.

Osteoconduction refers to the ability of material to serve as a substrate for cell adhesion and function while facilitating bone growth throughout a three-dimensional scaffold across a defect. Hence, a porous architecture that allows bone ingrowth and vascularization throughout the scaffold is necessary. Ideally, scaffolds may be designed to maximize porosity and maintain mechanical properties with interconnected pores of approximately 200-400 nm. This type of architecture can provide a large surface area for cell attachment, growth, and function, as well as a large void space for bone formation and vascularization.

Biodegradable biomaterials are highly preferred over non-degradable materials, however, they are generally weaker. Controlled degradation of a scaffold allows for gradual load transfer to bone, increasing space for bone growth, and eventual filling of a defect with natural bone, as opposed to a permanent biomaterial which may cause stress-shielding or infection.

Scaffolds must not elicit a significant inflammatory response that may result in fibrous capsule formation around the implant, rendering it ineffective. Toxic response of the tissues surrounding a biomaterial can cause cell death and worsen the injury.

Finally, biomaterial scaffolds must be sterilized without loss of function, e.g. sterilization process must not alter the chemical composition of material, which may further affect its bioactivity, biocompatibility, or degradation properties.

## **2.2 Osteogenesis: cell-based strategies** (Bruder and Fox, 1999; Mistry and Mikos, 2005)

Cell based strategies for bone tissue engineering involve in the transplantation of osteogenic cells into a defect. Cells used for cell-based therapies may be transplanted in various forms including fresh bone marrow, MSCs expanded in culture, or osteoblasts differentiated in culture.

The key factor for the success of bone marrow in healing non-unions of injured bone is the presence of MSCs. These progenitor cells are promising tools for regenerative therapy due to proliferation capabilities, preservation of bioactivity after freezing, and the ability to build new tissue in a defect. However, these cells make up less than 0.001% of the cellular content of bone marrow, and even less as age increases. The limited quantity of MSCs in marrow has led to the strategy to isolate MSCs from bone marrow, expand *in vitro* and seed onto a carrier for implantation into a defect.

MSCs are capable of differentiation into cells of a variety of musculoskeletal tissues. Isolated MSCs in culture can be selectively differentiated into osteoblasts with media supplements such as dexamethasone, ascorbic acid, and  $\beta$ -glycerophosphate. Additionally, MSCs can be harvested from marrow, expanded in culture, and differentiated into osteoblasts prior to implantation. These osteogenic cells can begin building new osteoid immediately upon arrival at an injury site. Biomaterial carriers, such as biodegradable polymers and ceramics, have been used to deliver differentiated MSCs to a defect site.



### **2.3 Osteoinduction: growth factor-based strategies** (Bruder and Fox, 1999; Mistry and Mikos, 2005)

Growth factors are signaling polypeptide molecules that regulate a multitude of cellular functions including migration, adhesion, proliferation, differentiation, and gene expression. Growth factors bind to specific surface receptors of target cells to induce a response, usually in the form of new mRNA or protein synthesis. A single growth factor may induce the same or different response in various cell types. In addition, many cell types secrete the same growth factors, though not always with the same effect. A number of osteoinductive growth factors have been identified, two of the most common groups are bone morphogenetic proteins (e.g. BMP-2, BMP-7) and transforming growth factor- $\beta$  (e.g. TGF- $\beta$ 1). BMPs are cytokines that stimulate MSC differentiation into osteoblasts. TGF- $\beta$ s are growth factors that stimulate MSC differentiation towards chondrocytes and proliferation of osteoblasts and chondrocytes.

### **3. Biomaterials** (Cao et al., 2005; Nedović and Willaert, 2005)

The selection of biomaterial plays a key role in the design and development of tissue engineering product. A biomaterial must interact with tissue to repair, rather than act simply as a replacement. Furthermore, biomaterials used directly in tissue repair or replacement applications must elicit a desirable cellular response.

A wide variety of polymeric and ceramic materials have been studied for use as biomaterials for bone tissue engineering. Biopolymers offer one major advantage over ceramics that is flexibility. The mechanical and degradation properties of a polymer can be modified by composition and processing conditions. The three main material types which have been successfully used in developing scaffolds for bone tissue engineering include:

- (1) Natural polymers: such as collagen, glycosaminoglycan, chitin, starch, cellulose
- (2) Synthetic polymers: such as polylactic acid (PLA), polyglycolic acid (PGA), and their co-polymer (PLGA)
- (3) Ceramics: such as hydroxyapatite (HA) and  $\beta$ -tricalcium phosphate ( $\beta$ -TCP)

Synthetic materials can be easily processed into various structures and can be produced easily and reproducibly. Moreover, it is possible to tightly control various properties such as mechanical strength, hydrophobicity, and degradation rate. Natural

biomaterials must be isolated from plant, animal, or human tissue. They are typically expensive and differ from large batch-to-batch variations. Furthermore, natural materials sometimes exhibit a limited range of physical properties and can be difficult to isolate and process. Although they have some limitations, there are some important advantages of using natural materials, for example, they have specific biological activity and generally do not elicit unfavorable host tissue response. Some synthetic polymers, in contrast, can elicit a long-term inflammatory response from the host tissue. Ceramics have also been widely used, due to their high biocompatibility and resemblance to the natural inorganic component of bone and teeth. Ceramics are inherently brittle so that their applicability in soft tissue engineering is limited.

### **3.1 Demineralized bone powder**

Demineralized bone powder (DBP) is a human allograft bone that is washed, demineralized with organic solvents, dried, prepared, and sterilized. As first described by Urist in 1960s (Urist and Dowell, 1968; Urist et al., 1967). The DBP can be generated by the hydrochloric acid extraction process of allograft bone, giving rise to a demineralized matrix consisting of osteoconductive type 1 collagen and non-collagenous proteins, including osteoinductive bone morphogenetic proteins (BMPs) that shown to possess inherent osteoconductive and osteoinductive properties including stimulate the formation of bone at a defect site (Urist et al., 1967).

Recent research has proven that cortical bone is the preferred choice for DBM synthesis as it is more osteoinductive with a lower antigenic potential than cancellous bone (Urist and Dawson, 1981). Sampath (1981) described the histological process by which new bone is formed under the influence of DBP in ectopic sites (Sampath and Reddi, 1981, 1983). The tissue is initially infiltrated by inflammatory and mesenchymal stem cells (Urist et al., 1967).

The DBP serve as an insoluble scaffold. Although the soluble extract or insoluble collagen scaffolds are not osteoinductive alone, when recombined and reconstituted together it can restore bone induction. Therefore, there is collaboration between a soluble signal and an insoluble substratum of collagen to initiate new bone formation. The soluble signal was purified by heparin affinity chromatography, hydroxyapatite columns, and molecular sieve chromatography. The final purification was accomplished by preparative gel electrophoresis and novel BMPs were isolated (Table 2.1). The sequential cellular responses to implants of demineralized bone materials include chemotaxis, attachment of progenitor cells to the

matrix, proliferation and differentiation of progenitor cells into chondrocytes, cartilage mineralization, vascularization, resorption of the induced cartilage, and ultimately new bone formation (Muthukumaran and Reddi, 1985).

Nowadays, DBP has been extensively utilized in orthopaedics, periodontal, maxillofacial, and hand reconstruction applications. DBP comprises bone morphogenetic proteins (BMPs) that are essential regulators for endochondral bone formation (Murugan and Ramakrishna, 2005).

**Table 2.1** The superfamily of BMPs

<b>BMP Subfamily</b>	<b>BMP Designation*</b>
BMP-2/4	BMP-2, BMP-4
BMP-3	BMP-3, BMP-3B
OP-1 / BMP-7	BMP-5, BMP-6, BMP-7, BMP-8, BMP-8B
Others	BMP-9, BMP-10, BMP-11, BMP-15
Cartilage-Derived Morphogenetic Proteins (CDMPs)	BMP-14/CDMP-1/GDF-5
	BMP-13/CDMP-2/GDF-6
Growth/Differentiation Factors (GDF)	BMP-12/CDMP-3/GDF-7

\* BMP-1 is procollagen C-proteinase related to *Drosophila* Tolloid and does not contain the canonical seven cysteines of classical BMPs listed in this Table. BMP-1 is copurified with the osteogenic BMPs such as BMP-2.

Table 2.1 summarizes the fifteen known BMPs in mammals that are related to members of the TGF- $\beta$  superfamily. BMPs are dimers that held together by a critical intermolecular disulfide linkage. The dimeric conformation is critical for bone induction and morphogenesis. Each of the two monomers is biosynthesized as a precursor molecule of over 400 amino acids. However, mature BMP monomer derived from proteolytic processing is an approximately 120 amino acid polypeptide. BMPs are pleiotropic signals. Pleiotropy is the property of a gene or protein to act in a multiplicity of steps. BMPs act on the three key steps in the sequential cascade of bone morphogenesis such as chemotaxis, mitosis and differentiation of transient stage of cartilage and the permanent induction of bone.

## **3.2 Collagen**

### **3.2.1 The nature of collagen**

Collagen is the most abundant fibrous protein in mammals, which is commonly found in skin, bone, teeth, tendons, cartilage, blood vessels, and connective tissue. More than 90% of the extracellular protein in tendon and bone and more than 50% in skin consist of collagen. Collagen provides strength and elasticity to tissues. Also, it is the main component of ligaments and tendons. Collagen plays an important role in the formation of tissues and organs. It is also involved in various functional expressions of cells. Collagen is a good surface-active agent, exhibits biodegradability, weak antigenicity and superior biocompatibility compared with other natural polymers, such as albumin, alginate and cellulose.

### **3.2.2 Classification of collagen**

Collagen can be found in many parts throughout the body. It is classified in different forms known as type. Different collagen types are necessary to confer distinct biological features to the various types of connective tissues in the body. Currently at least 13 collagen types which vary in the amino acid composition, the length of the helix, the nature and size of non-helical portions have been isolated, as listed in Table 2.2.

**Table 2.2** Chain composition and body distribution of collagen types (Friess, 1998).

Collagen type	Chain composition	Tissue distribution
I	$(\alpha 1(\text{I}))_2\alpha 2(\text{I})$ or trimer $(\alpha 1(\text{I}))_3$	Skin, tendon, bone, cornea, dentin, fibrocartilage, large vessels, intestine, uterus, dentin, dermis, tendon
II	$(\alpha 1(\text{II}))_3$	Hyaline cartilage, vitreous, nucleus pulposus, notochord
III	$(\alpha 1(\text{III}))_3$	Large vessels, uterine wall, dermis, intestine, heart valve, gingiva (usually coexists with type I except in bone, tendon, cornea)
IV	$(\alpha 1(\text{IV}))_2\alpha 2(\text{IV})$	Basement membranes
V	$\alpha 1(\text{V})\alpha 2(\text{V})\alpha 3(\text{V})$ or $(\alpha 1(\text{V}))_2\alpha 2(\text{V})$ or $(\alpha 1(\text{V}))_3$	Cornea, placental membranes, bone, large vessels, hyaline cartilage, gingiva
VI	$\alpha 1(\text{VI})\alpha 2(\text{VI})\alpha 3(\text{VI})$	Descemet's membrane, skin, nucleus pulposus, heart muscle
VII	$(\alpha 1(\text{VII}))_3$	Skin, placenta, lung, cartilage, cornea
VIII	$\alpha 1(\text{VIII}) \alpha 2(\text{VIII})$ chain organization of unknown helix	Produced by endothelial cells, Descemet's membrane
IX	$\alpha 1(\text{IX})\alpha 2(\text{IX})\alpha 3(\text{IX})$	Cartilage
X	$(\alpha 1(\text{X}))_3$	Hypertrophic and mineralizing cartilage Cartilage, intervertebral disc, vitreous humour
XI	$\alpha 1(\text{XI})\alpha 2(\text{XI})\alpha 3(\text{XI})$	Chicken embryo tendon, bovine periodontal ligament
XII	$(\alpha 1(\text{XII}))_3$	
XIII	Unknown	Cetal skin, bone, intestinal mucosa

### 3.2.3 Three dimensional structure of type I collagen

Type I collagen is predominant in higher order animals especially in the skin, tendon, and bone where extreme forces are transmitted. It is a compound of three chains, two of which are identical, termed  $\alpha 1(I)$ , and one  $\alpha 2(I)$  chain with different amino acid compositions, or it can rarely represent a trimer built of three  $\alpha 1(I)$  chains. Each of the  $\alpha$ -chains is composed of about 1,000 amino acid residues with Gly-X-Y repeating sequence. For type I collagen, X and Y residues are proline and hydroxyproline in every six residues. Only glycine residue is facing toward the center of the chain and the other hydrophobic amino acid residues are all facing outside. This is related closely to the low solubility of collagen in water. The  $\alpha$ -chains form a helical structure by rotating counterclockwise with 3.3 amino acid residues per rotation. Helical structure is presented at the center and relaxed structure is presented at both ends of the collagen molecule as shown in Figure 2.4 (a). Furthermore, the three  $\alpha$ -chains as a whole form a helical structure by rotating clockwise with 30-45 residues per rotation. When the triple helix is denatured and becomes gelatin, polypeptides are separated to one  $\alpha$ -chain, two  $\beta$ -chains, and three  $\gamma$ -chains.

The denaturing temperature of collagen from various animal species is different since it is related to the temperature of the environment surrounding the cells. For example, the denaturing temperature of human or higher order animals is 40°C, whereas that of the fish in Antarctic is about 5°C. Furthermore, it is known that collagen in different tissues of the same animal has different denaturing temperature. Hydroxyproline plays an important role in heat stability of the collagen molecule. Introduction of —OH group in proline facilitates the formation of hydrogen bonds within the molecule through water molecules. Thus, the denaturing temperature is high in collagen molecules which have high hydroxyproline content.

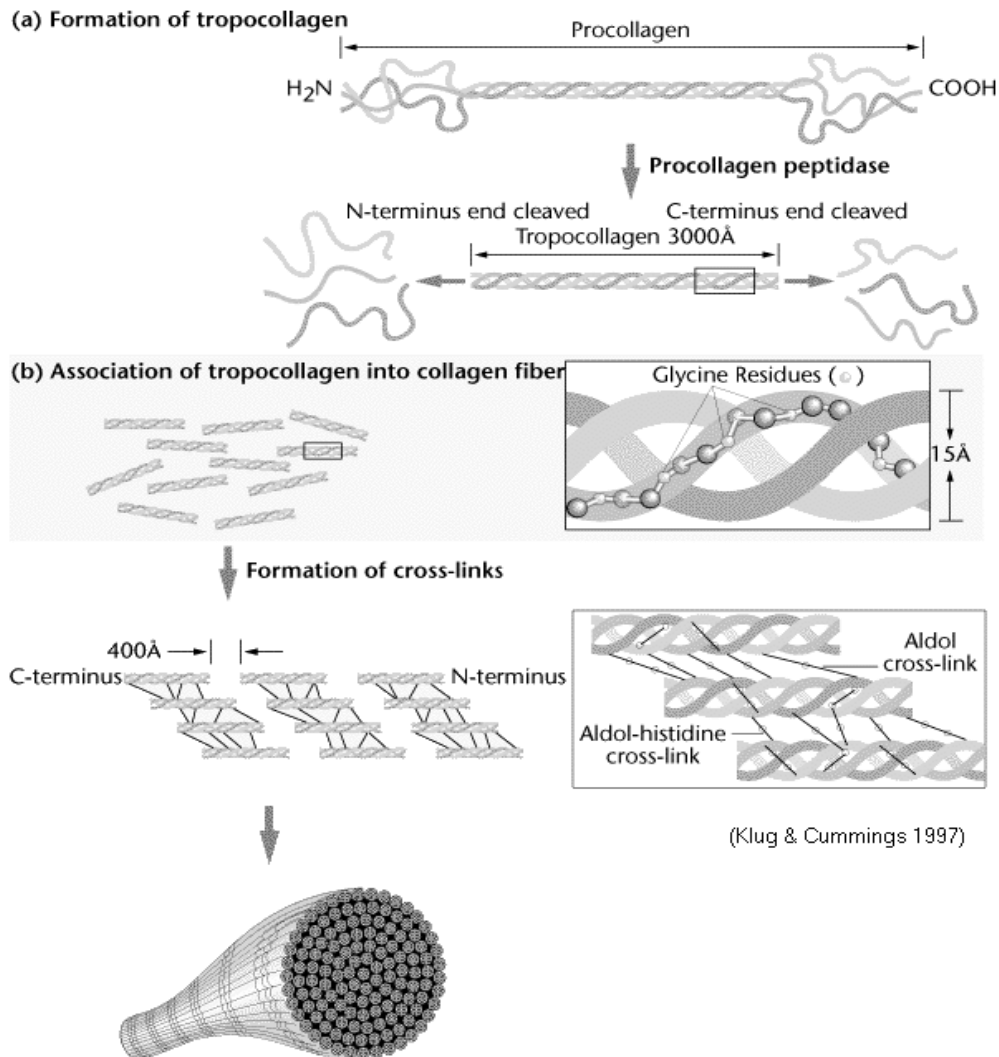


**Figure 2.4** Molecular structure of collagen  
 ([http://www.mun.ca/biology/scarr/collagen\\_structure](http://www.mun.ca/biology/scarr/collagen_structure))

### 3.2.4 Amino acid composition

Within collagen molecules, approximately 1/3 of the total amino acid residues is composed of glycine and 2/9 are amino acids, i.e. proline and hydroxyproline. Hydrophilic amino acid residues are very few. Telopeptide regions (non-helical regions of the molecule) are denoted for regions of 9–26 amino acids at the amino and carboxyl terminal chain ends of the molecule that are not incorporated into the helical structure. Table 2.3 represents the amino acid composition of  $\alpha$ -chains in bovine collagen.

**Table 2.3** Amino acid composition of bovine collagen  $\alpha$ -chains (Miller and Lunde, 1973)

Amino acid	Residues/1,000 residues			
	$\alpha$ 1(I)	$\alpha$ 2(I)	$\alpha$ 1(II)	$\alpha$ 1(III)
3-Hydroxyproline	1	-	2	-
4-Hydroxyproline	85	85	91	127
Aspartic acid	45	47	43	48
Threonine	16	17	22	14
Serine	34	24	26	44
Glutamic acid	77	71	87	71
Proline	135	120	129	106
Glycine	327	328	333	366
Alanine	120	101	102	82
Cysteine	-	-	-	2
Valine	18	34	17	12
Methionine	7	4	11	7
Isoleucine	9	17	9	11
Leucine	21	34	26	15
Tyrosine	4	3	1	3
Phenylalanine	12	16	14	9
Hydroxylysine	5	11	23	7
Lysine	32	21	15	25
Histidine	3	8	2	8
Arginine	50	57	51	44

Primary structure of collagen is characterized by the presence of Gly-X-Y repeating sequence. The presence of glycine in every three residues is essential for the formation of helical structure. X and Y represent other amino acid residues. The frequency of amino acids in these positions is different in different species of collagen. For type I collagen, proline and hydroxyproline exist in X and Y, respectively. Such a regular sequence is not found in the telopeptide regions.



### **3.3 Gelatin** (Tabata and Ikada, 1998)

#### **3.3.1 The nature of gelatin**

Gelatin is a natural protein which is derived from collagen, a main component that found in any connective tissue of human and animals. Gelatin can be obtained from hydrolysis reaction of collagen with subsequent purification, concentration, and drying operations. This process can break the triple-helix structure of collagen into single-stranded macromolecules. Gelatin is a vitreous, brittle, tasteless and odorless.

The important property of gelatin in aqueous solution is a thermal reversible conformational transition, which is responsible for gelation upon cooling from solution below the specific gel point of gelatin as the chains undergo a conformational coil-to-helix transition during they try to recover the collagen triple-helix structure. When heat the gelatin at body temperature (37°C), the triple-helices will be denatured and reversed to gel again to become fully soluble. The gel point depended on the source of the raw material. Gelatin extracted from the tissues of warm-blooded animals has a gel point in the range of 30-35°C and gelatin extracting from the skin of cold-water ocean fish has a gel point in the range of 5-10°C. When immerse the gelatin in cold water, the granules were hydrated into discrete, swollen particles. While it is heated, gelatin disperses into the water, resulting in a stable suspension. Gelatin is stable in aqueous solutions of polyhydric alcohols such as glycerin and propylene glycol. It is insoluble in most organic solvents.

#### **3.3.2 Types of gelatin**

There are two types of gelatin, depending on the preparation process (Figure 2.5). Gelatin can be divided into 2 types based on the production process

Type A gelatin (basic gelatin) is produced from acid process. This process is mainly applied to porcine skin. The isoelectric point (pI) of type A gelatin are in the range of 7-9. Acid process is faster than alkaline process and normally requires 10 to 48 hours of denaturation.

Type B gelatin (acidic gelatin) is produced form alkaline process. It is mainly applied to cattle skin and bone, in which the triple-helix collagen molecule is more densely crosslinked and complex. Type B gelatin has a pI from 4.7 to 5.4. This process requires longer time for several weeks. Typical specifications for type A and B gelatin are shown in Table 2.4.

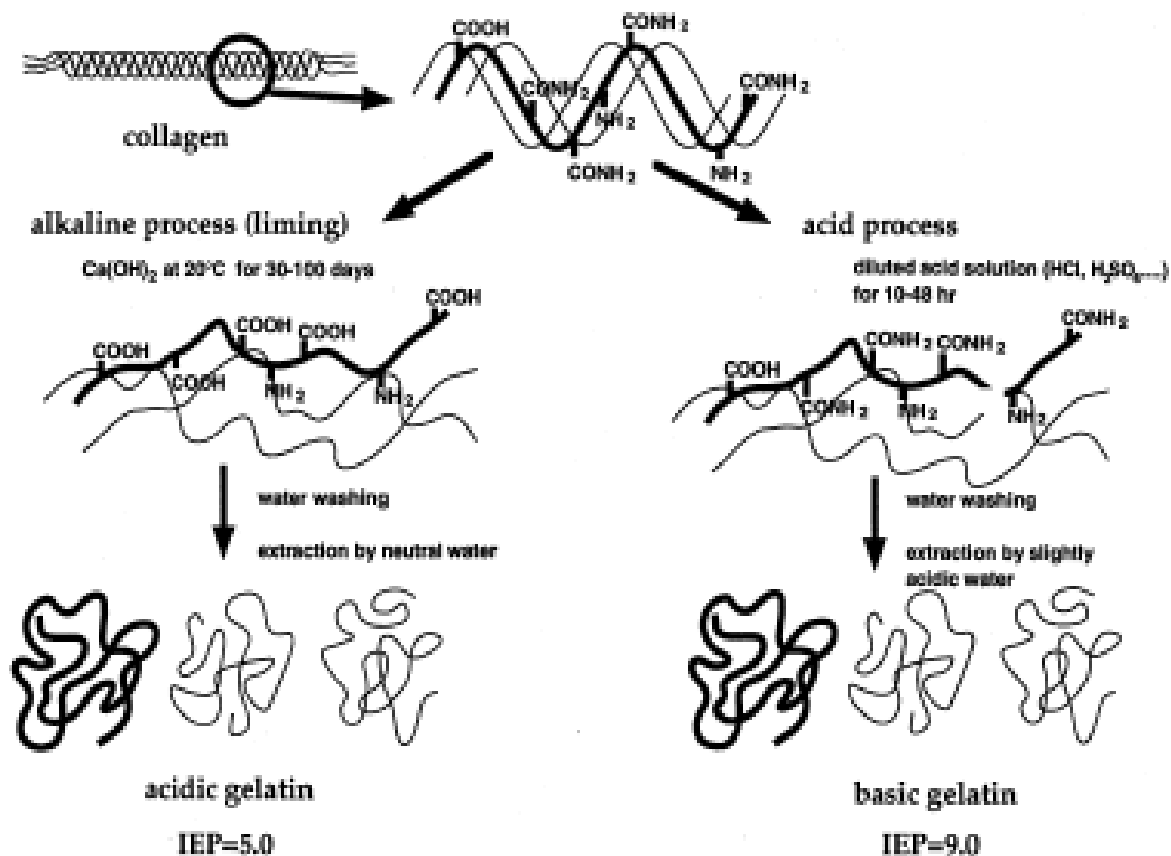


**Figure 2.5** Preparation processes for acidic and basic gelatins from collagen  
(Tabata and Ikada, 1998)

**Table 2.4** Typical specifications for gelatin

([http://www.gelatin-gmia.com/html/rawmaterials\\_app.html](http://www.gelatin-gmia.com/html/rawmaterials_app.html))

Properties	Type A	Type B
pH	3.8-5.5	5.0-7.5
Isoelectric Point	7.0-9.0	4.7-5.4
Viscosity (mps)	15-75	20-75
Ash (%)	0.3-2.0	0.5-2.0

### 3.3.3 Structure and composition of gelatin (Wahl and Czernuszka, 2006)

Gelatin is a denatured form of collagen. Gelatin has random coil structure which can be readily soluble in water. It contains many glycine (almost 1 in 3 residues, arranged every third residue), proline and 4-hydroxyproline (4-Hyp) residues. A typical structure is -Ala-Gly-Pro-Arg-Gly-Glu-4Hyp-Gly-Pro- as shown in Figure 2.6.

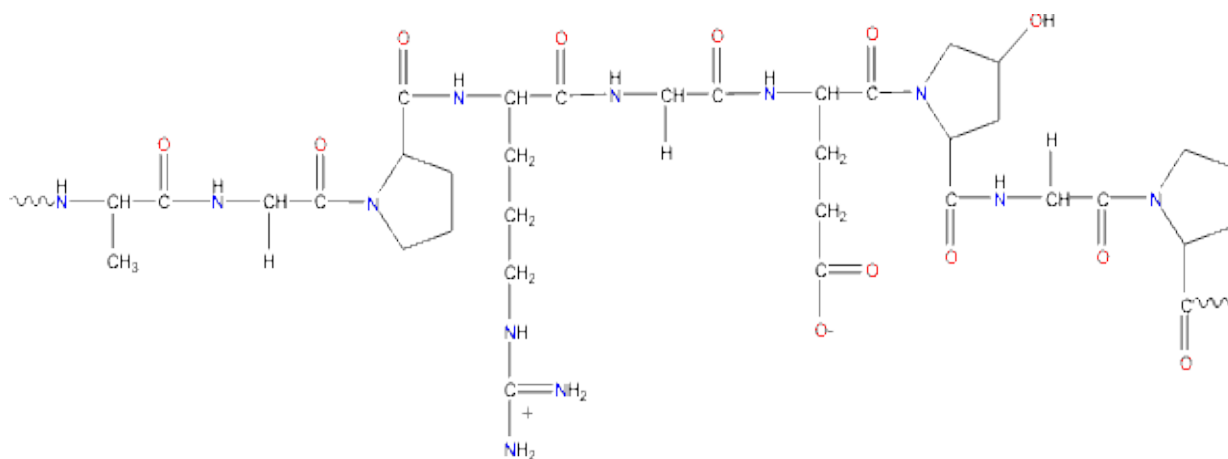


**Figure 2.6** Structure of the gelatin

([http://www.niroinc.com/food\\_chemical/spray\\_drying\\_gelatin.asp](http://www.niroinc.com/food_chemical/spray_drying_gelatin.asp))

Gelatin is a high molecular weight protein. Generally, gelatin contains 84-90% protein, 1-2% mineral salts and 8-15% water. It contains specific amounts of 18 different amino acids (Table 2.5). The molecular weight of these large protein structures typically ranges between 20,000-250,000 Dalton.

### 3.3.4 Applications of the gelatin

Gelatin is biocompatibility, biodegradability and non-immunogenicity. Therefore, it is suitable for biomedical applications such as vascular prosthetic sealants, wound dressing, tissue engineering scaffolds, and drug delivery system. They were modified to various forms including hard and soft capsule, hydrogel, or microsphere. In addition, it has been commonly used in pharmaceutical, photography and cosmetic manufacturing.

**Table 2.5** Amino acid compositions of gelatin

([http://www.gmap-gelatin.com/about\\_gelatin\\_comp.html](http://www.gmap-gelatin.com/about_gelatin_comp.html))

<b>Amino acid</b>	<b>%Weight</b>
Glycine	21.4
Proline	12.4
Hydroxyproline	11.9
Glutamic acid	10.0
Alanine	8.9
Arginine	7.8
Aspartic acid	6.0
Serine	3.6
Lycine	3.5
Leucine	3.3
Phenylalanine	2.4
Valine	2.2
Threonine	2.1
Isoleucine	1.5
Hydroxylysine	1.0
Histidine	0.8
Methionine	0.7
Tyrosine	0.5
Total	100.0

### 3.4 Chitosan (Jung et al., 2007)

#### 3.4.1 The nature of chitosan

Chitin is a biosynthetic polysaccharide that extracted from various animals and plants. Chitin is the abundant biopolymer mainly found in cell walls of some microorganisms such as fungi, yeast and in exoskeletons of invertebrates such as crustaceans, mollusks, crabs, shrimps, lobsters, squids and insects. Chitosan, a derivative of chitin, exists naturally only in a few species of fungi. Chitin and chitosan are copolymers consisting of 2-acetamido-2-deoxy- $\beta$ -D-glucose (N-acetyl-glucosamine) and 2-amino-2-deoxy- $\beta$ -D-glucose (N-glucosamine) as repeating units. The repeating units are randomly distributed throughout the biopolymer chains depending on the processing method used to derive the biopolymer. When the number of N-acetyl-glucosamine units is lower than 50%, the biopolymer is referred as chitosan. The term “degree of deacetylation (%DD)” is higher than 50%, it can be named as chitosan. In contrast, when the number of N-glucosamine units is lower than 50%, the term chitin is used (Figure 2.7).

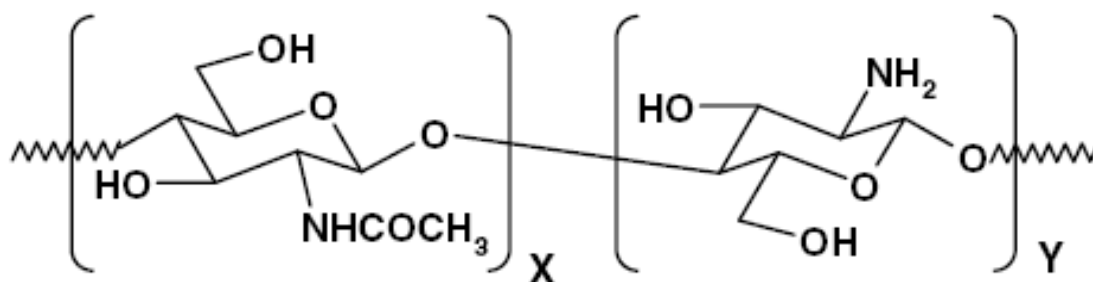


**Figure 2.7** Co-polymer structure of chitin (X) and chitosan (Y)

(Jung et al., 2007)

### 3.4.2 Preparation of chitin and chitosan

Chitosan is produced from shellfish waste by a multistage process. First the salt is washed out and the shellfish is shredded. The shredded shellfish is decalcified in dilute aqueous HCl solution and deproteinized in dilute aqueous NaOH solution. Then it is decolorized and dried to obtain chitin. Deacetylation in hot concentrated NaOH solution is used to convert the chitin into chitosan. The chitosan obtained is then neutralized and dried (Figure 2.8).

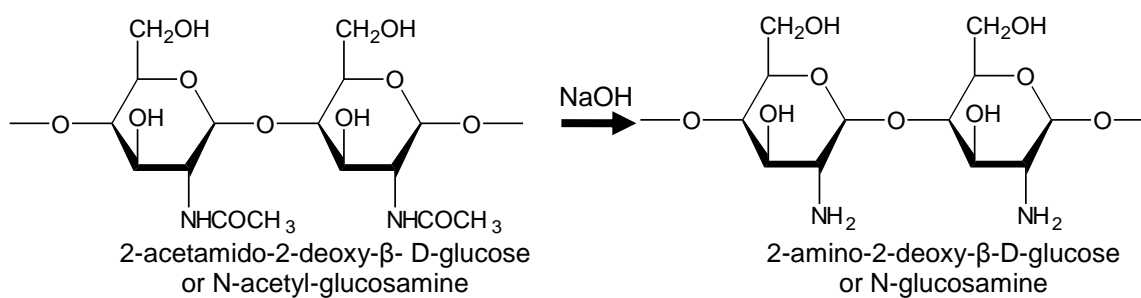


**Figure 2.8** The chitosan produced from deacetylation of chitin

(Jung et al., 2007)

### **3.4.3 Properties of chitosan**

The amino group in chitosan has a pKa of 6.5, thus, chitosan is positively charged and soluble in acidic to neutral solution with a charge density dependent on pH and %DD value. In other words, chitosan is bioadhesive and readily binds to negatively charged surfaces such as mucosal membranes.

There are two advantages of chitosan over chitin. Firstly, chitosan is readily dissolved in agents such as 1-10% (v/v) aqueous acetic acid whereas highly toxic co-solvents such as lithium chloride and dimethylacetamide (DMAc) must be used to dissolve chitin. The second advantage of chitosan is the presence of the free amino group that not only renders a polyelectrolytic effect to the polymer backbone, but also presents an active site upon which many chemical reactions may be applied.

Due to the solubility of chitosan in acidic solvent below pH 6, organic acid such as acetic, formic, and lactic acids are used for dissolving chitosan and most commonly used is 1% acetic acid solution (pH around 4.0). Solubility in inorganic acids is quite limited. At higher pH, precipitation or gelation will be occurred. Chitosan solution forms polycation complex with anionic hydrocolloid and provides gel.

Molecular weight and %DD of chitosan strongly affect on its properties such as solubility and biological properties. Furthermore, it was reported that %DD affected the hydrophilicity and biocompatibility of the chitosan while molecular weight affected degradation rate and the mechanical property.

### **3.4.4 Characteristics of chitosan for tissue engineering applications**

The uses of chitosan in biomedical applications have been of interest because of its advantages such as its biocompatibility, biodegradability, non-toxicity. It can extend into three-dimensional structures and has many biofunctionalities (such as antithrombogenic, hemostatic, acceleration of wound healing, antimicrobial activity).

### 3.5 Chitooligosaccharide

Chitosan is a polysaccharide having high molecular weight and insoluble at neutral pH, therefore its use is sometimes limited, especially in human body. This problem can be overcome by water-soluble chitosan called chitooligosaccharide (COS) as shown in Figure 2.9.

Chitooligosaccharide can be synthesized from chitosan by several techniques such as enzymatic, acid or free radical hydrolysis. COS is then a saccharide which composed of 2-8  $\beta$ -(1, 4)-D-glucosamine repeating units with a structure of chitosan characteristic. Structure of COS is excellent absorption and water soluble. It plays a principal role in a variety of application, for example, immune enhancement, anti-cancer function, anti-bacterial function, suppressive function for blood sugar increase, cholesterol control effect, calcium absorption acceleration effect and improvement effect of liver function.

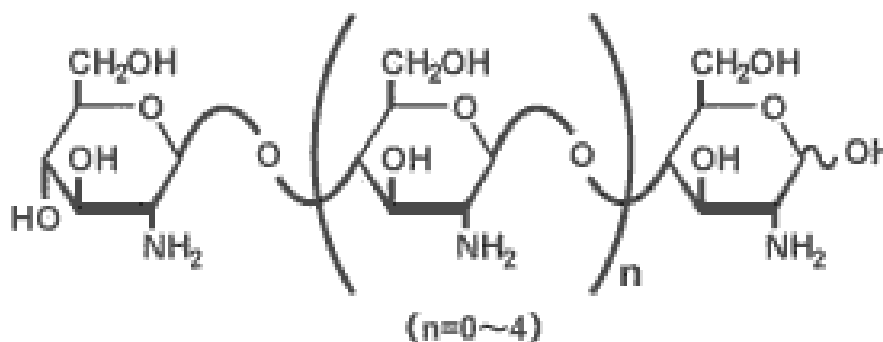


**Figure 2.9** The structure of chitooligosaccharide  
([http://www.yskf.jp/yskf\\_en/yskf\\_en\\_03\\_06.html](http://www.yskf.jp/yskf_en/yskf_en_03_06.html))



## 4. Mesenchymal Stem Cells

Mesenchymal stem cells are found in all multi-cellular organisms and defined by two properties as follows:

- (1) Self-renewal: the ability to go through numerous cycles of cell division while maintaining the undifferentiated state.
- (2) Potency: the capacity to differentiate into specialized cell types yielding an organized tissue.

### 4.1 Sources of mesenchymal stem cells

Within bone marrow, there are two main types of stem cells, namely hematopoietic stem cells (HSCs) and mesenchymal stem cells (MSCs). Hematopoietic stem cells include both lymphoid and myeloid lineages that finally produce blood circulating cells and organ resident cells of the immune response. Mesenchymal stem cells are defined as self-renewal, multipotent progenitor cells with the capacity to differentiate into tissues of mesodermal origin (adipoblasts, osteoblasts, chondroblasts, tenoblasts, myoblasts and stromal cells, as shown in Figure 2.10). Tissues of ectodermal origin (neurons), and tissues of endodermal origin (hepatocytes). Sources of mesenchymal stem cells are bone marrow, fat, hair follicles, periodontal ligament, thymus, spleen, placenta, and umbilical cord blood.

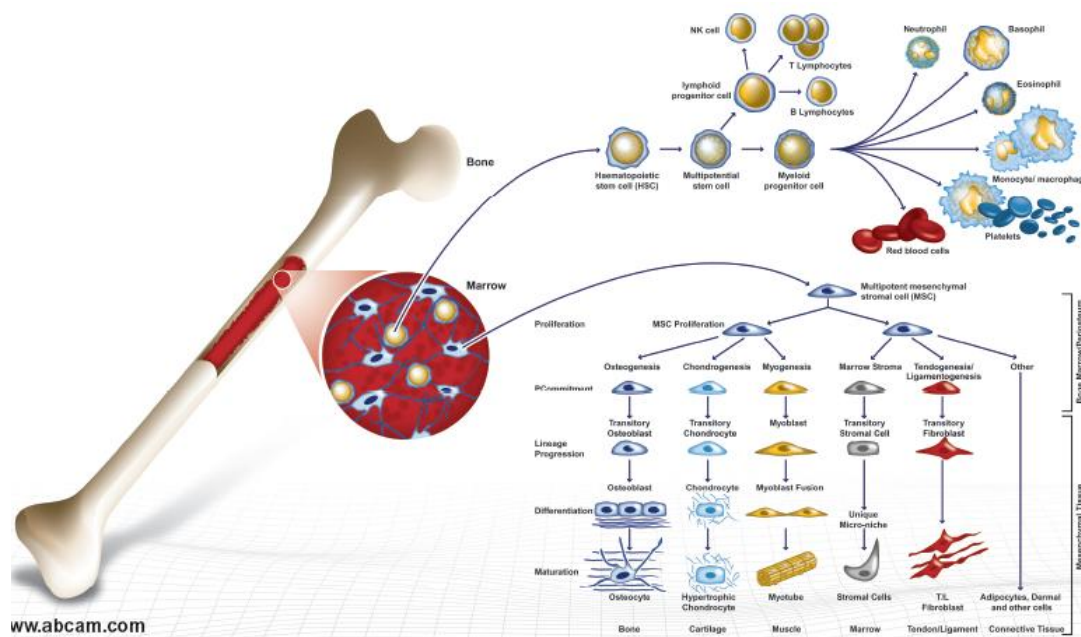


**Figure 2.10** The MSCs capacity to differentiate into tissues of mesodermal origins (Murugan and Ramakrishna, 2005)

## 4.2 Phenotype and characteristics of mesenchymal stem cells

When stem cells are isolated and cultured *in vitro*, the adherent population indicating mesenchymal stem cells tends to form colonies of spindle-shaped cells (fibroblast-like) termed as colony forming unit-fibroblast (CFU-F). The CFU-F property is frequently used when studying the proliferative capacity of mesenchymal stem cells in culture.

Initially, the cultured fibroblast-like cells are observed to be alkaline phosphatase-positive, collagen IV-positive and fibronectin-positive. In addition, collagen type I and laminin of the basement membrane are found in the extracellular matrix surrounding the cultured mesenchymal stem cells. A wide range of cell surface antigens such as CD73, CD105 as well as other adhesion molecules and growth factor/ cytokine receptors including CD29, CD90, CD117, CD166, CD54, CD102, CD121a, CD121b, CD123, CD124, and CD49 have been targeted in these initial mesenchymal stem cell populations using a wide panel of antibodies, as presented in Table 2.6.

**Table 2.6** Type of Mesenchymal stem cell surface markers

Types of markers	Characteristics
Specific antigens	SH2, SH3, SH4, STRO-1, $\alpha$ -smooth muscle actin, MAB1740
Extracellular matrix	Collagen type I, III, IV, V, VI, proteoglycans, fibronectin, hyaluronan, laminin
Growth factor & cytokines	Interleukins: $\alpha$ 1, 6, 7, 8, 11, 12, 14, and 15 LIF, SCF, Flt-3 ligand, GM-CSF, G-CSF, M-CSF
Growth factor & cytokine Receptors	IL-1R, IL-3R, IL-4R, IL-6R, IL-7R, PDGFR, TNF-IR, TNF-IIR, TGF $\beta$ - IR, TGF $\beta$ - IIR, IFN- $\gamma$ R, 6FGFR, EGFR, LIFR, G-CSFR, S-CFR, transferrin
Adhesion molecules	Integrins: $\alpha$ v $\beta$ 3, $\alpha$ v $\beta$ 5 Integrin chains: $\alpha$ 1, $\alpha$ 2, $\alpha$ 3, $\alpha$ 4, $\alpha$ 5, $\alpha$ v, $\beta$ 1, $\beta$ 3, $\beta$ 4 ICAM-1, ICAM-2, VCAM-1, ALCAM-1, LFA-3, L-selectin, endoglin, CD44

### 4.3 Growth and differentiation of mesenchymal stem cells

MSCs and colony forming unit-fibroblastic (CFU-F) can be induced *in vitro* to expand and differentiate into the osteoblastic lineage using dexamethasone, ascorbic acid, and  $\beta$ -glycerophosphate. Under this condition the cells undergo the following sequences: (1) proliferation, (2) differentiation, and (3) maturation. Growth or proliferation is marked by many-fold increase in cell number. Synthesis of collagen I and alkaline phosphatase indicate osteogenic differentiation. Maturation is noticed by formation of multilayer nodules, secretion of osteocalcin, and mineralization of the extracellular matrix (ECM).

During embryogenesis, bone tissues are formed through two distinct pathways: intramembranous ossification and endochondral ossification (Lanza and Vacanti, 2007). In the case of intra-membranous ossification, osteoblasts differentiate directly from mesenchymal cell condensations, whereas in the case of endochondral ossification, the condensed mesenchymal cells differentiate into chondrocytes and form a cartilaginous template. Then the surrounding mesenchymal cells immediately differentiate into osteoblasts after maturation of hypertrophic chondrocytes in the template suggesting that osteoblasts and chondrocytes are derived from a common progenitor cells (Figure 2.11). Furthermore, it is well known that osteoblasts, chondrocytes, adipocytes, myoblasts, tendon cells, and fibroblasts differentiate from the common precursor of bone marrow mesenchymal stem cells (Komori et al., 2006). The lineages are determined by different transcription factors. The transcription factors Runx2 and Osterix regulate osteoblast differentiation, Sox family proteins (Sox9, Sox5 and Sox6) regulate chondrocyte differentiation, MyoD transcription factors (MyoD, Myf5 and Myogenin) regulate myogenic differentiation, and PPAR- $\gamma$  transcription factors regulate adipocyte differentiation. Runx2 first directs multipotent mesenchymal cells to a preosteoblastic state, after which Osterix and Runx2 together convert the cells into mature osteoblasts (Jimi et al., 2010).

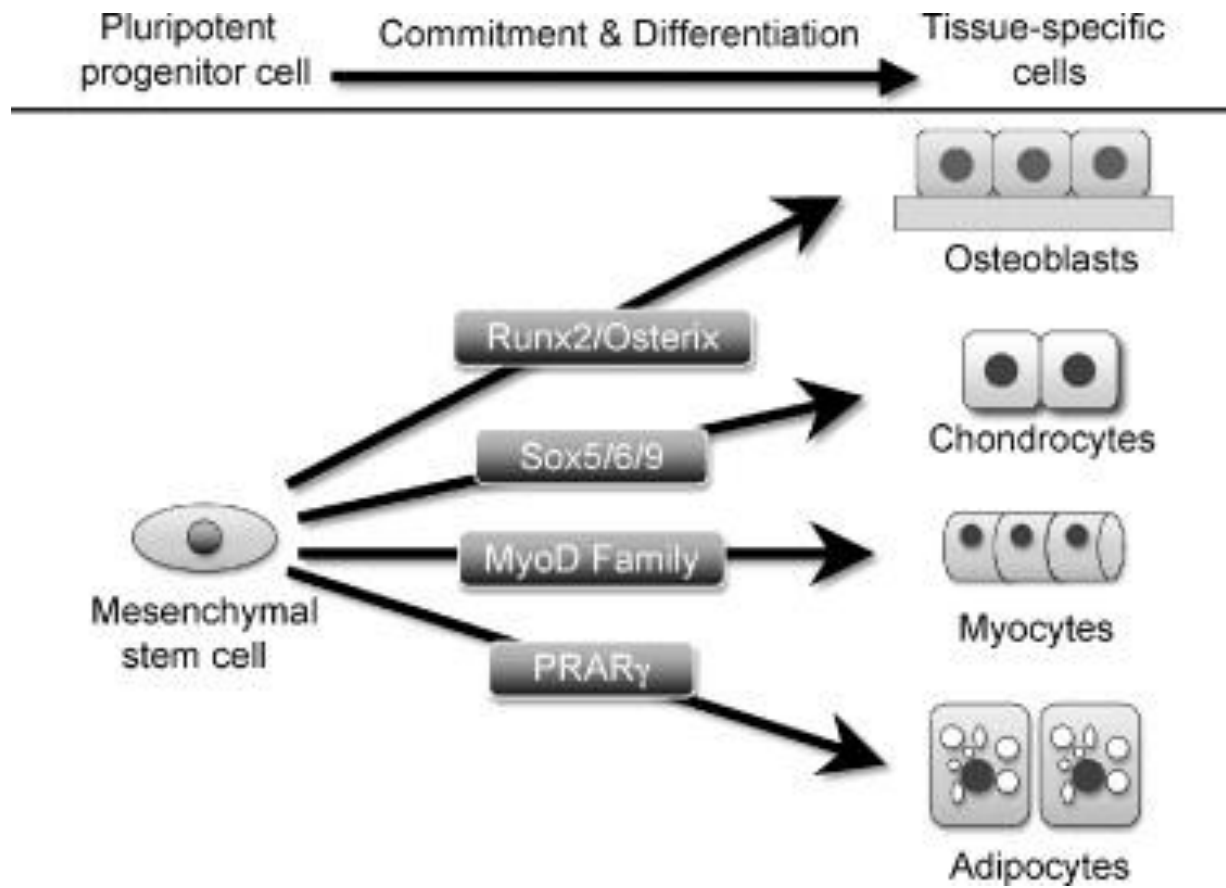


**Figure 2.11** Schematic model for differentiation of a mesenchymal stem cell into tissue specific cells by specific transcription factors. (Jimi et al., 2010)

## 5. Fabrication technique of the scaffolds

Fabrication techniques are important factors that present many challenges in obtaining specific physical and biological properties of the scaffolds, including high porosity, surface area, structural strength, and specific three-dimensional shapes. These characteristics are determined by the scaffold fabrication technique, which must be developed such that it does not adversely affect the biocompatibility of the construct material.

The major requirement of any proposed polymer processing technique is not only the utilization of biocompatible materials but the process should not affect the biocompatibility of the polymer. The processing technique should also allow the manufacture of scaffolds with controlled porosity and pore size. A highly porous scaffold is desirable to allow cell seeding or migration throughout the material. Pore size plays a critical role in both tissue ingrowth and the internal surface area available for cell attachment. A large surface area is required so that a high number of cells, sufficient to replace or restore organ function, can be cultured.

The mechanical properties of the scaffold are often of critical importance especially when regenerating hard tissue like bone and cartilage. Although the properties of the solid polymer and the porosity of the scaffold have a profound effect on its mechanical properties, polymer processing can also be influential in this respect. The shape of a hard tissue is often important to its function and in such cases the processing technique must allow the preparation of scaffold with irregular three dimensional geometries.

The techniques used to manufacture scaffolds for tissue engineering is dependent on the properties of the polymer and its intended application. These include solvent casting and particulate leaching, gas leaching, gas foaming, fiber meshes/fiber bonding, phase separation, melt molding, emulsion freeze-drying, and freeze-drying.

### 5.1 Freeze-drying technique

One method to fabricate polymer scaffolds with variable porosity and pore size utilizes a freeze drying process. Freeze drying or lyophilization is an ideal method of preserving products, and active ingredients such as proteins, enzymes, microorganisms, chemical and natural products. Freeze drying is the only way that water can be successfully removed from an organic substance or material without damaging the cell structure and losing of volatile components.

The first step in lyophilization is to convert the product into a frozen state. It is important that during the freezing process, the solvent or water is crystallized. The formation of ice crystals results in a separation of the solutes and the solvent. The concentration of the solvent is generally greater than that of the solutes, the formation of ice forces the solutes into a region between the crystals known as the interstitial. Thus the second function of the freezing process is to cause a separation of the solutes and the solvent.

The second step is sublimation. Once frozen, the product is placed under vacuum and gradually heated without melting the product. This process, called sublimation, transforms the ice directly into water vapor, without first passing through the liquid state. Because the process of sublimation occurred at atmospheric pressures is quite slow, we can increase the sublimation rate by decreasing the pressure above the ice surface. This is accomplished by placing the frozen material into a chamber and removing the gases to create a vacuum. The water vapor given off by the product in the sublimation phase condenses as ice on a collection trap, known as condenser, within the vacuum chamber of the lyophilizer. The lyophilized product should contain 3% or less of its original moisture content and should be properly sealed. The result of these two steps is the porous scaffold. Pore size, porosity, and interconnected pore of this scaffold depend on concentration of solution and freezing rate.

## **5.2 Cross-linking technique**

To enhance mechanical property and decrease biodegradation rate, the scaffolds have to be cross-linked. Cross-linking can be done by various methods such as chemical treatment, dehydrothermal treatment, ultraviolet irradiation, and electron beam irradiation. Two widely used methods described here are chemical and dehydrothermal cross-linking.

### **5.2.1 Chemical cross-linking**

Among chemical cross-linking agents used, glutaraldehyde is the most widely used due to its high efficiency in the stabilization of collagenous materials. Cross-linking of collagenous samples with glutaraldehyde involves the reaction of free amino groups of lysine or hydroxylysine residues of polypeptide chains with the aldehyde groups of glutaraldehyde. It is likely that glutaraldehyde can crosslink between two amino residues of collagen chains. Moreover, other chemical such as formaldehyde and 1-ethyl-3-(3-dimethyl aminopropyl)carbodiimide (EDC) are mostly found as the cross-linking agents. The disadvantage of chemical cross-linking is that some chemical agents, which are toxic to cells, can be left over in the scaffold and can cause the irritation to patients when using the scaffolds as the skin substitutes.

### **5.2.2 Dehydrothermal cross-linking**

The scaffold can be cross-linked by the method of dehydrothermal (DHT) treatment in a vacuum oven at temperature above 100°C. Dehydrothermal treatment generates chemical bonding between the amino acid and carboxyl groups of collagen molecules due to thermal dehydration. Dehydrothermal cross-linking can occur only if the amino acid carboxyl groups are close to each other. Thus, it is believed that dehydrothermal treatment allows scaffolds to crosslink to a less extent than chemical treatment.

## 6. Related researches

### 6.1 Mesenchymal stem cell for tissue engineering

Zhang et al. (2006) studied on a tissue-engineered bone using rhBMP-2 induced periosteal cells with a porous nano-hydroxyapatite/collagen/poly(L-lactic acid) scaffold. In this study, the cell-scaffold construct was cultured *in vitro* for 2 weeks, followed by subcutaneous implantation in nude mice. The assessments of the cell viability and osteoinductive capability were performed both *in vitro* and *in vivo* to determine the osteoinductive potential of cell-scaffold construct for bone repair. The results of scanning electron microscopy suggested that the scaffold supported adhesion and proliferation of periosteal cells. New bone formation was observed only in experimental groups with cell transplants 8 weeks post-implantation. The animals of the control groups did not show bone formation. The results strongly support the approach of the transplantation of rhBMP-2 induced periosteal cells within a suitable carrier structure for bone regeneration.

### 6.2 Demineralized bone matrix for bone tissue engineering

Walsh (1995) studied the organic matrix remaining after removal of the mineral phase by chelation with EDTA or solubilized in HCl as a template for mineral deposition and the production of mineral organic composites. Different pH conditions were employed to alter the inorganic phase which was deposited within the organic matrix. The results shown that EDTA and HCl were completely demineralized the mineral phase from the composite. HCl demineralization resulted in an increase in strain and energy at peak load compared to EDTA demineralized samples. SEM and elemental analysis confirmed complete demineralization of the samples with HCl and EDTA and smooth collagen.

Piattelli (1996) studied and compared bone regeneration processes between mineralized freeze-dried bone allografts (FDBA) and demineralized freeze-dried bone allografts (DFDBA) as substitutes for autologous bone in oral surgery. The demineralization process has been shown to determine osteoinduction. The histological results showed that the DFDBA particles near the host bone were involved in the mineralization processes, while the FDBA particles that were farthest from the host bone were lined by osteoblasts, actively secreting osteoid matrix and newly formed bone. These results demonstrate the highly osteoconductive effect of FDBA.



Mizuno (1996) showed that implantation of demineralized bone powder (DBP) into muscle for stimulating chondrogenesis and inducing ectopic bone formation. They designed 3D collagen sponge for packing density of DBP implants. The DBP packed between two layers of a porous collagen was used to assess the chondroblastic differentiation of human dermal fibroblasts. Human dermal fibroblasts were seeded onto the composite sponge, migrated through the collagen into the packet of DBP and deposited extracellular matrix amongst the particles of DBP.

Mauney (2004) investigated the human bone marrow mesenchymal stem cells (BMSCs) that cultured on 3D partially demineralized bone (DMB) scaffolds in bioreactor. They prepared partially DMB scaffolds from the femoral condyles of bovine cancellous bone. The residual cleaned sample was sectioned and partially demineralized in 0.6 N HCl. After cultivation of DMB-treated cells for 16 days, they found that DMB promoted osteogenic differentiation of BMSCs and induced high levels of alkaline phosphatase activity, bone-specific protein transcript levels (alkaline phosphatase and osteopontin), and mineralized matrix production of BMSCs.

Zhou (2005) showed that demineralized bone powder (DBP) promoted chondrogenesis or osteogenesis of hMSCs in 3D collagen sponge culture. They prepared porous 3D collagen sponges from pepsin-digested bovine collagen and fabricated by lyophilization. Bilaminar collagen sponges were inserted with DBP between the two layers. And then sponges were transferred to seeding chambers. They found that DBP noticeably enhanced chondrogenesis of hMSCs in 3D sponges for 21 days and stimulated expression of chondrocyte-specific genes aggrecan, COL II, and COL X. Moreover, DBP induced hMSCs to express osteoblastic gene markers such as ALP and osteocalcin.

### 6.3 Gelatin for bone tissue engineering

Takahashi (2005) studied the osteogenic differentiation of MSCs in gelatin-based biodegradable sponges. In this study, gelatin sponges and  $\beta$ -tricalcium phosphate ( $\beta$ -TCP) were prepared by chemical crosslinking of gelatin with glutaraldehyde in the presence of  $\beta$ -TCP. The obtained scaffolds showed the average pore size of 180–200  $\mu$ m and well distribution of  $\beta$ -TCP.  $\beta$ -TCP composition play significant role in cell attachment, proliferation, and osteogenic differentiation of MSCs. Furthermore,  $\beta$ -TCP at 50 wt% showed the best results on cell attachment, proliferation, and osteogenic differentiation (Takahashi et al., 2005a).

Takahashi (2005) fabricated biodegradable gelatin sponges at different contents of  $\beta$ -TCP to allow BMP-2 to incorporate into them. They revealed that BMP-2 was released *in vivo* at a similar time profile, irrespective of the  $\beta$ -TCP content. The *in vivo* time period of BMP-2 retention was longer than 28 days. The osteoinductivity of gelatin or gelatin- $\beta$ -TCP sponges incorporating BMP-2 was studied following the implantation into the back subcutis of rats in terms of histological and biochemical examinations. The extent of bone formation was higher in the sponges with the lower contents of  $\beta$ -TCP. On the other hand, the level of alkaline phosphatase activity and osteocalcin content at the implanted sites of sponges decreased with an increase in the content of  $\beta$ -TCP. The gelatin sponge exhibited significantly higher osteoinduction activity than other gelatin- $\beta$ -TCP sponges. In addition, the *in vitro* collagenase digestion experiments revealed that the gelatin- $\beta$ -TCP sponge collapsed easier than the gelatin sponge without  $\beta$ -TCP incorporation. These results suggest that the maintenance of the intrasponge space is necessary for the osteoinduction and is one factor contributing to the osteoinduction extent of BMP-2-incorporating sponges (Takahashi et al., 2005b).

#### **6.4 Chitosan and other polymer scaffolds for bone tissue engineering**

Zhao (2002) prepared biodegradable hydroxyapatite/chitosan-gelatin (HA/CS-Gel) composite scaffold by phase separation method. The HA granules were dispersed uniformly in the organic network via pulverizing and ultrasonically treating commercial available HA particles. The rat osteoblasts were used to examine the proliferation and functions in the scaffolds. They found that collagen I and proteoglycan-like substrate were synthesized, while osteoid and bone-like tissue formed during the culture period. Furthermore, the cell/scaffold constructs had good biomineralization effect after 3 weeks in culture.

Zhao (2006) compared the effects of human mesenchymal stem cells (hMSCs) cultured on two types of composite materials, chitosan–gelatin (CG) and hydroxyapatite/chitosan–gelatin (HCG), and examined the hMSC adhesion and three-dimensional construct development. They found that HA promoted protein and calcium ion adsorption of the 3D porous scaffolds in the complete tissue culture media. Moreover, hMSCs exhibited higher initial cell adhesion efficiency to 2D HCG membranes and maintained higher proliferation rates in the 3D HCG than CG scaffolds over a 35-day period. Differentiation assays indicated that the 3D HCG scaffolds have higher alkaline phosphate activity upon osteogenic induction than CG scaffolds. These findings suggest high osteogenic differentiation potential of HCG scaffold.

Peng (2006) prepared porous chitosan/collagen (CS/COL) scaffolds by freezing and lyophilization methods. They investigated morphology and distribution of human periodontal ligament cells (PDLCs) on the scaffolds compared to a single component scaffold. The addition of collagen to chitosan increased the swelling ability and decreased the contraction. The adherence and growth of PDLCs cultured within the CS/COL scaffolds were better than that within either CS or COL scaffolds alone.

Jung (2007) evaluated the effect of chitosan with absorbable collagen sponge (ACS) carrier on bone formation in the rat calvarial defect model. These results showed that new bone area and defect closed to the chitosan/ACS group were significantly greater than those of the others at 8 weeks postsurgery. Chitosan reconstituted with ACS has significant potential to induce the regeneration of bone in rat calvarial critical size defects.

Arpornmaeklong (2007) investigated the microstructure and biocompatibility of CS/COL composite scaffolds. Mouse pre-osteoblast, MC3T3-E1, was cultivated on the sponges in osteogenic condition medium for 21 days. They found that the combination of CS/COL matrices created a well defined porous microstructure and biocompatible scaffolds.

CS/COL composite sponges promoted growth and differentiation of osteoblasts into the mature stage.

Arpornmaeklong (2008) investigated the effects of a combined chitosan and collagen (CS/COL) scaffolds on osteogenic differentiation of rat-bone marrow stem cells (BMSCs). The scaffolds were fabricated via freeze-drying. They found that the expression of ALP and osteocalcin on CS/COL composite scaffolds were greater than that on chitosan alone. Moreover, CS/COL scaffolds showed a higher resistance to enzymatic degradation and collagen scaffolds. CS/COL scaffolds demonstrated higher compressive strength than collagen alone. Therefore, combined CS/COL scaffolds promoted osteoblastic differentiation of BMSCs and improved the mechanical and physical properties of the scaffolds.

She (2008) fabricated 3D porous silk fibroin/chitosan (SFCS) scaffolds with freeze-drying method. They investigated *in vitro* degradation behaviors of SFCS scaffolds for 8 weeks in phosphate buffer saline (PBS) solution at 37°C. SFCS scaffolds maintained its porous structure until 6 weeks of degradation. The scaffolds were degraded much more rapidly during the first 2 weeks, and the weight loss reached 19.28 wt% after 8 weeks of degradation. The degradation process affects little SFCS scaffolds' swelling properties.

Xianmiao (2009) prepared nano-hydroxyapatite (n-HA)/chitosan (CS) composite membranes by solvent casting and evaporation methods for study the function of bone regeneration. The results showed that the surface roughness and micropores of the composite membranes increased with the rise of n-HA content. They are suitable for adhesion, and proliferation of cells. The n-HA content and solvent evaporation temperature have influence on the swelling ratio, tensile strength and elongation rate of the composite membranes. n-HA and its content can affect the proliferation of cells. The n-HA/CS composite membranes have no negative effect on the cell morphology, and possess good biocompatibility.

Peter (2010) prepared chitosan–gelatin/nanophase hydroxyapatite (CG/nHA) composite scaffolds by blending chitosan and gelatin with nanophase hydroxyapatite. The composite scaffolds were highly porous with a pore size of 150–300 µm. They showed good swelling character, which could be modulated by varying ratio of chitosan and gelatin. The composite scaffolds in the presence of nHA showed a decreased degradation rate and increased mineralization. The nanocomposite scaffolds could be improved MG-63 cell attachment, proliferation in comparison with chitosan–gelatin (CG) scaffold.

### **6.5 Chitooligosaccharide for tissue engineering**

Ohara (2004) analyzed gene expression of osteoblasts cultured with water-soluble and low molecular chitooligosaccharide (COS). They cultured osteoblastic cell line in  $\alpha$ -MEM supplemented with 10% FBS and 0.005% COS for 3 days. They found that ALP activity was significantly high compared with the control culture group. Human 1.0<sup>®</sup> cDNA microarray analysis revealed that 16 genes were expressed at  $\geq 1.5$ -fold higher signal ratio levels in the experimental group compared with the control group after 3 days. Furthermore, the expression of mRNAs for BMP-2 slightly increased after 7 days of culture with COS. These results suggest that a super-low concentration of COS could modulate the activity of osteoblasts through mRNA levels and the genes concerning cell proliferation and differentiation can be controlled by water-soluble COS.

Ratanavaraporn (2009) studied the physical and biological characteristics of very low molecular weight chitooligosaccharide (COS, 1.4 kDa) film that prepared from high molecular weight chitosan (1,000 kDa) via free radical degradation process. The results showed that COS film presented more hydrophilic property than chitosan film. The number of mesenchymal stem cells proliferated on COS film was higher than that on chitosan film. In addition, COS film enhanced osteogenic differentiation potential of MSCs, as observed in the alkaline phosphatase activity assay and calcium deposition assay.

## **6.6 Bone tissue engineering in animal model**

Bayat (2010) compared the quantity and quality of osseous healing of bone matrix gelatin (BMG) with autogenous bone graft (ABG) in cat models. Osseous defects (5x5 mm) were made through upper alveolar bone distal to the canines in the left and right quadrants (maxilla) in each of 12 Persian male cats and filled randomly with BMG and ABG. The repair response was examined on days 14, 28, and 56 after surgery (n = 4 per bone substitute per time point). Qualitative histological and quantitative histometric analysis including percentage of new formed bone fill (BF) and density were done. The inter-treatment comparison of mean levels of BF at specific time points showed consistently greater levels within BMG treated defects and reached significance on days 14, 28, and 56. On day 56, BF was significantly higher within BMG group. Intra-treatment evaluation of bone formation in each group showed that BD significantly increased during treatment, and BF in BMG group reached significance at every time point but in ABG group only increase from day 28 to 56 reached significance. The results support the use of BMG to treat bone defects.

Kohles (2000) developed demineralized freeze-dried bone allografts (DFDBA) combined with collagen for used as an effective filling material. They evaluated the regenerative healing response of five allograft mixtures via the morphology of filled, periodontal defects. Critical size mandibular and maxillary osseous defects were surgically created in six adult baboons. The filling response of four combinations of DFDBA and tendon collagen was compared with an all collagen graft after 3 months of implantation. The overall results indicated that all combinations of DFDBA and collagen provided a better filling response than the all collagen matrix. All of the combinations were similar with 60:40 of collagen to DFDBA mass ratio resulting in the largest defect filling response.

# CHAPTER III

## MATERIALS & METHODS

### 1. Raw materials, Chemicals & Reagents

#### 1.1 Raw materials

1. Bovine Achilles tendon type I collagen powder (Sigma-Aldrich, USA)
2. Type A gelatin powder (pI 9, Nitta Gelatin Inc., Japan)
3. Alaska crab chitooligosaccharide (MW 2,000 Da, Hangzhou, China)

#### 1.2 Chemicals & Reagents

1. Agarose molecular biology grade (Sigma, USA)
2. Alcian blue
3. 2-amino-2-methyl-1-propanol (Sigma-Aldrich, USA)
4. L-ascorbic acid ( $C_6H_8O_6$ , MW 176.12 g/mol)
5. BisBenzimide fluorescent dye (Hoechst 33258)
6. Bovine serum albumin (Sigma-Aldrich Co., USA)
7. Brij35 (Sigma-Aldrich, USA)
8. Calcium carbonate ( $CaCO_3$ , Analar, England)
9. *o*-Cresolphthalein (OCPC,  $C_{22}H_{18}O_4$ , MW 346.38 g/mol)
10. Type I collagenase (Sigma-Aldrich Co., USA)
11. Dexamethasone ( $C_{22}H_{29}FO_5$ , MW 392.46 g/mol)
12. Dulbecco's modified eagle medium (DMEM, Hyclone, USA)
13. Ethanol (99.7-100%, VWR International Ltd., UK)
14. Ethanolamine ( $NH_2CH_2CH_2OH$ , MW 61.08 g/mol)
15. Ethidium bromide (Sigma Aldrich, USA)
16. Fetal bovine serum (FBS, Hyclone, USA)
17. Formalin solution (HCHO and  $CH_3OH$  in water, MW 30.03 g/mol)
18. Glacial acetic acid ( $CH_3COOH$ , MW 60.05 g/mol)
19. Glutaraldehyde solution (25% v/v, MW 100.12 g/mol)
20.  $\beta$ -glycerol phosphate ( $C_3H_7Na_2O_6P \cdot 5H_2O$ , MW 306.11 g/mol)
21. Glycine ( $C_2H_5NO_2$ , MW 75.07 g/mol)

22. Hydrochloric acid (Merck, USA)
23. Hydrogen peroxide ( $\text{H}_2\text{O}_2$ , MW 18.016 g/mol)
24. Insulin ( $\text{C}_{254}\text{H}_{377}\text{N}_{65}\text{O}_{75}\text{S}_6$ , MW 5733.49 g/mol)
25.  $\beta$ -Mercaptoethanol (Sigma-Aldrich, USA)
26. Alpha- minimal essential medium ( $\alpha$ -MEM, Hyclone, USA)
27. Dimethylsulfoxide (DMSO, Sigma-Aldrich, Germany)
28. MTT [3-(4,5-dimethylthiazol-2-yl)-2,5-diphenyltetrazolium bromide]
29. 2,4,6-trinitrobenzene sulfonic acid (TNBS,  $\text{C}_6\text{H}_3\text{N}_3\text{O}_9\text{S}$ , MW 293.17 g/mol)
30. *p*-nitrophenyl phosphate liquid substrate (Sigma Aldrich, USA)
31. *p*-nitrophenol (Sigma Aldrich, USA)
32. Oil red O ( $\text{C}_{26}\text{H}_{24}\text{N}_4\text{O}$ , MW 408.49 g/mol)
33. PCR marker (Bio-Rad, USA)
34. Penicillin/Streptomycin antibiotic (100 U/ml, Hyclone, USA)
35. Phosphate buffer saline (PBS, pH 7.4, Hyclone, USA)
36. Povidone betadine
37. Isopropyl alcohol ( $\text{CH}_3(\text{CH}_2)_2\text{OH}$ , MW 60.1 g/mol)
38. Sodium Azide (Labchem, APS, Austraria)
39. Silk suture (Dacron 4-0)
40. Silver nitrate ( $\text{AgNO}_3$ , MW 169.87 g/mol)
41. Sodium citrate ( $\text{HOC}(\text{COONa})(\text{CH}_2\text{COONa})_2 \cdot 2\text{H}_2\text{O}$ , MW 294.10 g/mol)
42. Sodium chloride ( $\text{NaCl}$ , MW 58.44 g/mol)
43. Sodium dodecylsulfate (SDS,  $\text{C}_{12}\text{H}_{25}\text{OSO}_3\text{Na}$ , MW 288.38 g/mol)
44. Sodium hydrogen carbonate ( $\text{NaHCO}_3$ , MW 84.01 g/mol)
45. Sodium hydroxide ( $\text{NaOH}$ , Analar, England)
46. Sulfuric acid ( $\text{H}_2\text{SO}_4$ , MW 98.08 g/mol)
47. Thiopental sodium
48. Transferrin
49. Tryphan blue (0.4%, Sigma-Aldrich, Germany)
50. Trypsin-EDTA (0.25% trypsin with EDTA.4Na, Hyclone, USA)
51. Triton X 100 (Sigma, USA)
52. Tween-20 (Sigma-Aldrich Co., USA)



### 1.3 Equipments

1. Auto-pipettes (10, 100, 1000, 5000  $\mu$ l)
2. Beaker
3. Cell culture flask : T25, T75 (Falcon, USA)
4. Centrifuge (Eppendorf, USA)
5. Centrifugal tubes (Corning, USA)
6. CO<sub>2</sub> incubator (Forma Scientific, England)
7. Cryovial tube
8. Cuvette
9. Cylinder
10. Digital balance
11. Digital timer
12. Disposable gloves
13. DNA Thermal cycler (Thermo Hybaid, USA)
14. Energy-dispersive X-ray spectroscopy (EDX, Philip Model XP 30 CP)
15. Electrophoresis chamber set (BIO-RAD, USA)
16. Erlenmeyer Flask
17. Flow cytometer (BD Dickinson, USA)
18. Forceps, operation blade
19. Fourier transform infrared spectroscopy (FT-IR, Spectrum GX, Perkin Elmer, UK)
20. Freezer (-80°C, Forma Scientific, USA)
21. Gel Doc analyzer (BIO-RAD, USA)
22. Gel permeation chromatography (GPC, PL-GPC 110, Polymer laboratories, Shropshire SY6 6AX, UK)
23. Glass slip (15 mm in diameter, Matsunami, Japan)
24. Homogenizer (T 25 digital, Ultra-turrex, Ika Co., Germany)
25. Laminar flow hood (Gelman Science)
26. Lint-freed paper (Kimwipe, USA)
27. Lyophilizer (Heto, PowerDry LL3000, USA)
28. Microplate reader
29. Microcentrifuge
30. Micro centrifuge tube 0.2 ml, 0.5 ml, 1.5 ml (BIO-RAD, USA)
31. Multi-channel pipette

32. Orbital shaker
33. Parafilm (American National Can, USA)
34. Phase-contrast microscope (IX70, Olympus Optical Co., Japan)
35. pH meter (Eutech Cybernataics)
36. Sanitary tissue paper (Celox, Thailand)
37. Scanning electron microscopy (SEM, Jeol JSM 5400)
38. Spectrophotometer (Versa Max, Molecular Device Japan Co., Japan)
39. Syringe with 18-gauge needle (Corning, USA)
40. Tissue culture flasks (Corning, USA)
41. Ultrasonicator
42. Universal Testing Machine (Instron 5567, USA)
43. UV Transilluminator (Fotodyne, USA)
44. Vacuum drying oven and pump (VD23, Binder, Germany)
45. Vortex mixer (Scientific Industry, USA)
46. Water purification equipment (Water pro Ps, Labconco USA)
47. Water bath, Thermostat shaking (Mettler, Germany)
48. 6-, 24-, 48-, and 96-well sterile plate (Corning, USA)

## 2. Experimental Procedures

Experimental works are divided into 3 parts. Part I is the study on characterization of mesenchymal stem cells (MSCs) isolated from human periosteum in order to apply in bone tissue engineering. Part II is the investigation on the size effect of demineralized bone powder on the physical and chemical properties of blended collagen scaffolds including *in vitro* osteogenic properties when cultured with MSCs. Part III is the study on the osteogenic differentiation of the novel scaffolds made from gelatin/chitooligosaccharide/demineralized bone powder both *in vitro* and *in vivo* bioassays. The systems of gelatin/chitooligosaccharide/demineralized bone powder were developed for bone tissue engineering applications using human MSCs for *in vitro* study and Wistar rats for *in vivo* study.

### Part I: Characterization of MSCs from human periosteum

Figure 3.1 shows the summary of experimental procedure of Part I: Characterization of MSCs from human periosteum.

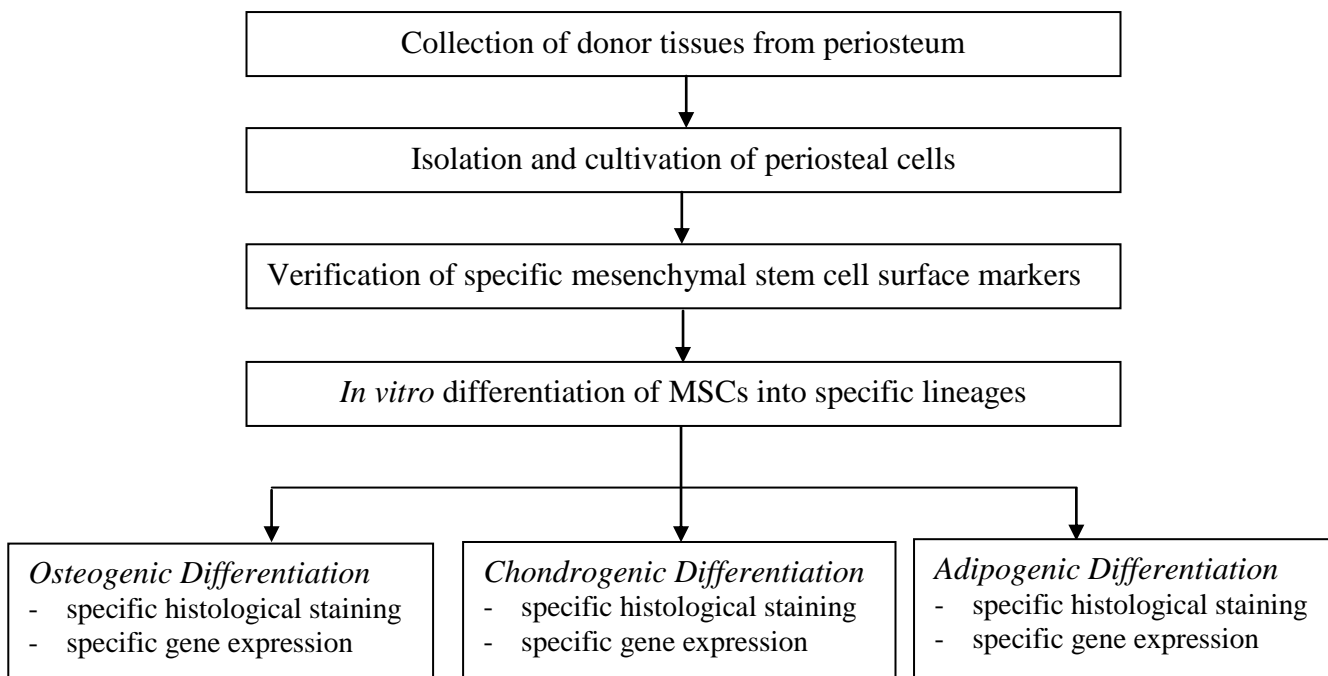


**Figure 3.1** Diagram of experimental procedures (Part I).

## Part II: Osteogenic characterization of collagen/demineralized bone powder scaffolds

Figure 3.2 shows the summary of experimental procedure of Part II: Osteogenic characterization of collagen/demineralized bone powder scaffolds.

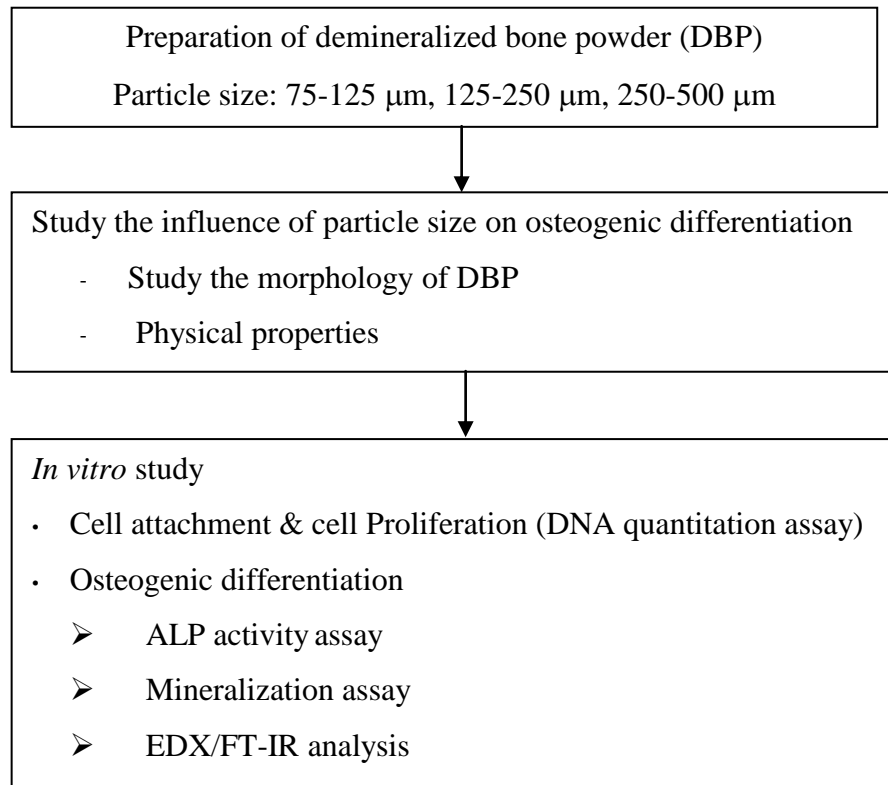


**Figure 3.2** Diagram of experimental procedures (Part II).

### Part III: Gelatin/chitooligosaccharide/demineralized bone powder scaffolds for bone tissue engineering

Figure 3.3 shows the summary of experimental procedure of Part III: Gelatin/chitooligosaccharide/demineralized bone powder scaffolds for bone tissue engineering.

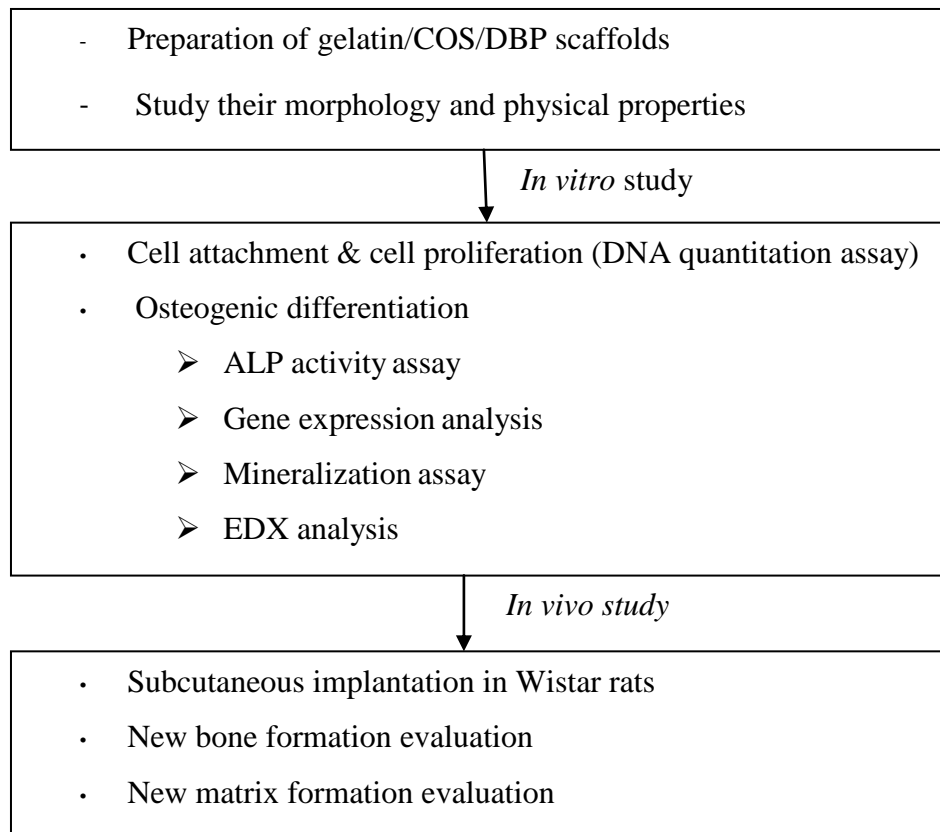


**Figure 3.3** Diagram of experimental procedures (Part III).

## **Part I. Characterization of periosteum-derived cells as mesenchymal stem cells**

### **2.1 Isolation and cultivation of mesenchymal stem cells**

In this study, mesenchymal stem cells (MSCs) were isolated from the human periosteum explants of 25-year-old male donor using primary culture technique. Initially, the tissues were washed with alpha-minimum essential medium ( $\alpha$ -MEM) containing 200 units/ml penicillin, and 100  $\mu$ g/ml streptomycin to remove blood and remain debris away. Next, the periosteum-tissues were cut into very small pieces, 1 mm x 1 mm, and placed on sterile tissue culture flasks. They were cultured in  $\alpha$ -MEM supplemented with 10% fetal bovine serum (FBS), 100 units/ml penicillin, and 50  $\mu$ g/ml streptomycin. The culture flasks were maintained in an incubator at 37°C, 5%CO<sub>2</sub>, 95% humidity and culture medium was changed twice a week. The small pieces of tissues were continuously cultured until observing an outgrowth of periosteum-derived cells (PD cells) the tissues. When PD cells suitably proliferate on T-25 tissue culture flask, the primary cells were collected by trypsinization. Briefly, the old medium were removed and replaced with 0.25% Trypsin/EDTA solution. The culture flask was incubated at 37°C, 5%CO<sub>2</sub> for 5 min. After cells were detached, Trypsin was inactivated with 10%FBS culture medium and centrifuged with 1,500 rpm for 5 min. The supernatant was removed and the pellet was resuspended with fresh culture medium and then recultured the cells in the new tissue culture flask with the same condition. The PD cells were maintained in the incubation until further experiments.

### **2.2 Analysis of the specific cell surface of PD cells**

The characterization of PD cells from the immunophenotype properties was analyzed using specific cell surface antigens, and specific cell staining. Briefly, the PD cells were collected from the tissue by trypsinization technique. The cell pellets were washed with 1X PBS supplemented with sodium azide and bovine serum albumin (BSA). They were centrifuged with 1,500 rpm for 5 min 3 times. The pellet cells were collected in sterile conical tube more than  $5 \times 10^5$  cells/tubes. The specific CD marker antibodies were used in this study including CD29, CD44, CD90, and CD105 for the mesenchymal stem cells markers; CD34, and CD45 for hematopoietic stem cell markers. 10  $\mu$ l each antibody was aliquoted and incubated on ice in the dark for 20 min. Then, the cells were washed in PBS solution for 3 times (centrifuged at the same condition). Next, the cells were fixed in PBS solution supplemented with 0.5% formaldehyde for 5 min in the dark. In the last step, the stained cells were placed in the flow cytometer and analyzed the data with BD Cell Quest Pro Software.

### **2.3 *In vitro* functional characterizations of periosteum-derived cells**

The PD cells were maintained culture in the incubator at the same condition until they reached confluence. Next, the PD cells were trypsinized for subculture and induced with specific differentiation medium to be three lineages of PD cells including osteogenic, chondrogenic, and adipogenic lineages. Each lineage of differentiated cells was verified by specific staining assay and specific gene expression analysis.

#### **2.3.1 Osteogenic differentiation study of periosteum-derived cells**

Osteogenic differentiation of PD cells were induced using osteogenic medium ( $\alpha$ -MEM supplemented with 10% FBS, 100 units/ml penicillin, and 50  $\mu$ g/ml streptomycin,  $10^{-8}$  M dexamethasone, 50  $\mu$ g ascorbic acid and  $10^{-9}$  M  $\beta$ -glycerophosphate) and compared with the control group in control medium ( $\alpha$ -MEM supplemented with 1% FBS) for all experiments. They were maintained in an incubator at 37°C, 5%CO<sub>2</sub>, 95% humidity approximately 3 weeks. The specific staining assessments were performed after 7 days incubation for alkaline phosphatase (ALP) staining, and after 21 days for von Kossa and alizarin red S staining, respectively. For the specific osteogenic gene expression, total RNA of the differentiated cells were extracted using standard protocol. Then, reverse transcription-polymerase chain reaction (RT-PCR) was performed for specific genes such as runt-related transcription factor 2 (RUNX2), alkaline phosphatase (ALP), and osteopontin (OPN). The glyceroldehyde-3-phosphate dehydrogenase (GAPDH) was used as internal loading control.

#### **2.3.2 Chondrogenic differentiation study of periosteum-derived cells**

The 3D pellet culture of PD cells was transferred to sterile polypropylene culture tubes (volume 15 ml). Firstly, the cell pellets were washed with PBS and soaked in control medium on orbital shaker at 75 rpm. After the initial 24 hours of seeding and culture, the culture medium was replaced by chondrogenic medium (DMEM supplemented with 1% FBS, 100 units/ml penicillin, and 50  $\mu$ g/ml streptomycin, 6.25  $\mu$ g/ml, insulin transferrin selenium (ITS supplement), and 10 ng/ml TGF- $\beta$ 3). The experiment was compared with the control group in control medium (DMEM supplemented with 1% FBS) for all experiments. The medium was changed 3-times a week. Finally, the cell pellets were washed with PBS, fixed with formaldehyde solution, dehydrated through ethanol, embedded in paraffin, and sectioned at a thickness of 5  $\mu$ m, deparaffinized, and rehydrated. For the specific chondrogenic

staining, the differentiated MSCs were stained with alcian blue. For the specific chondrogenic gene expression, total RNA of differentiated cells were extracted using with standard protocol. Then, reverse transcription-polymerase chain reaction (RT-PCR) was performed for specific genes such as Sox-9. The glyceroldehyde-3-phosphate dehydrogenase (GAPDH) was used as internal loading control.

### **2.3.3 Adipogenic differentiation study of periosteum-derived cells**

Adipogenic differentiation of PD cells were induced using adipogenic medium (DME/Ham's F12 medium containing 3%FBS, 100 units/ml penicillin, and 50 µg/ml streptomycin insulin, 3,5,3'-triiodothyronine, transferrin, calcium pantotenate, biotin and dexamethasone) and compared with the control group in control medium (DME/Ham's F12 medium supplemented with 1% FBS) for all experiments. They were maintained in an incubator at 37°C, 5%CO<sub>2</sub>, 95% humidity for 21 days. For the specific staining, the differentiated PD cells were stained with oil red O solution. For the specific adipogenic gene expression, the differentiated cells were extracted total RNA followed with standard protocol. Then, the RNA was performed reverse transcription-polymerase chain reaction (RT-PCR) for specific genes such as PPAR-γ and lipoprotein lipase (LPL). The glyceroldehyde-3-phosphate dehydrogenase (GAPDH) was used as internal loading control for every gene.



## **Part II. Osteogenic characterization of collagen/demineralized bone powder scaffolds**

### **2.4 Preparation of the demineralized bone powder**

The human bone allograft was obtained from donors at the Chulalongkorn King's Memorial Hospital. The allograft from cancellous bone was kept in freezer at  $-80^{\circ}\text{C}$  before use. The frozen bone was thaw at room temperature until the ice crystal was evaporated. The bone were removed tissue and cleaned as follows: the cleaning bone in the large beaker was placed in the ultrasonic bath (sonicator) filled with distilled water and was performed frequencies approximately 18,000 cycles per second. First, the bone pieces were placed in the large beaker filled with 0.01X Allowash (Brij 35) solution for 15 minutes (3 times), each time with sterile distilled water for 15 min. Next, the bone pieces were replaced in 3% hydrogen peroxide ( $\text{H}_2\text{O}_2$ ) solution for 15 min (3 times), each time with sterile deionized water for 15 min, respectively. After that, the washed bone allograft was continually washed with 70% isopropyl alcohol for 15 min (3 times), each time with sterile DI water, respectively. (Honsawek et al., 2010).

The cleaned bone was dried by lyophilization technique. They were placed in sterile Petri dish and covered with foiled paper with many small pinholes. The freeze dry temperature is  $-55^{\circ}\text{C}$  under vacuum overnight until the samples were completely dried. The dried bone was pulverized using a ball mill grinder. They were rapidly chilled in liquid nitrogen solution during pulverization process. The ground bone was sieved in order to separate the particle size into 3 ranges; 75-125  $\mu\text{m}$ , 125-250  $\mu\text{m}$ , and 250-500  $\mu\text{m}$ , prior to demineralization process. (Honsawek et al., 2010).

The dried bone was demineralized using acid extraction process (Honsawek et al., 2005). They were placed in the large Erlenmeyer flask filled with 0.1N hydrochloric acid (HCl) solution in proportion of 100 mg bone powder to 10 ml gram of HCl. The flask was continuously shaken in the incubator shaker at  $4^{\circ}\text{C}$  all the time with frequencies at 250 rpm. After every 30 min, they were rinsed by taking supernatant solution away and replaced with the new HCl solution. They were continuously performed demineralization around 16 times. After that, the demineralized bone was washed with large amount of distilled water around 15 minutes for 3 times followed with 70% isopropyl alcohol for 15 min (3 times). Finally, they were alternatively washed with sterile distilled water and left to be dried. The demineralized bone was refreeze-dried and stored at  $-20^{\circ}\text{C}$  until further use.

## 2.5 Fabrication of collagen/demineralized bone powder scaffolds

To fabricate the scaffolds, firstly 2 wt% aqueous pure collagen solution was prepared by weighting and swelling Type I bovine Achilles tendon collagen powder 2 g in 100 ml of 1% (v/v) acetic acid solution (pH 2.5) for 2 h at 4°C. Next, the mixed component was homogenized using a homogenizer at 10,000 rpm for 1 min each time until the solution was homogeneous. The pure collagen solution was added with 25% (v/v) glutaraldehyde solution (6.25 µl/ml solution) and allowed for cross-linking under stirring for 15 min. (Song et al., 2006; Tangsadthakun et al., 2007; Rattanavaraporn et al., 2009)

For preparation of the demineralized bone based collagen scaffolds, the demineralized bone was classified into 3 groups: the particle size in range 75 to 125 µm (D125), 125 to 250 µm (D250), and 250 to 500 µm (D500), respectively. Each group of the demineralized bone was mixed in the cross-linked homogeneous collagen solution using a homomixer at the weight blending ratio of collagen to demineralized bone 60/40. As a result, four types of material solutions were obtained:

- (1) 2 wt% aqueous pure collagen solution
- (2) 2 wt% aqueous pure collagen solution mixed with D125 (60/40)
- (3) 2 wt% aqueous pure collagen solution mixed with D250 (60/40)
- (4) 2 wt% aqueous pure collagen solution mixed with D500 (60/40)

0.25 ml of material solution was loaded into each well of sterile 48-well culture plates which were wrapped with aluminium foil and pre-freezed at -20°C for 12 h and then freezed at -80°C for 12 h. The sample solution was freeze-dried using a lyophilizer under vacuum for 24 h. The obtained scaffolds were immersed in 0.1M glycine solution at room temperature for 2 h to block the non-reacted aldehyde groups and washed repeatedly with DI water before refreeze-drying. The scaffolds were sterilized using ethylene oxide before cultivation.

## **2.6 Physical and chemical characterization of the scaffolds**

### **2.6.1 Morphology observation of the scaffolds**

The morphology of cross-sectioned scaffolds was determined using scanning electron microscopy (SEM). The samples were put on a copper stub and then sputter-coated with gold prior to SEM observation at an accelerating voltage of 12-15 kV. The average pore sizes of the scaffolds were analyzed using Image J program.

### **2.6.2 Mechanical test of the scaffolds**

The universal testing machine (Instron 5567, USA) was used to determine the slope from 5 to 30% of the stress-strain curves of the scaffolds (13 mm in diameter and 3 mm in thickness) a constant compression rate of 0.5 mm/min both dry and wet conditions. The compressive modulus was analyzed and presented as the mean  $\pm$  standard deviation (n=5).

### **2.6.3 Swelling ability of the scaffolds**

Water absorption capacity of the swollen scaffold was determined. The known weight of the dry scaffold was immersed in PBS (pH 7.4) at 37°C for 24 h. The wet scaffold was weighted after blotting the scaffold using lint-freed paper (Kimwipe) to remove excess PBS. The swelling ratio of the scaffold ( $W_s$ ) was calculated from the equation:

$$W_s = \frac{(W_w - W_d)}{W_d}$$

$W_w$  and  $W_d$  represented weight of the wet and dry scaffolds, respectively. The values were represented as the mean $\pm$ standard deviation (n=5).

#### **2.6.4 Cytotoxicity test of the scaffolds**

The assay was modified according to the biological evaluation of medical devices-Part 5 (ISO 10993-5: 1999). The scaffolds were soaked in 2 ml of DMEM supplemented with 10% fetal bovine serum (FBS) and kept at 37°C for 24 hours. Next, the scaffolds were removed and the remainder (sample extract) would be used in the experiment. DMEM supplemented with 10% FBS and DMEM supplemented with 10% FBS and containing 20 ppm of zinc acetate were used as negative and positive controls, respectively. The L929 fibroblasts were evaluated the test. The cells were seeded in 24-well plate and incubated at 37 °C including 5% CO<sub>2</sub> for overnight. Hereafter, the medium from each well was removed and replaced with sample extract, negative control and positive control. All wells were further incubated for 24 hours. The cells viability was measured using MTT assay (Bernas and Dobrucki, 2002). Briefly, the samples were washed with PBS. The MTT solution was added into each sample and incubated at 37°C for 30 min. Next, MTT [3-(4, 5 dimethylthiazolyl)-2, 5-diphenyltetrazolium bromide] solution was removed and DMSO was used to solubilize the formazan crystals to the yellow tetrazolium rings of MTT. Finally, the absorbance of the solution was measured at 570 nm.

### **2.7 *In vitro* biological characterizations of PD cells onto the collagen/demineralized bone powder scaffolds**

#### **2.7.1 *In vitro* cell culture of PD cells**

The sterilized scaffolds were seeded with PD cells. The cell-seeded scaffolds were cultured in  $\alpha$ -MEM supplemented with 10% FBS, 100 U/ml Penicillin/Streptomycin at 37°C, 5% CO<sub>2</sub>, 95% humidity. When the cells reached confluence, they were trypsinized for subculture as their suitable.

For initial attachment and proliferation assay, the PD cells ( $5 \times 10^5$  cells/scaffold) were seeded onto the scaffolds using orbital shaking at 250 rpm and cultured in proliferating medium ( $\alpha$ -MEM supplemented with 15% FBS) at 37°C, 5% CO<sub>2</sub>. The numbers of cells from 6 hours to 5 days after seeding were quantified by DNA assay. Briefly, the cell samples were lysed in sodium citrate-buffered saline solution (SSC, pH 7.4) containing sodium dodecylsulfate (SDS) at 37°C for overnight. Then, 100  $\mu$ l of cell lysates were mixed with a fluorescent dye solution (Hoechst 33258 dye) in a 96-well black plate. The mixed solutions were spontaneously measured their fluorescence intensities at the excitation and emission

wavelengths of 355 and 460 nm, respectively. The standard curve between the DNA and known cell number was prepared (Takahashi et al., 2005b).

### **2.7.2 *In vitro* osteogenic differentiation of PD cells**

The PD cells were seeded on the scaffolds ( $1 \times 10^6$  cells/scaffold) the same as the seeding method in section 2.7.1 and were cultured in culture medium for 1 day. Next, they were fed with osteogenic medium and then cultured from 1 day to 28 days. The MSCs cultured scaffolds were performed experiments as follows:

For alkaline phosphatase (ALP) activity assay (Hofmann et al., 2007; Marolt et al., 2006), the cultured cells were removed old medium and added SDS solution 1 ml and then incubated for 2 h at 37°C. Next, the cell lysate suspension was reacted with *p*-Nitrophenyl phosphate (pNPP) liquid substrate at 37°C for 15 min. During incubation, the ALP converted pNPP to the soluble yellow end product of *p*-Nitrophenol (pNP). The reaction was stopped with NaOH and absorbance of the solution was immediately measured at 405 nm by a spectrophotometer. The calibration curve was prepared from the pNP standard solution. The ALP activity value was normalized using DNA content of each condition.

The number of cells determined by DNA quantitation assay and also used to normalize ALP activity and calcium content. The cells lysates were prepared from the cell samples and cell standard ( $10^6$  cells/vial). They were frozen at -80°C and thaw at room temperature for several cycles to break the cell membrane. Next, each sample was added with SDS lysis buffer, sonicated and incubated at 37°C for 1 h. After that, the cell lysates, cell standards, and blank were pipetted into the 96-well black plate. Then, the Hoechst 33258 was thawed at room temperature. Hoechst, SSC buffer, and DI water were mixed for preparing Hoechst solution. The solution was added into each well and immediately measured the fluorescent intensity at 355 nm (Excitation) and 460 nm (Emission) using fluorescence microplate reader.

For calcium determination assay, the calcium reagent Arsenazo III assay were utilized as manufacturer's instruction. First, the calcium in cell lysate was extracted with equal volume of HCl at 4°C for 4 h. 25 µl of calcium extracted lysate was mixed with 200 µl of Arsenazo reagent and then leave the reaction approximately 60 s. The absorbance of the solution mixture was measured at 650 nm by a spectrophotometer to assess total calcium content. The calibration curve was prepared from calcium carbonate standard (CaCO<sub>3</sub>).

### **2.7.3 The observation of cultured cells in the scaffolds**

After 7 days and 28 days of osteogenic differentiation (followed with the process in section 2.7.2, the cells seeded scaffolds were washed with PBS to remove non-adherent cells and then fixed in 2.5wt% glutaraldehyde solution in PBS at 4°C for 1 hr. Next, the scaffolds were gently dried using critical point dry technique. Finally, the dried scaffolds were cross-sectional cut and observed under SEM (followed with the process in section 2.6.1).

### **2.7.4 Elemental analysis of cultured cell in the scaffolds**

The surface elements, especially calcium (Ca), phosphorous (P), and oxygen (O) on the cell surface of MSCs cultured scaffolds for 28-days in osteogenic media were analyzed by energy-dispersive X-ray spectroscopy technique (EDX, Philip Model XP 30 CP). The same cell seeded scaffold constructs used in SEM observation were employed for EDX analysis.

### **Part III Gelatin/chitooligosaccharide/demineralized bone powder scaffolds for bone tissue engineering**

#### **2.8 Fabrication of the gelatin/chitooligosaccharide/demineralized bone scaffolds**

Two wt% aqueous pure gelatin solution was prepared by dissolving 2 g of Type A gelatin powder in 100 ml of 1% (v/v) acetic acid (pH 2.5) for 2 h at 60°C with a hotplate stirrer. The other blending ratio of gelatin to chitooligosaccharide (G/C) 70/30 for 2 wt% aqueous solution was prepared in the same solvent and condition. The solutions were added with 25% (v/v) glutaraldehyde solution (6.25 µl/ml solution) and allowed stirring for 15 min. After that, the solutions were kept crosslinking under 4°C for 12 h. The blended gelatin/chitooligosaccharide (G/C) 70/30 solution was added with demineralized bone (size range 250-500 µm) at the ratio of 60/40 and then mixed with a magnetic stirrer for 2 h.

Three types of material solutions were obtained as follows:

- (1) 2 wt% aqueous pure gelatin (G) solution
- (2) 2 wt% aqueous gelatin solution mixed with chitooligosaccharide (G/C) (70/30)
- (3) 2 wt% aqueous gelatin solution mixed with chitooligosaccharide (G/C) and demineralized bone

0.25 ml of material solutions were loaded into each well of sterile 48-well culture plate which was wrapped with aluminium foil and pre-frozen at -20°C for 12 h and then frozen at -80°C for 12 h. The sample solution was freeze dried using a lyophilizer under vacuum for 24 h. The obtained scaffolds were immersed in 0.1M glycine solution at room temperature for 2 h to block the non-reacted aldehyde groups and washed repeatedly with DI water before refreeze-drying. The scaffolds were sterilized using ethylene oxide before cultivation.

## **2.9 Physical and chemical characterization of the gelatin/chitooligosaccharide/demineralized bone scaffolds**

### **2.9.1 Morphological observation of the scaffolds**

The morphological observation of the unseeded scaffolds was evaluated using SEM as explained in section 2.6.1.

### **2.9.2 Mechanical test of the scaffolds**

Compressive modulus of the dry and wet scaffolds was evaluated using a universal testing machine as explained in section 2.6.2.

### **2.9.3 Swelling ability of the scaffolds**

Water sorption capacity of the swollen scaffolds was determined as explained in section 2.6.3.

### **2.9.4 *In vitro* biodegradation test of the scaffolds**

Degradation ratio of sterilized scaffold was evaluated as explained in section 2.6.4.



## **2.10 *In vitro* biological characterizations of PD cells onto the gelatin/chitooligosaccharide/demineralized bone powder scaffolds**

### **2.10.1 *In vitro* cell culture of PD cells cultured in scaffolds**

The sterilized scaffolds were seeded with PD cells. The cell-seeded scaffolds were cultured in  $\alpha$ -MEM supplemented with 10% FBS, 100 U/ml Penicillin/Streptomycin at 37°C, 5% CO<sub>2</sub>, 95% humidity. When the cells reached confluence, they were trypsinized for subculture and placed in new sterilized culture flasks.

For initial attachment and proliferation assay, was evaluated as explained in section 2.7.1.

### **2.10.2 *In vitro* osteogenic differentiation of PD cells cultured in scaffolds**

The PD cells were seeded on the scaffolds ( $1 \times 10^6$  cells/scaffold) following the seeding method in section 3.3.2 and then cultured in normal culture medium for 1 day. Next, the medium was changed to osteogenic medium. The culture was continued at 37°C, 5% CO<sub>2</sub> for 28 days. The MSCs cultured scaffolds were performed experiments as follows.

For alkaline phosphatase (ALP) activity assay, DNA quantitative assay, and calcium determination assay, were applied as explained in section 2.7.2.

### **2.10.3 The observation of PD cells cultured in scaffolds**

After 7 days and 28 days of osteogenic differentiation (followed the process in section 2.7.2), the cell seeded scaffolds were prepared and observed under SEM (followed the process in section 2.6.1).

### **2.10.4 Elemental analysis of PD cells cultured in scaffolds**

The surface elements on the cell surface of PD cells cultured scaffolds for 28-days in osteogenic media were analyzed by EDX as explained in section 2.9.

### 2.10.5 Study of biological properties of the scaffolds in animal model

Twelve male Wistar rats (8 weeks of age; average weight 275-300g) were used in this study. Before surgery, the animals were anesthetized with a mixture of Thiopental sodium solution (60 mg/kg body weight). All procedures were followed by Home office guidelines on the scientific use of animal (Scientific procedures) Act 1986.

For the insertion of implants, the skin of animal was shaved, washed, and disinfected with povidone betadine. Their skins were cut for making small pockets around 13 mm and then inserted the sterile scaffolds inside. Next, each pocket was closed with the sterile wound suture (Dacron 4-0). After surgery the animals were randomly assigned into two groups. The first group (n=6) was maintained for 4 weeks and the second group (n=6) was maintained for 8 weeks. The illustration of the implantation site was shown in the figure 1.

The samples were explanted after completion of implantation period. Briefly, the animals were sacrificed using overdose of Thiopental sodium (200 mg/kg body weight). Each sample was separated into 2 parts. The first part was immersed in 10% formalin solution for 24 h and was evaluated the bone formation using histochemical staining (stained for H&E, and von Kossa). The second part was dried, placed in 1 ml of 1N HCl and then heated at 90 °C until the tissue completely dissolved in the solution. The solutions were quantitated the calcium content using Arsenarzo III reagent kit in section 2.7.2 and normalized with the non-implanted scaffolds.

For the histochemical staining, the H&E staining was used for evaluation of the *in vivo* osteoid formation. Briefly, the explants that fixed in 10% formalin solution were dehydrate, immersed in hot paraffin basin, and placed in the plastic blocks. Each sample was gently cut into 3 sections using a microtome with the thickness of 5 µm/section and then placed on a glass slide. For evaluation of the osteoid formation, the slides were stained for H&E stain via pathologic technique. The scaffolds implanted at 4-weeks and 8-weeks were compared. The von Kossa staining method was used for evaluation of the *in vivo* mineralization in 8-weeks post-implantation. The stained slides were analyzed via microscopy and histomorphometry analyses were determined using Image Pro Plus program. Briefly, the bone formation area was quantified and then normalized with the total area. The data were presented as the mean  $\pm$  standard deviation.

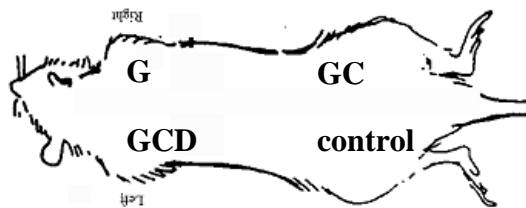


**Figure 3.1** Implanted sites of Wistar rat

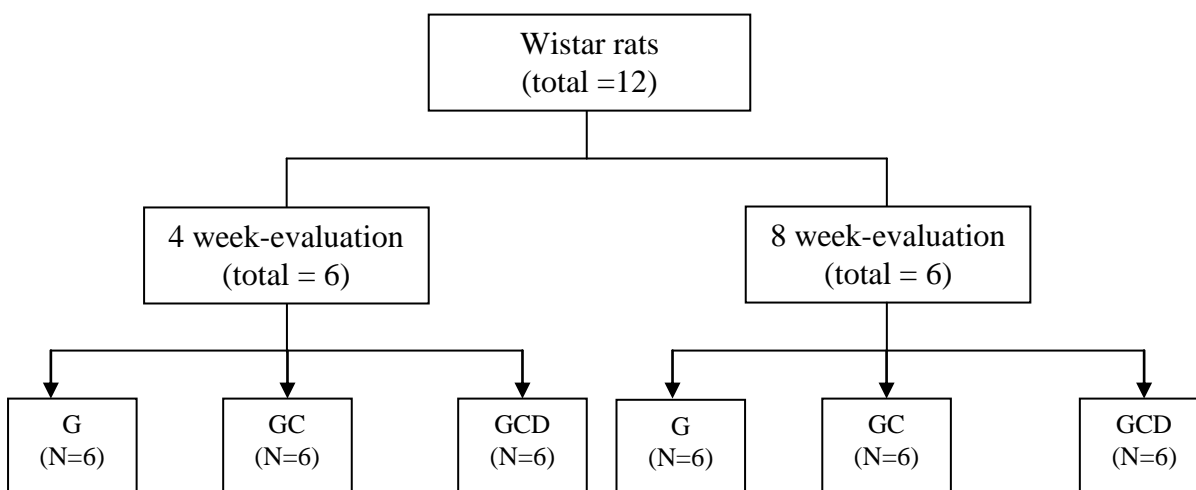


**Figure 3.2** The group and the number of Wistar rats used to evaluate *in vivo* osteogenic responses

### 2.11 Statistical Analysis

The data were expressed as means with error bars representing standard error of the mean (S.E.). Analysis of variance (ANOVA) was used to determine the significant differences among treatment groups. Turkey-type multiple comparison tests were used for comparing means of more than two groups in one way ANOVA analyses. *P*-value less than 0.05 was considered to be statistically significant.

## CHAPTER IV

### RESULTS

#### Part I: Mesenchymal stem cells for bone tissue engineering

##### 1. Characteristics of periosteum-derived cells

For bone tissue engineering application, the mesenchymal stem cells (MSCs) is needed for the study. The MSCs derived from the human periosteal tissue are interested because they are easy for cultivation and maintenance. The MSCs were isolated from periosteal tissue using primary culture technique under sterile condition. Briefly, the tissue was cultured in culture medium ( $\alpha$ -MEM supplemented with 10% FBS, 200U Penicillin, 100  $\mu$ g Streptomycin) and the medium was changed three times a week. The out-growing cells were collected using trypsinization and then recultivation in the culture plate. They attached on the culture plate in monolayer quite orderliness. Furthermore, the morphology of periosteum-derived (PD) cells are spindle and stellate shape in normal condition (Figure 4.1A) whereas more round and cuboidal shape in osteogenic condition was observed (Figure 4.2A). Therefore, the different condition of medium had influenced to change their morphology. The proliferation of PD cells was studied for evaluation of population doubling time (PDT) and specific growth rate ( $\mu$ ). The results found that PD cells had PDT around 30.473 hours whereas they had specific growth rate ( $\mu$ ) around  $2.28 \times 10^{-2} \text{ hour}^{-1}$ . The results showed that PD cells from periosteal tissue had rapid proliferation rate suitable for bone tissue engineering.

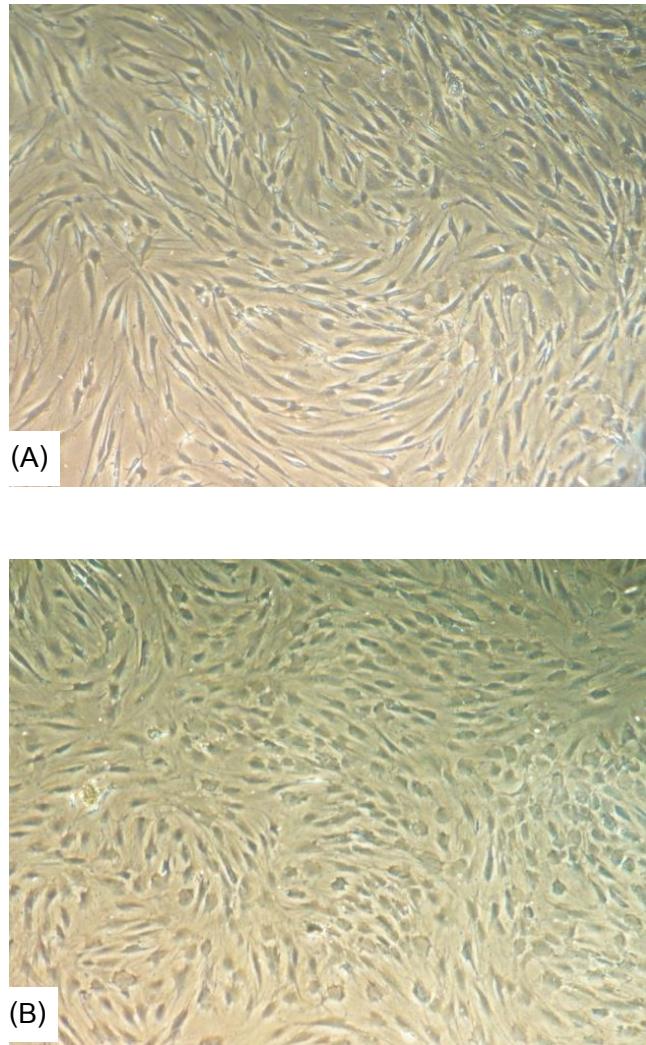


**Figure 4.1** Periosteum-derived cells from primary outgrowth technique. (A) cultivation in culture medium (B) cultivation in osteogenic medium (10X magnification)

## 2. Cell surface marker characteristics of periosteum-derived cells

In fact, each cell type has specific expression of cell surface markers. To confirm the MSC characteristics of the isolated PD cells population for this study, flow cytometry was performed using validated cell surface markers relating to MSCs. For verification of MSCs, the cells should be proved that they have cell surface markers specific for MSCs but have no cell surface markers specific for hematopoietic stem cells (HSCs). In this study, the PD cells were fixed and stained with specific antibodies such as CD29, CD44, CD90, and CD105 for detection MSC characteristics (inclusion criteria) whereas CD34 and CD45 for hematopoietic markers (exclusion criteria). The cells stained with specific antibody were analyzed via flow cytometer. The black lines represent the fluorescence intensity of cells stained with the indicated antibodies and the blue lines represent the negative control cells, which were stained with a nonimmunoreactive isotype control antibody (Figure 4.2). The results found that PD cells had highly expression of MSC markers. They had expression of CD29, CD44, CD90, and CD105 approximately 92.99%, 98.04%, 99.43%, and 55.47%, respectively. By the way, they had very low expression of HSC markers such as CD34 and CD45 approximately, 0.02% and 0.29%, respectively. Therefore, most population of PD cells had expression of MSC cell surface characteristics which they need to investigate their function that they can activated into MSC lineages (bone, cartilage, fat) by using *in vitro* functional specific differentiation assay in the next experiment.

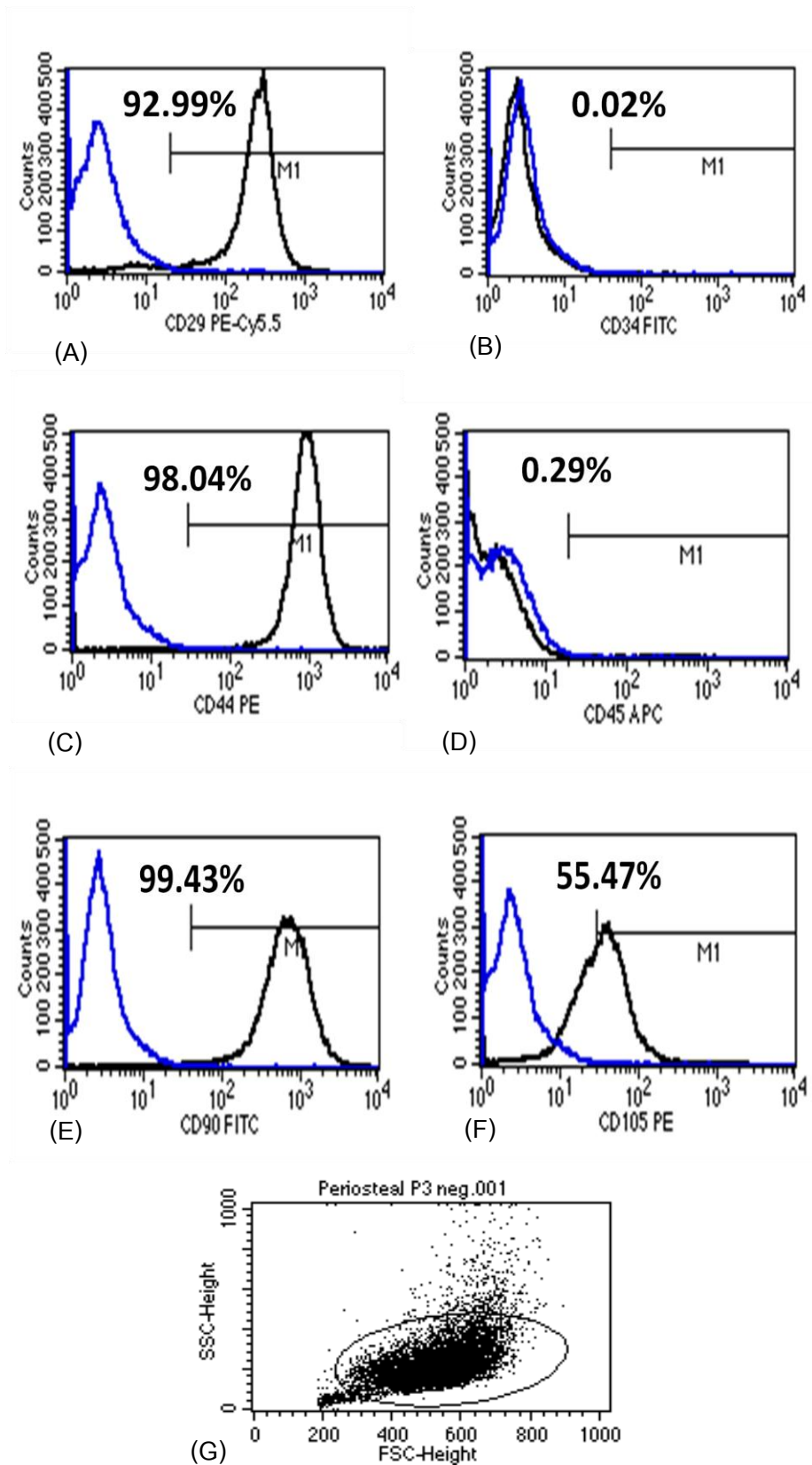


**Figure 4.2** FACS histogram of periosteum-derived cells performed specific antibody staining (A) CD29 (B) CD34 (C) CD44 (D) CD45 (E) CD90 (F) CD105 and (G) cell population characteristic

### **3. *In vitro* osteogenic, chondrogenic, and adipogenic differentiation of periosteum-derived cells**

In terms of cells, MSCs isolated from periosteal tissue were cultured on tissue culture plates under normal condition. MSCs at the 3<sup>rd</sup> passage were prepared for further use in this study. Due to the fact that MSCs can differentiate into osteoblasts, chondroblasts, and adipocyte, *in vitro* functional assay of PD cells were investigated to verify their differentiation potential to osteogenic, chondrogenic, and adipogenic lineages.

For osteogenic differentiation assay, PD cells were cultured on tissue culture plates under osteogenic medium (OM:  $\alpha$ -MEM supplemented with 10% FBS, 100 units/ml penicillin, and 50  $\mu$ g/ml streptomycin,  $10^{-8}$  M dexamethasone, 50  $\mu$ g ascorbic acid and  $10^{-9}$  M  $\beta$ -glycerolphosphate) for 4 weeks, compared to those cultured under the control medium (CM:  $\alpha$ -MEM supplemented with 1% FBS, 100 units/ml penicillin, and 50  $\mu$ g/ml streptomycin). The alkaline phosphatase (ALP) activity and mineralization assays were selected for the key indicators for osteogenic differentiation. In this work, ALP staining, Alizarin red S staining, and von Kossa staining assays were performed in PD cells cultured under osteogenic induction, as shown in Figure 4.3. Our findings revealed that PD cells in OM were stained purple color spreading in all the cultured areas indicating high ALP activities. On the other hand, PD cells in CM were stained light blue color in the most areas implying ALP activities. Furthermore, the mineralization was selected to confirm the osteogenic differentiation using Alizarin red S staining and von Kossa staining assays. For Alizarin red S staining, the results showed that the PD cells cultured in OM stained deep red colour representing for calcium nodules whereas the PD cells cultured in CM were stained weak. For von Kossa staining, the results showed that the PD cells cultured in OM were stained strong black brown color which representing for calcium nodules whereas the PD cells cultured in CM were stained very light brown color. The results were confirmed by osteogenic specific gene expression using RT-PCR. Total RNA from the PD cells cultured both in OM and CM for 3 weeks were extracted under standard protocol and then were performed RT-PCR for RUNX2, ALP, COL1, and Osteopontin. The GAPDH was used as normalized control gene. The results displayed that the PD cells cultured in OM had high expression for RUNX2, ALP, COL1, and Osteopontin. In contrast, the PD cells cultured in CM exhibited low expression of ALP, COL1, and Osteopontin and no expression of RUNX2 (Figure 4.6). These data suggested that osteogenic differentiation potential of PD cells cultured in OM were remarkably higher than that of PD cells cultured in CM.



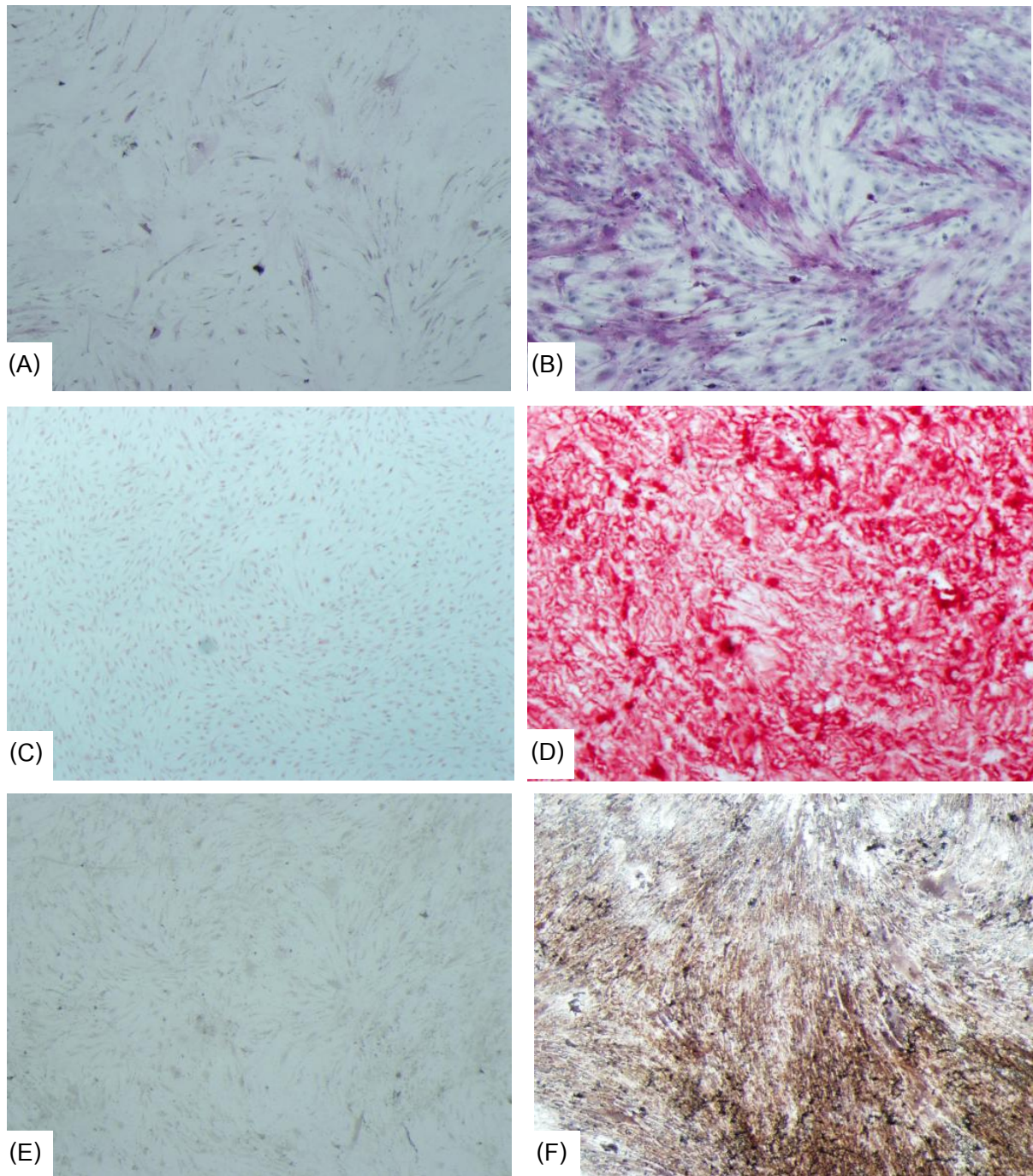


**Figure 4.3** Specific chemical staining of cultured periosteum-derived cells for osteogenic differentiation. (A, B) ALP staining at day 7 (C, D) Alizarin red S staining at day 28 (E, F) von Kossa staining at day 28. (A, C, E in the presence of control medium and B, D, F in the presence of osteogenic medium).

For induction of chondrogenesis, PD cells were cultured on tissue culture plates under chondrogenic medium (CHM: DMEM supplemented with 1% FBS, 100 units/ml penicillin, and 50  $\mu\text{g/ml}$  streptomycin, 6.25  $\mu\text{g/ml}$ , insulin transferrin selenium (ITS supplement), and 10 ng/ml TGF- $\beta$ 3) for 3 weeks, compared to PD cells cultured under control medium (CM: DMEM supplemented with 1% FBS, 100 units/ml penicillin, and 50  $\mu\text{g/ml}$  streptomycin). The sulfated glycosaminoglycans (sGAG) formation is a key indicator for chondrogenic differentiation. In this study, Alcian blue stained sGAG content in the extracellular matrix was found in PD cells cultured under chondrogenic induction, as shown in Figure 4.4. It was exhibited that PD cells cultured in CHM were stained blue color which representing for sGAG content spread around the cultured area whereas PD cells cultured in CM were stained very light blue color. The result was confirmed by chondrogenic specific gene expression using RT-PCR. Total RNA were extracted from the PD cells cultured in both CHM and CM for 3 weeks under standard protocol. Then RT-PCR analysis was performed for Sox-9. The GAPDH was used as normalized control gene. The results represented that the PD cells cultured in CHM had high expression for Sox-9. On the contrary, the PD cells cultured in CM possessed very low expression of Sox-9 (Figure 4.6). The chondrogenic differentiation potential of PD cells cultured in CHM was much higher than of PD cells cultured in CM.

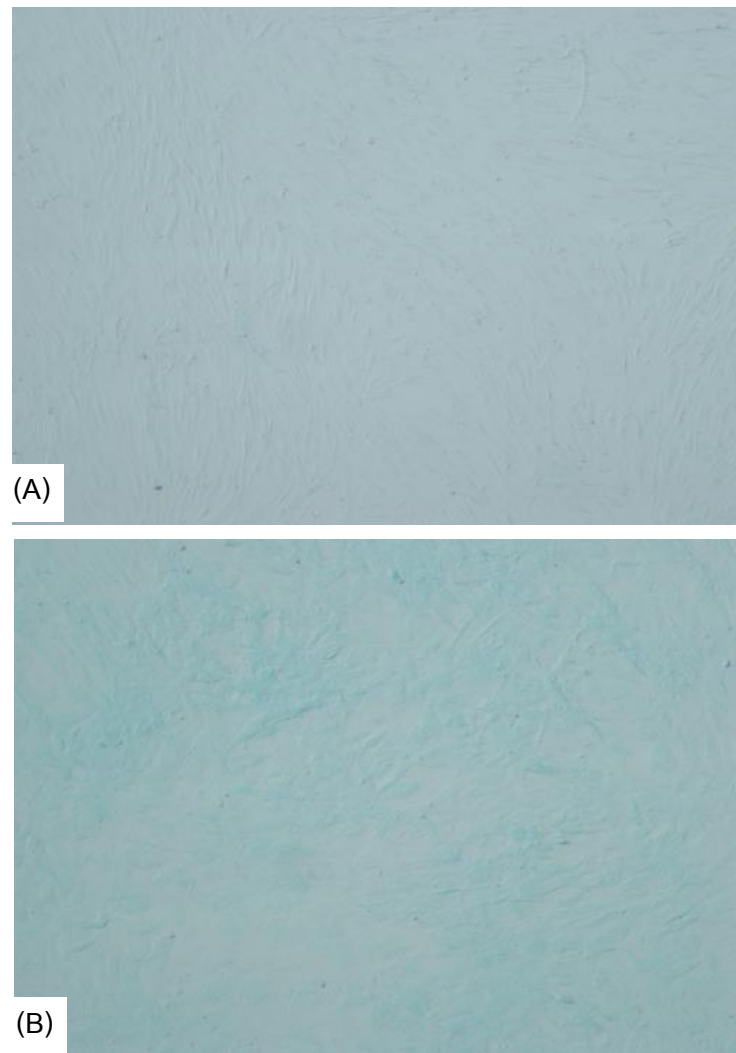


**Figure 4.4** Specific chemical staining of cultured periosteum-derived cells for chondrogenic differentiation at day 21. (A) Alcian blue staining for PD cells cultured in control medium (B) Alcian blue staining for PD cells cultured cells in the presence of chondrogenic medium.

For the induction of adipogenesis, PD cells were cultured on tissue culture plates under adipogenic medium (AM: DME/Ham's F12 medium containing 3%FBS, 100 units/ml penicillin, and 50 µg/ml streptomycin, 0.05 µM insulin, 0.2 nM 3,5,3'-triiodothyronine, 100 nM transferrin, and 100 nM dexamethasone) for 4 weeks, compared to PD cells cultured under control medium of (CM: DME/Ham's F12 medium supplemented with 1% FBS, 100 units/ml penicillin, and 50 µg/ml streptomycin). The lipid droplet formation is a key marker for adipogenic differentiation. Oil red O was used to stain lipid droplet created by stem cell underwent adipogenic differentiation. In this work, Oil red O stained lipid droplet formed by PD cells cultured under adipogenic induction was showed in Figure 4.5. It was presented that PD cells cultured in AM were found red stained of intracellular lipid vacuoles spread around the cultured area whereas PD cells cultured in CM did not detected red stained. The result was confirmed by adipogenic specific gene expression using RT-PCR. Total RNA were extracted from the PD cells cultured in both AM and CM for 4 weeks under standard protocol. Then RT-PCR analysis was performed for LPL, PPAR- $\gamma$ . The GAPDH was used as normalized control gene. The results showed that the PD cells cultured in AM had high expression for LPL and PPAR- $\gamma$ . In contrast, the PD cells cultured in CM not found expression of LPL and possessed very low expression of PPAR- $\gamma$  (Figure 4.6). The adipogenic differentiation potential of PD cells cultured in AM was much higher than of PD cells cultured in CM.

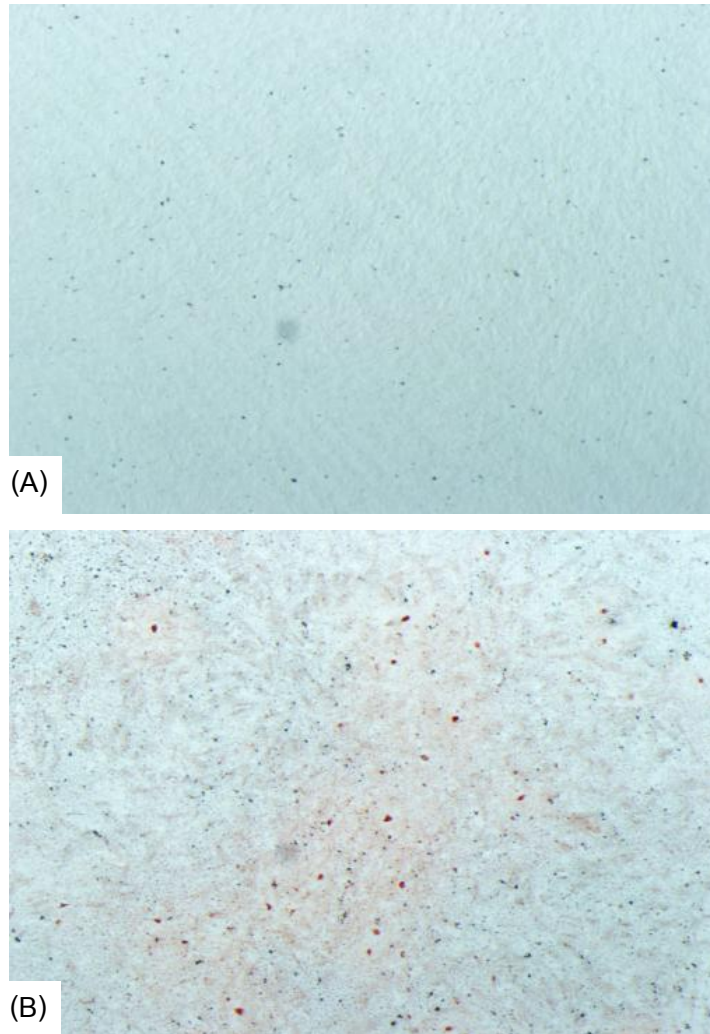


**Figure 4.5** Specific chemical staining of cultured periosteum-derived cells for adipogenic differentiation at 28 days. (A) Oil red O staining for PD cells cultured in control medium (B) Oil red O staining for PD cells cultured in adipogenic medium.

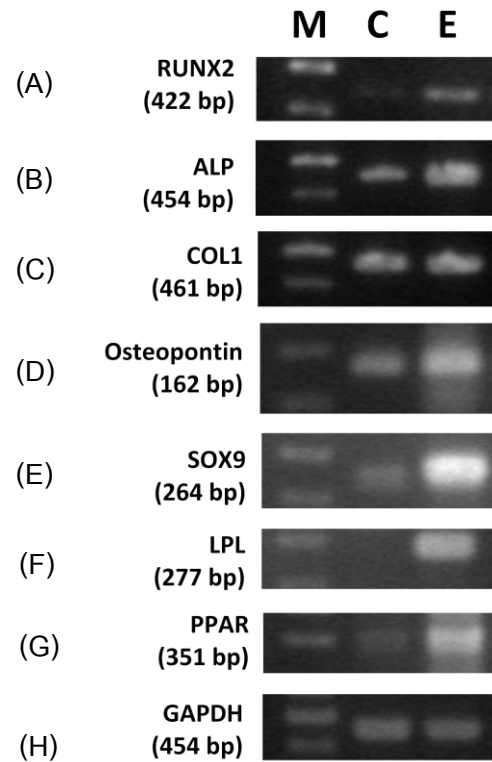


**Figure 4.6** A typical result of gel-electrophoresis of PCR products to evaluate the expression of MSC-specific genes in control medium and conditioned medium. (A, B, C, D) osteogenic genes: RUNX2, ALP, COL1, and Osteopontin (E) chondrogenic gene: Sox-9 (F, G) adipogenic genes: LPL and PPAR- $\gamma$ . The amount of total RNA was standardized by the expression level of GAPDH (H). Lane M = DNA markers, lane C = PD cells cultured in control medium, lane E = PD cells cultured in conditioned medium

#### **4. Summary**

It could be concluded from this part of study that primary cell isolated from human periosteum showed mesenchymal characteristics when investigated their functional properties. Briefly, the illustration of cells showed their morphology in spindle shape like fibroblast cells and showed more cuboidal shape in condition of osteogenic medium. Moreover, MSC surface markers (CD29, CD44, CD90, CD105) could be detected but HSC surface markers (CD34 and CD45) could not be detected via flow cytometry technique. Furthermore, the isolated cells from human periosteum showed the MSC phenotypes, which can be differentiated into osteogenic, chondrogenic, and adipogenic lineages in condition of differentiated medium. Differentiated MSCs have characteristics of osteocyte (ALP, mineralization), chondrocyte (GAG aggregation), and adipocyte (fat droplet formation) via specific pathologic staining. Furthermore, they have specific gene expression of their lineages in the treatment group but not in control group.

## **Part II: Osteogenic characterization of collagen/demineralized bone powder scaffolds**

### **5. Characteristic of the demineralized bone powder**

The demineralized bone powder (DBP) was prepared from ground bone allograft via acid extract-demineralization process. The particle sizes of demineralized bone were characterized through the scanning electron microscopy (SEM) as shown in Figure 4.7. The particle sizes of DBP were classified using a series of sieves including 500 micron, 250 micron, 125 micron, and 75 micron. The DBP was categorized into 3 ranges: 75-125 micron (Figure 4.7A, average =  $106.72 \pm 22.82$  micron), 125-250 micron (Figure 4.7B, average =  $199.73 \pm 34.23$  micron), and 250-500 micron (Figure 4.7C, average =  $354.58 \pm 69.25$  micron). The DBP showed random polygon spindle shape.

### **6. Morphology of various demineralized bone powder blended collagen scaffolds**

The three dimensional scaffolds were fabricated from various demineralized bone powder and collagen Type I. The scaffolds were developed into 4 types: (1) pure collagen scaffold (COL), (2) collagen scaffold blended with demineralized bone size 75-125 micron (D125), (3) collagen scaffold blended with demineralized bone size 125-250 micron (D250), and (4) collagen scaffold blended with demineralized bone size 250-500 micron (D500). The fabricated scaffolds showed cylindrical shape and smooth surface. The immersion of scaffolds in PBS did not affect shape. This indicated that they were stable when soaking in the body fluid for a while. (Figure 4.8)

The morphology and pore size of three dimensional scaffolds were observed using SEM as shown in Figure 4.9. The average pore sizes of three dimensional scaffolds including COL scaffold, D125 scaffold, D250 scaffold, D500 scaffold are  $142.95 \pm 21.57$  micron,  $130.52 \pm 16.26$  micron,  $122.92 \pm 21.38$  micron, and  $113.03 \pm 19.11$  micron, respectively.



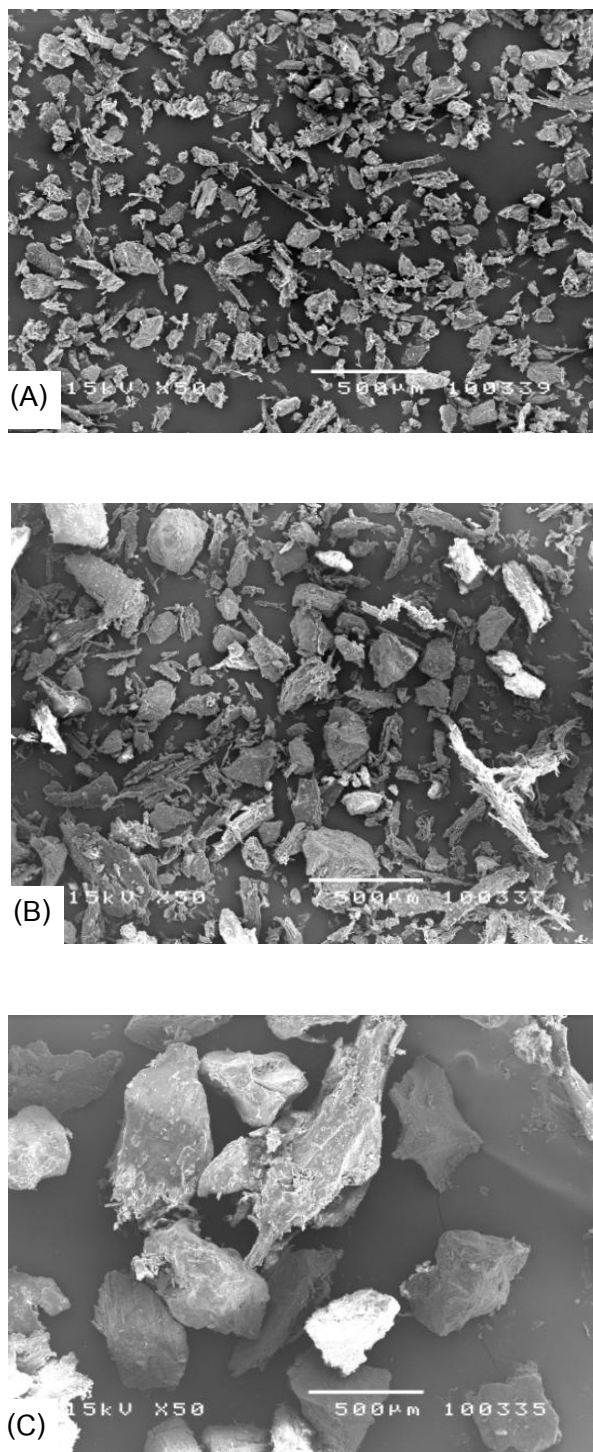


**Figure 4.7** The particle size of DBP in different ranges. (A) 75-125  $\mu\text{m}$  (B) 125-250  $\mu\text{m}$  (C) 250-500  $\mu\text{m}$  (white bar = 500  $\mu\text{m}$ , magnification 50X)

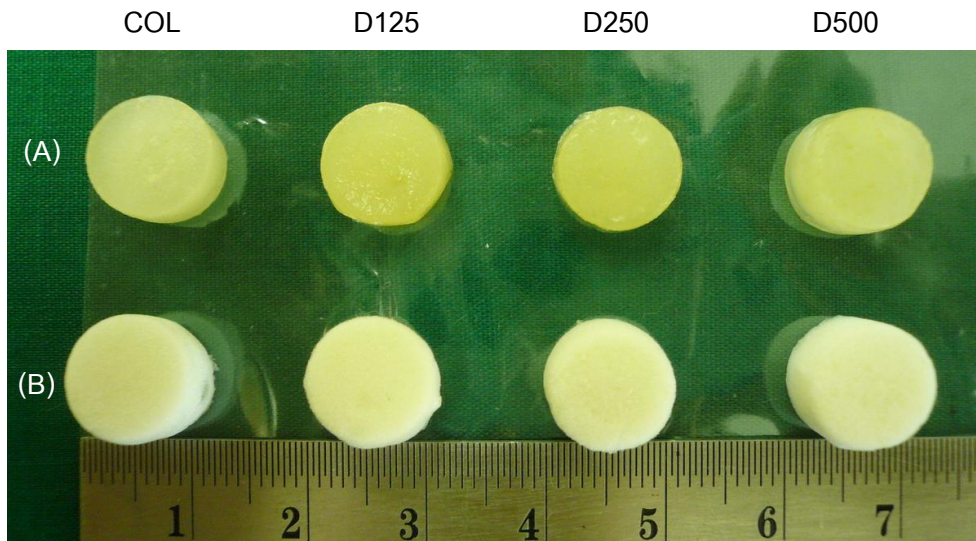


**Figure 4.8** Pure collagen scaffold and demineralized bone blended collagen scaffolds at different blending ratios. (A) Wet condition (B) Dry condition

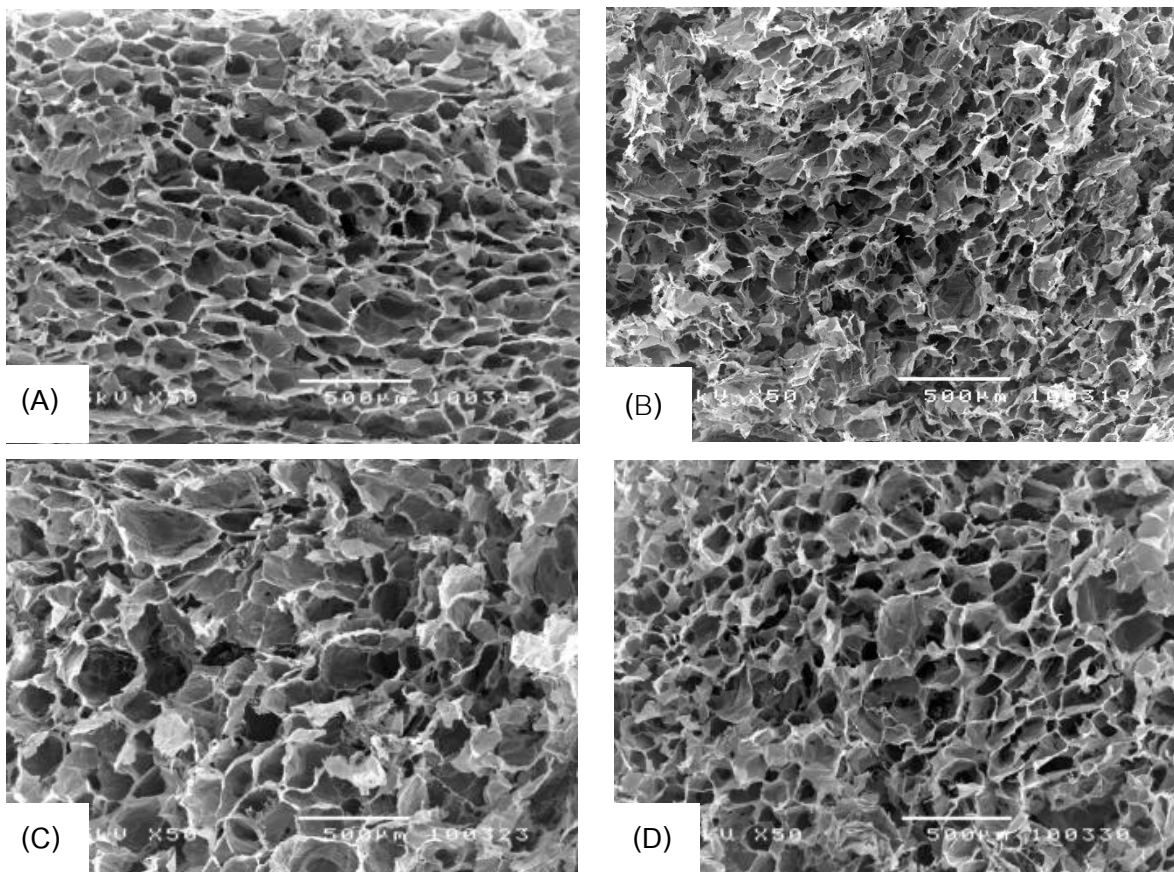


**Figure 4.9** The pore morphology of the pure collagen scaffold and various demineralized bone blended collagen scaffolds. (A) COL (B) D125 (C) D250 (D) D500 (white bar = 500 μm, magnification 50X)

### **7. Compressive modulus of the scaffolds**

The compressive modulus of three dimensional scaffolds was investigated using Universal testing machine (Instron55370) in order to evaluate the strength of scaffolds in dry and wet conditions (after swelling in PBS for 24 h). The result presented in Figure 4.10 showed that the compressive modulus of COL/DBP scaffolds with various particle size was higher than pure COL scaffolds. While in wet condition, the compressive modulus of all scaffolds was decreased. However, the compressive modulus of COL scaffolds and COL/DBP scaffolds did not have statistically significant difference.

### **8. Swelling property of the scaffolds**

The swelling ability is an important property of scaffold. The higher swelling ability could increase the bioactivity between cell and culture medium. The result on water absorption of pure collagen scaffold and collagen scaffold incorporated with demineralized bone powder was demonstrated in Figure 4.11. The highest relative swelling ratio, 59.5 times, was found in pure collagen scaffold. It was observed that the COL/DBP scaffolds resulted in the significantly lower swelling ability compared to the pure collagen scaffold ( $P < 0.001$ ). At the present of DBP in collagen scaffold, the relative swelling ratios of D125 scaffold, D250 scaffold, and D500 scaffold were approximately 17.4 times, 18.6 times, and 20.9 times, respectively. The lowest relative swelling ratio showed in the case of D125 scaffold (17.4 times) but no significant difference in among blended group.

The decreasing of water absorption might be due to the smaller pore size of scaffold with demineralized bone powder which was added. Furthermore, this might be because of the particle size of demineralized bone powder that inhibited the water absorption, resulting in the decrease of water absorption ability.

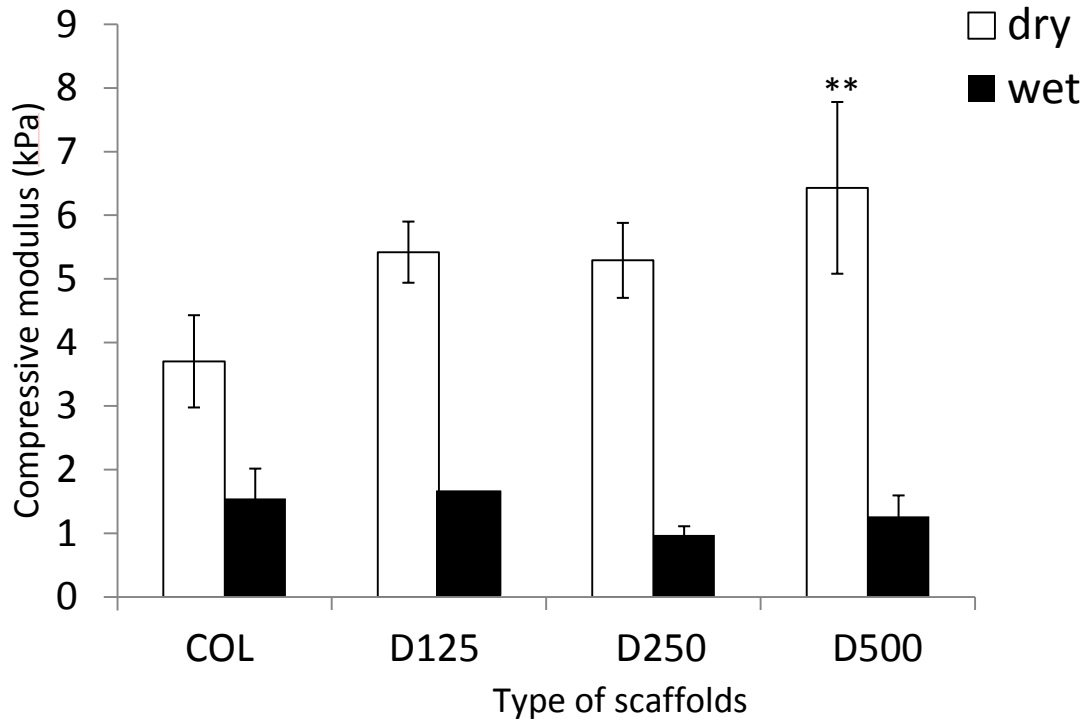


**Figure 4.10** The average compressive modulus of COL, D125, D250, and D500 scaffolds in dry and wet conditions. (\* represented statistically significant difference at  $P < 0.05$  compared with COL scaffold,  $n = 5$ ).

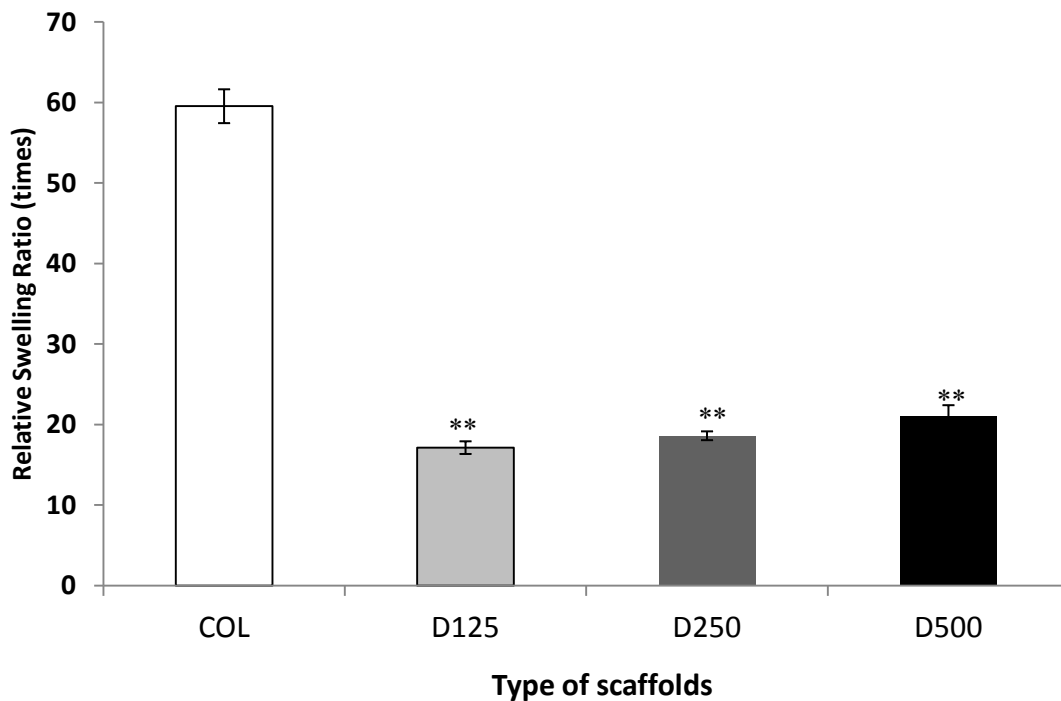


**Figure 4.11** The average swelling ability ratio of COL, D125, D250, and D500 scaffolds (\*\* represented statistically significant difference at  $P < 0.001$  compared with COL,  $n = 5$ ).

### 9. FT-IR analysis of the scaffolds

The chemical analysis of scaffolds was investigated by using FT-IR analysis. The FT-IR spectra obtained from collagen and demineralized bone powder scaffolds were displayed in Figure 4.12. From the spectrum of pure collagen, four characteristic absorption bands at the frequencies of 3300, 2925, 1660, and 1550 were observed. Generally, amide I bands ( $1660\text{ cm}^{-1}$ ) originated from C=O stretching vibrations coupled to N-H bending vibration. The amide II bands ( $1550\text{ cm}^{-1}$ ) arise from the N-H bending vibrations coupled to C-N stretching vibrations. The other two bands result from the stretching vibrations of free N-H group at  $2925\text{ cm}^{-1}$  and the vibration of hydroxyl group (-OH) at  $3300\text{ cm}^{-1}$  (Taravel et al., 1995; Tangsadthakun et al., 2007; Ratanavaraporn et al., 2009).

In contrast, the FT-IR spectra of D250 and D500 scaffolds at various particle sizes revealed the presence of  $\text{PO}_4^{3-}$  peak at  $1145\text{ cm}^{-1}$ .  $\text{HPO}_4^{2-}$  at  $875\text{ cm}^{-1}$  indicates the high levels of hydrogenphosphate ions (Šoptrajanov et al., 1999).  $\text{CO}_3^{2-}$  at  $1451\text{ cm}^{-1}$  demonstrates the carbonyl group (Frost et. al, 2009). These functional groups are the major components of carbonated hydroxyapatite in natural bone extracellular matrix

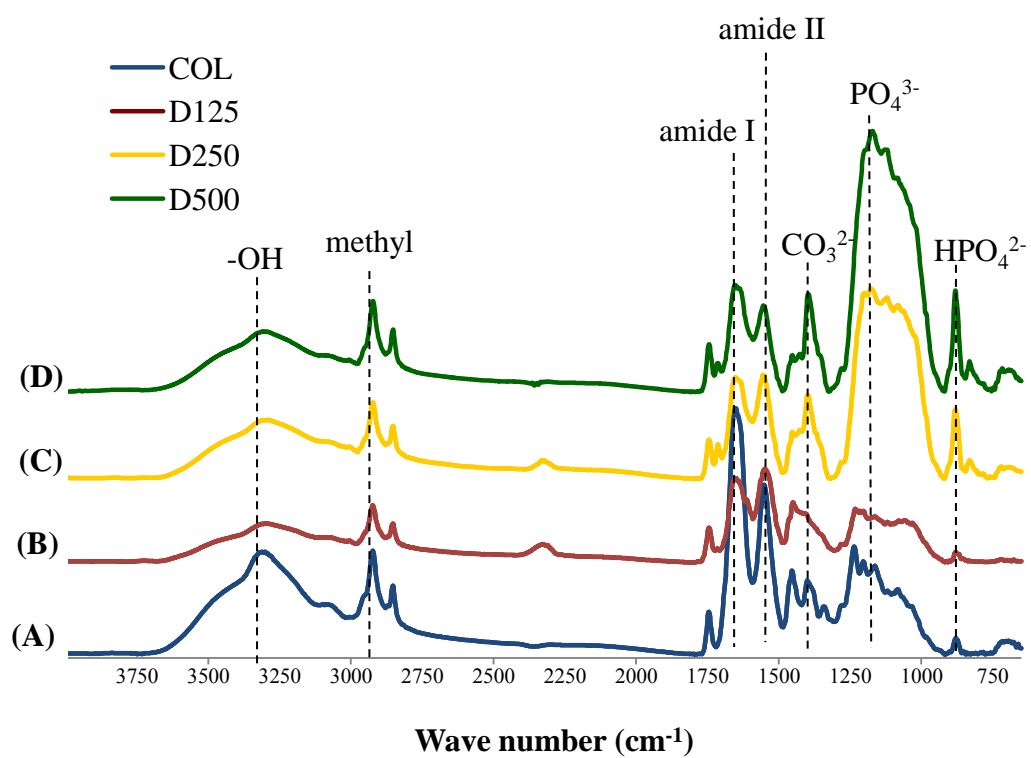


**Figure 4.12** FT-IR spectra of the different scaffolds (A) COL scaffold (B) D125 scaffold (C) D250 scaffold (D) D500 scaffold.

## **10. Biological characterization of the scaffolds**

### **10.1 Initial attachment and cell proliferation of PD cells cultured in collagen and demineralized bone powder scaffolds**

The evaluation of biological properties and osteogenic differentiation potential of the scaffolds were studied. Briefly, PD cells were seeded and cultured on pure collagen scaffold and collagen based scaffolds incorporated with DBP having various sizes for 6 hours, 1, 3 and 5 days. The attachment and proliferation of PD cells on scaffolds were analyzed by DNA quantitative assay as illustrated in Figure 4.13. It was observed that PD cells tended to attach and proliferate well on all scaffolds. It was also noticed that the number of PD cells proliferated on the collagen blended DBP were significantly lower than that on the pure collagen scaffold, indicating the hydrogel and biocompatibility effects of collagen which promote cell attachment and proliferation than collagen blended DBP scaffolds. In contrast, the number of PD cells which attached and proliferated on D125, D250, and D500 scaffolds were not different.

### **10.2 *In vitro* osteogenic differentiation test**

The scaffolds were investigated for osteogenic differentiation potential such as ALP activity and mineralization. For ALP activity, The PD cells were cultured on different scaffolds under osteogenic medium until 28 days. The ALP activity of PD cells was demonstrated in Figure 4.14. ALP activities of PD cells cultured on the D125, D250, and D500 scaffolds were significantly higher than that on the COL scaffold ( $P < 0.05$ ). In addition, it should be noticed that ALP activity on the COL scaffold blended DBP with the size of 250-500  $\mu\text{m}$  exhibited the maximum level among others.

For mineralization assay, the results showed that calcium content of PD cells cultured on the scaffolds were gradually increased until 28 days of culture. Calcium released from PD cells cultured on the D500 scaffolds were highest compared to other scaffolds. This finding is similar to the ALP activity result (Figure 4.15).

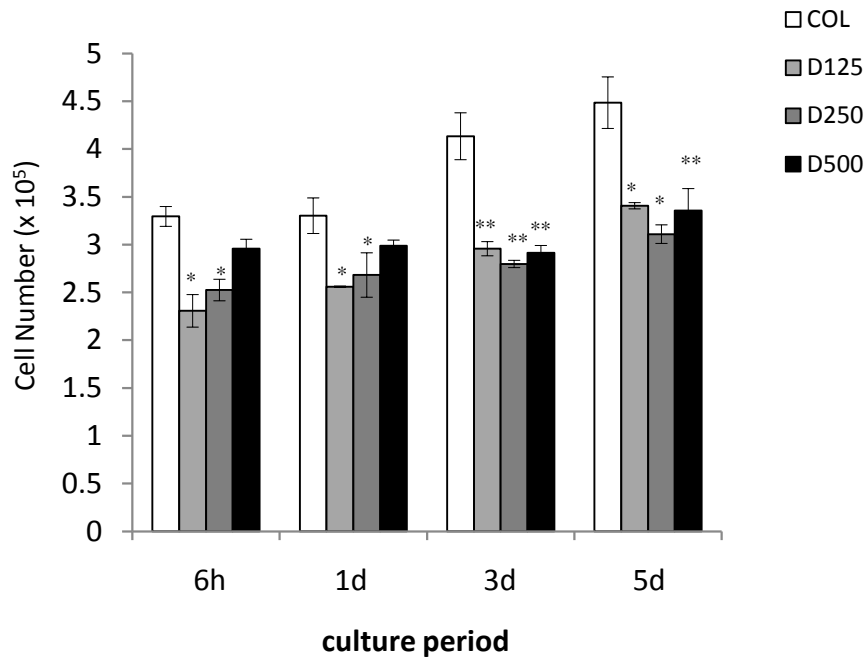


**Figure 4.13** Number of PD cells on COL, D125, D250, and D500 scaffolds at different blending ratios (\* and \*\* represented statistically significant difference at  $P < 0.05$  and  $P < 0.001$  relative to COL scaffold within each time period).

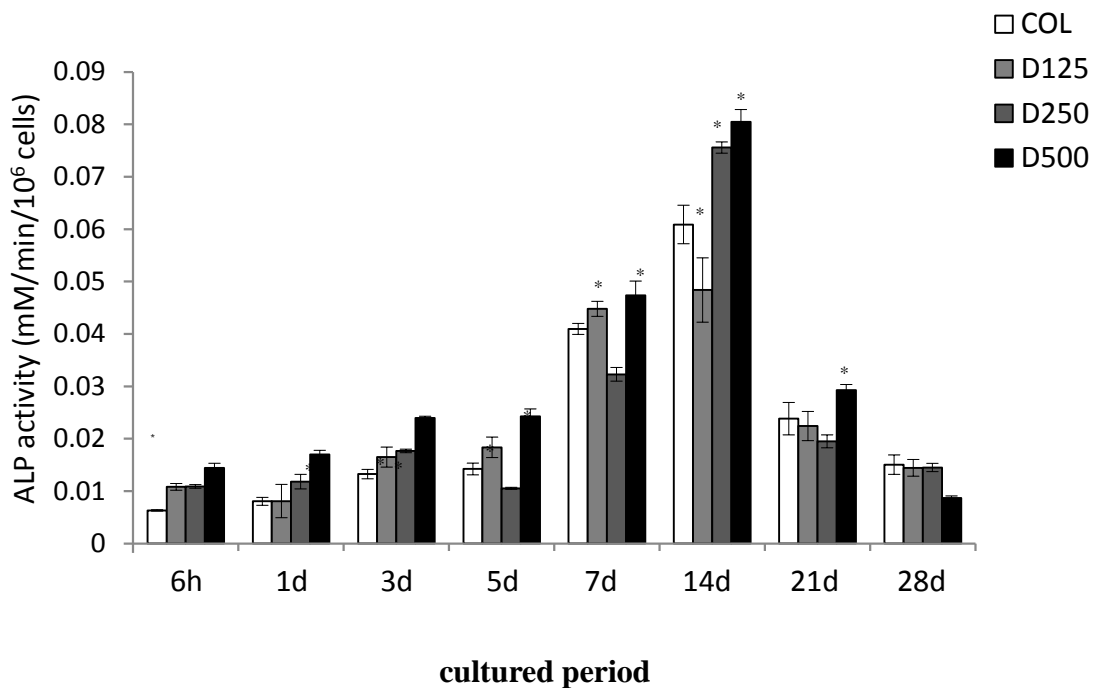


**Figure 4.14** ALP activity of PD cells cultured on COL, D125, D250, and D500 scaffolds in osteogenic medium (\* presented statistically significant difference at  $P < 0.05$  relative to COL within each time period).



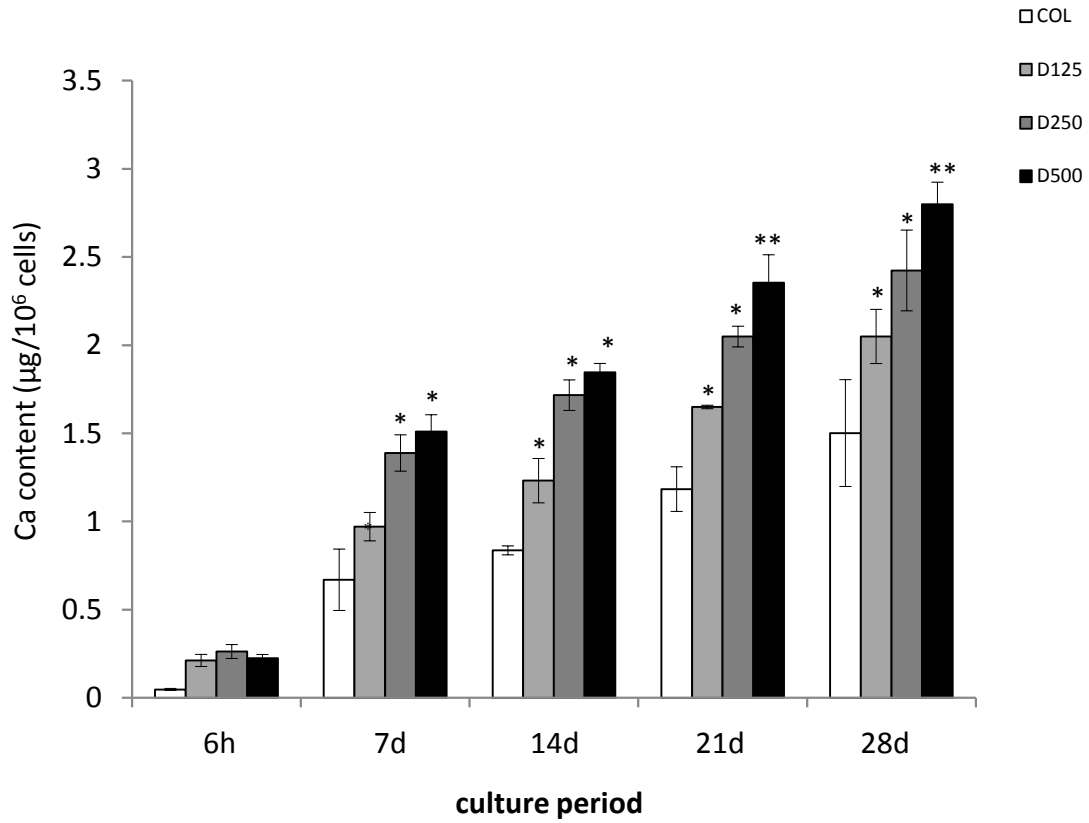


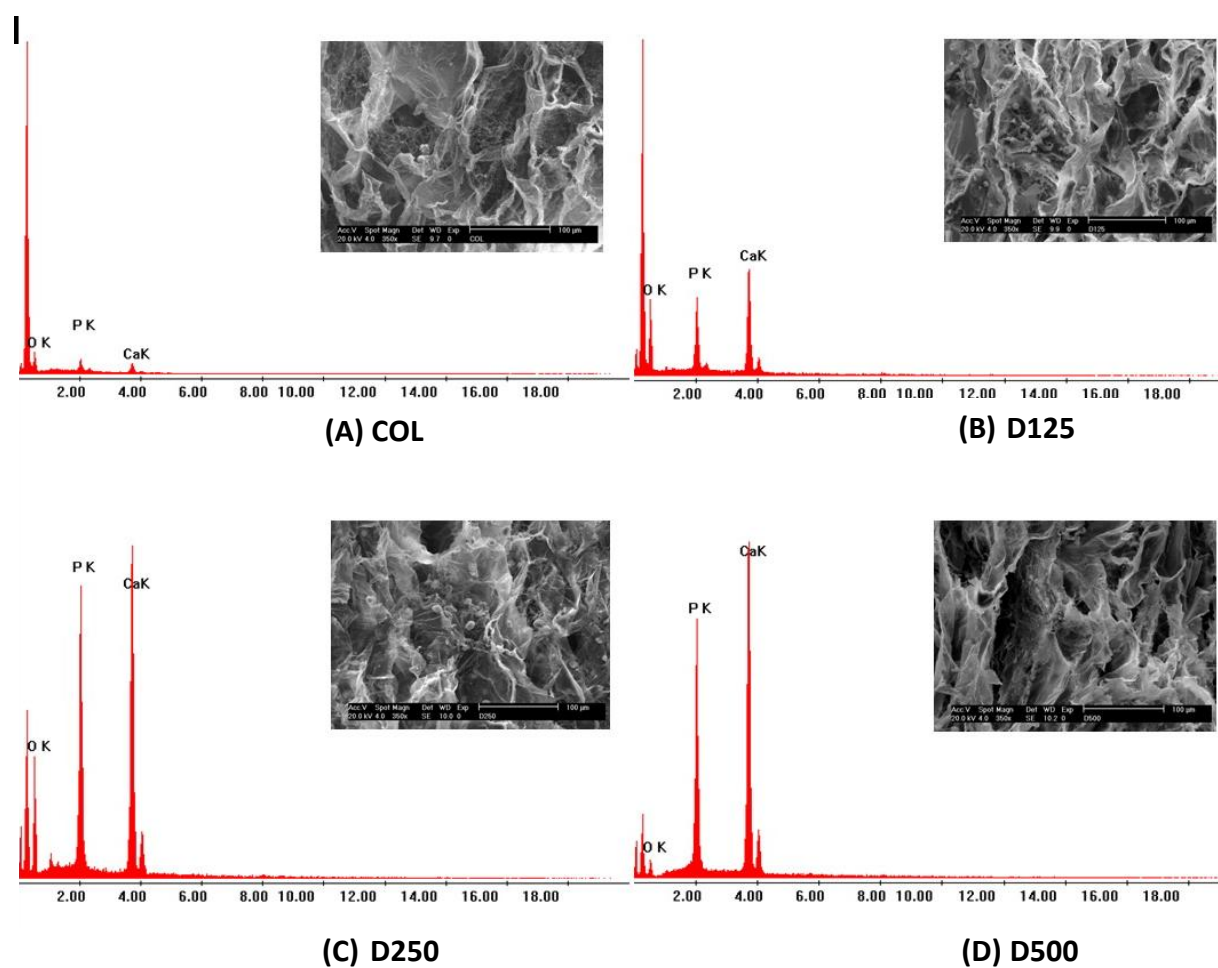
**Figure 4.15** Calcium level from the PD cells cultured on COL, D125, D250, and D500 scaffolds at different blending ratios for various times in osteogenic medium (\* and \*\* represented statistically significant difference at  $P < 0.05$  and  $P < 0.01$  relative to COL scaffold within each group).

Furthermore, the elements of cell surface were evaluated in order to prove that PD cultured cells in scaffolds were deposited minerals. After 28 days of culture under osteogenic condition, all samples were analyzed by energy dispersive X-ray spectroscopy (EDX). EDX results on the cell surface were summarized in Table 4.1. Calcium and phosphate contents on cell surface were found in all scaffolds. For the pure collagen scaffold (COL), the calcium deposited was approximately 6-15%. For the scaffold containing DBP, the calcium deposited observed in D125, D250, and D500 scaffolds was approximately 29-57%, 14-39%, and 22-31%, respectively. When we focused on the relative ratio of calcium to phosphorus (Ca : P), the results showed that for pure collagen scaffold, Ca : P ratio was in the range of 1.04–1.47 whereas the collagen scaffold containing demineralized bone powder showed higher ratios, 1.53–2.01, 1.32–1.61, and 1.58–1.74 in D125, D250, and D500 scaffolds, respectively (Figure 4.16).

In general, the Ca : P ratio of natural hydroxyapatite is estimatedly 1.67. It was found that D500 scaffold could provide nearest range of Ca : P among all scaffolds (1.58–1.74). The results suggested that Ca : P ratio of collagen scaffolds blended demineralized bone powder is higher than pure collagen scaffold. The incorporation of DBP into collagen scaffold showed relatively higher deposited calcium contents compared to the pure collagen scaffold. The EDX results corresponded to the calcium content reported in Figure 4.15.

**Table 4.1** Element analyses on PD cell surface after cultured on scaffolds

Type of scaffolds	O (%)	Ca (%)	P (%)	Ca : P
COL	71-90	6-15	4-14	1.04-1.47
D125	15-52	29-57	19-28	1.53-2.01
D250	38-82	14-39	9-23	1.32-1.61
D500	51-63	22-31	14-18	1.58-1.74

**Figure 4.16** Surface element of PD cells cultured on collagen and demineralized bone powder scaffolds under osteogenic medium for 28 days, analyzed by EDX. (A) COL (B) D125 (C) D250 (D) D500

### **10.3 Morphology of PD cells cultured collagen/demineralized bone powder scaffolds**

The morphology of PD cells cultured on pure collagen scaffolds and collagen scaffolds incorporated with various DBP was visualized by using SEM. Figure 4.17 (A, C, E, G) showed MSCs cultured on scaffolds in normal culture medium for 7 days. The results displayed that PD cells could be attached and proliferated on the surface of porous scaffolds.

For osteogenic differentiation, the PD cells were cultured in the condition of osteogenic medium for 28 days. Figure 4.17 (B, D, F, H) showed that PD cells in multi-layer and the extracellular matrix (ECM) of cells was observed on all scaffolds. The scaffolds incorporated with DBP at day 28 seemed to contain higher cell number and more ECM on the surface of scaffolds than those observed at day 7. The morphology of PD cells on collagen based scaffolds incorporated with DBP implied that all scaffolds were capable of supporting osteogenic differentiation of PD cells.

## **11. Summary**

From the results on characterization of three-dimensional collagen scaffolds blended with demineralized bone powder presented higher stability, and compressive modulus than pure collagen scaffold. Furthermore, COL/DBP scaffolds (D125, D250, and D500) were found to enhance osteogenic differentiation of PD cells when compared to pure collagen scaffold. The difference of ALP activity and calcium deposition between pure collagen scaffold and COL/DBP scaffolds were clearly observed.

Furthermore, collagen scaffold blended demineralized bone powder, particularly with the particle size of 250–500  $\mu\text{m}$ , showed excellent bioactivity for promoting osteogenic differentiation and mineralization when cultured with PD cells.

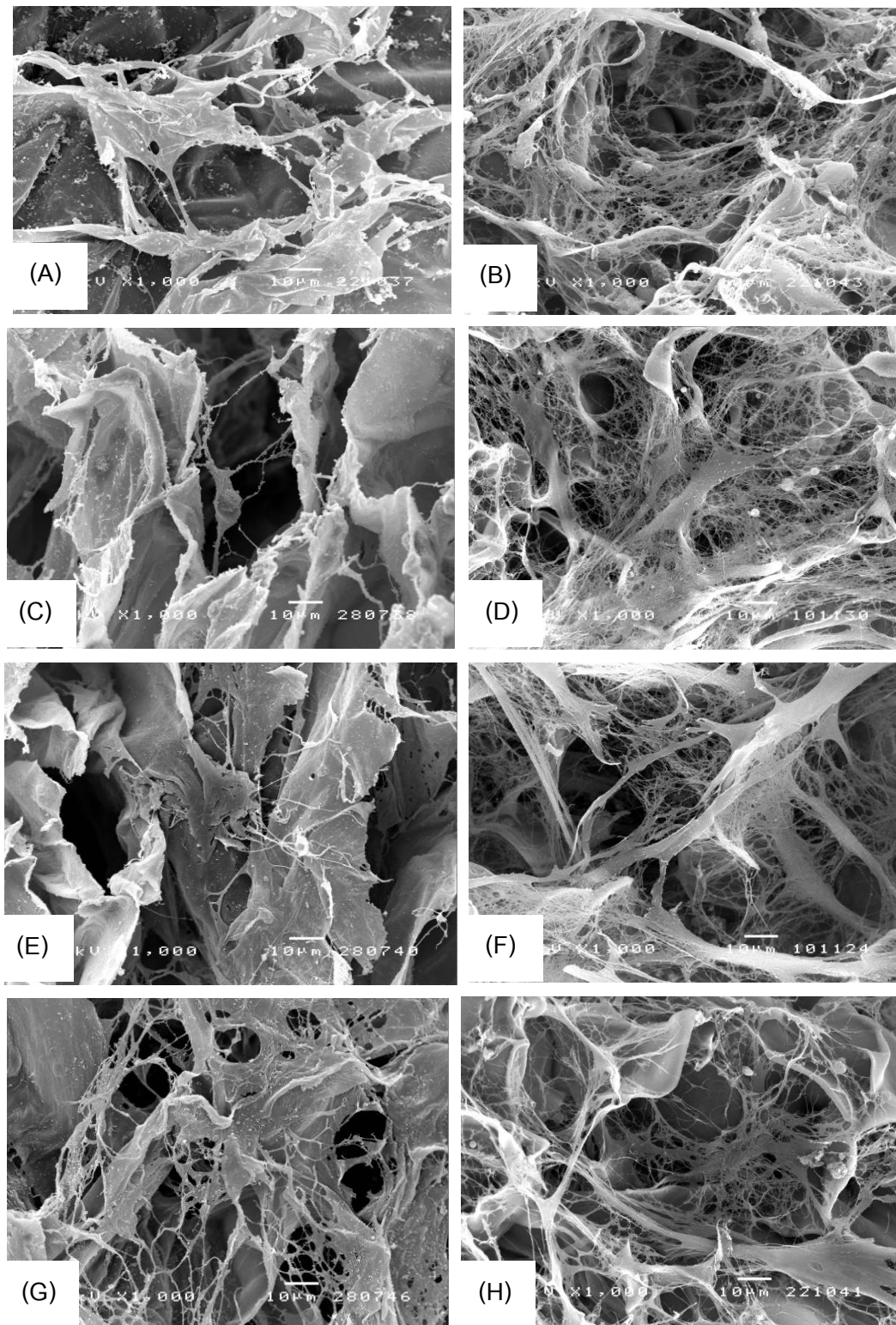


**Figure 4.17** The morphology of PD cells after cultured on scaffolds in normal culture medium at day 7. (A) COL (C) D125 (E) D250 (G) D500. The morphology of PD cells after cultured on scaffolds in osteogenic medium at day 28. (B) COL (D) D125 (F) D250 (H) D500 (white bar = 10  $\mu\text{m}$ , magnification 1000X)

### **Part III: Gelatin/chitooligosaccharide/demineralized bone powder scaffolds for bone tissue engineering**

After the study of the effects of the particle size of demineralized bone powder (DBP) which was blended with collagen scaffold on the morphology and mechanical properties of different scaffolds, DBP with the size of 250-500  $\mu\text{m}$  was selected. The DBP was blended with the combined material of gelatin and chitooligosaccharide (COS) in order to create the novel osteogenic potential scaffolds.

#### **12. Physical characterization of the scaffolds**

The novel scaffolds of gelatin, COS, and DBP were fabricated via freeze-drying and chemical crosslinking techniques. Glutaraldehyde was used as a crosslinking agent for these systems because it could crosslink between amino groups which were found in both gelatin and COS molecules. The glutaraldehyde-crosslinked scaffolds were washed with glycine and water to remove the residual aldehyde groups.

The scaffolds were vertically cut in order to observe the inner structure under SEM. The pore morphology of different scaffolds was shown in Figure 4.18. The average pore sizes of gelatin scaffold (G), gelatin/COS scaffold (GC), and gelatin/COS/DBP scaffold (GCD) were approximately  $125\pm 12$   $\mu\text{m}$ ,  $118\pm 17$   $\mu\text{m}$ , and  $111\pm 14$   $\mu\text{m}$ , respectively. The pore morphology illustration did not obviously different size but the average decreased pore size might be from the incorporation of COS and DBP into the blended solution.

The other physical properties of scaffolds including swelling ability ratio, percentage of weight loss, and percentage of porosity were shown in Table 4.2. The swelling ability is an important property of scaffold. The higher swelling ability could increase the bioactivity between cell and culture medium (Hutmacher et al., 2001).

The results on swelling ratio of G, GC, and GCD scaffolds were approximately 60.3 times, 39.5 times, and 20.7 times, respectively. The highest ratio of swelling ratio was found in G scaffold because gelatin could act as hydrogel which provided water or plasma inside. Furthermore, it was observed that the combined scaffolds such as GC scaffold and GCD scaffold showed decreasing of swelling ratio that might be associated with the decreasing of the amount of gelatin.

Porous structure is one of the main design criteria for bone tissue engineering scaffolds (Chen et al., 2008). The highly porous structures could improve mass transfer rate of oxygen and nutrients into the inner pores and also efficiently remove metabolic products (Li et al., 2003). In this study, the porosity of scaffolds measured by liquid displacement method was illustrated in Table 4.2. The result showed that all scaffolds showed high porosity. The highest porosity at 91% was found in G scaffold. It was also observed that the increase of the blended material resulted in the decrease of porosity in GC scaffold, and GCD scaffold approximately 88%, and 83%, respectively. Therefore, the addition of COS and DBP might reduce the porosity of the blended scaffolds.

The compressive modulus of G, GC, and GCD scaffolds were evaluated both dry and wet conditions, which were illustrated in Figure 14.19 (A) and (B), respectively. Firstly, in the case of dry scaffolds, compressive modulus of GCD scaffold (approximately 340 kPa) was significantly higher than that of the other blended and pure gelatin scaffolds. This might be due to the combination of demineralized bone powder which blended into the solution act as the reinforcing agents. However, in the wet state, compressive modulus of G, GC, and GCD scaffolds were approximately 36, 45, and 51 kPa but no statistical difference was found. The compressive modulus of all scaffolds was decreased in wet condition, approximately 4.6-6.7 times when compared to that in dry condition. Mostly, the protein based scaffold including gelatin which obtained from freeze-drying presented the high percentage of water absorption. Therefore, it acted as the hydrogel when it was wet, leading to a decreasing of mechanical strength (Drury and Mooney, 2003).

**Table 4.2** Physical characterization of the different scaffolds from gelatin, chitooligosaccharide, and demineralized bone powder

<b>Type of scaffolds</b>	<b>G</b>	<b>GC</b>	<b>GCD</b>
average pore size ( $\bar{x}$ )	125±12 $\mu\text{m}$	118±17 $\mu\text{m}$	111±14 $\mu\text{m}$
% porosity	90.6±5.3	88.2±3.5	82.9±4.6
swelling ratio (times)	60.3±5.4	39.5±4.3	20.7±2.9
% weight loss	11.6±4.2	11.0±2.2	4.6±2.0

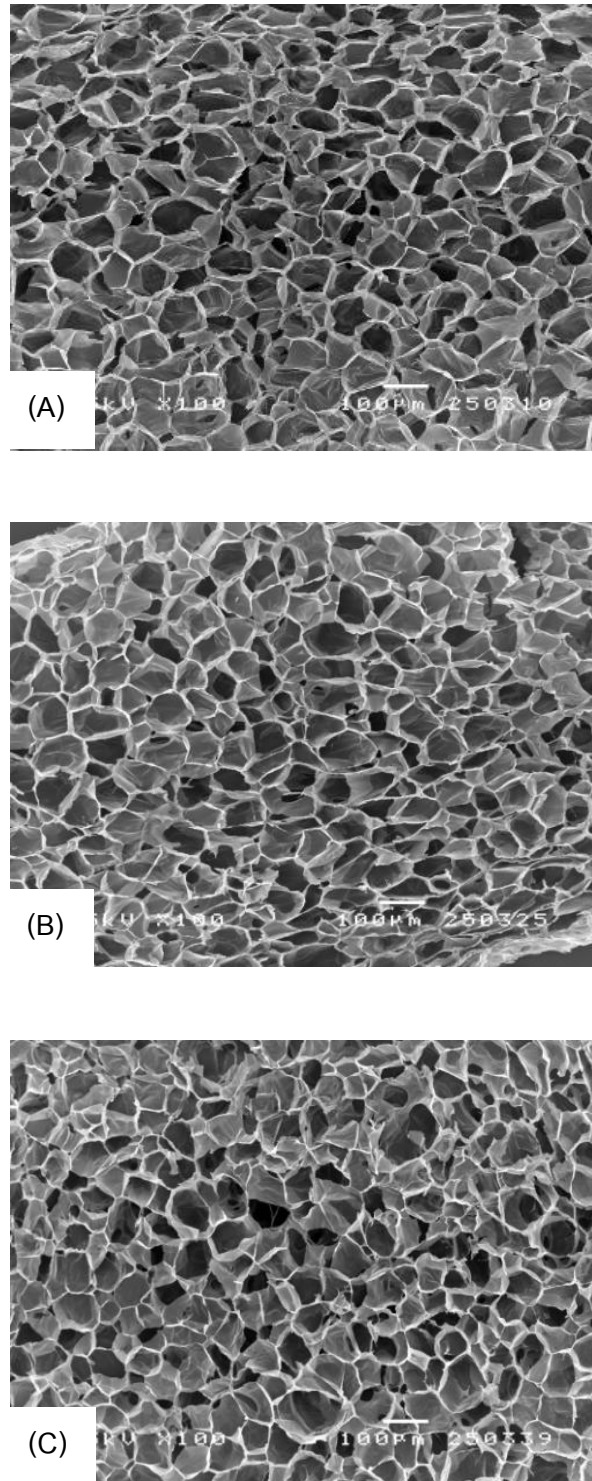


**Figure 4.18** The pore morphology of the gelatin/chitooligosaccharide/demineralized bone powder scaffolds. (A) G scaffold (B) GC scaffold (C) GCD scaffold (white bar = 100 µm, magnification 100X) G = gelatin scaffold, GC = gelatin/chitooligosaccharide scaffold, GCD = gelatin/chitooligosaccharide/demineralized bone powder scaffold



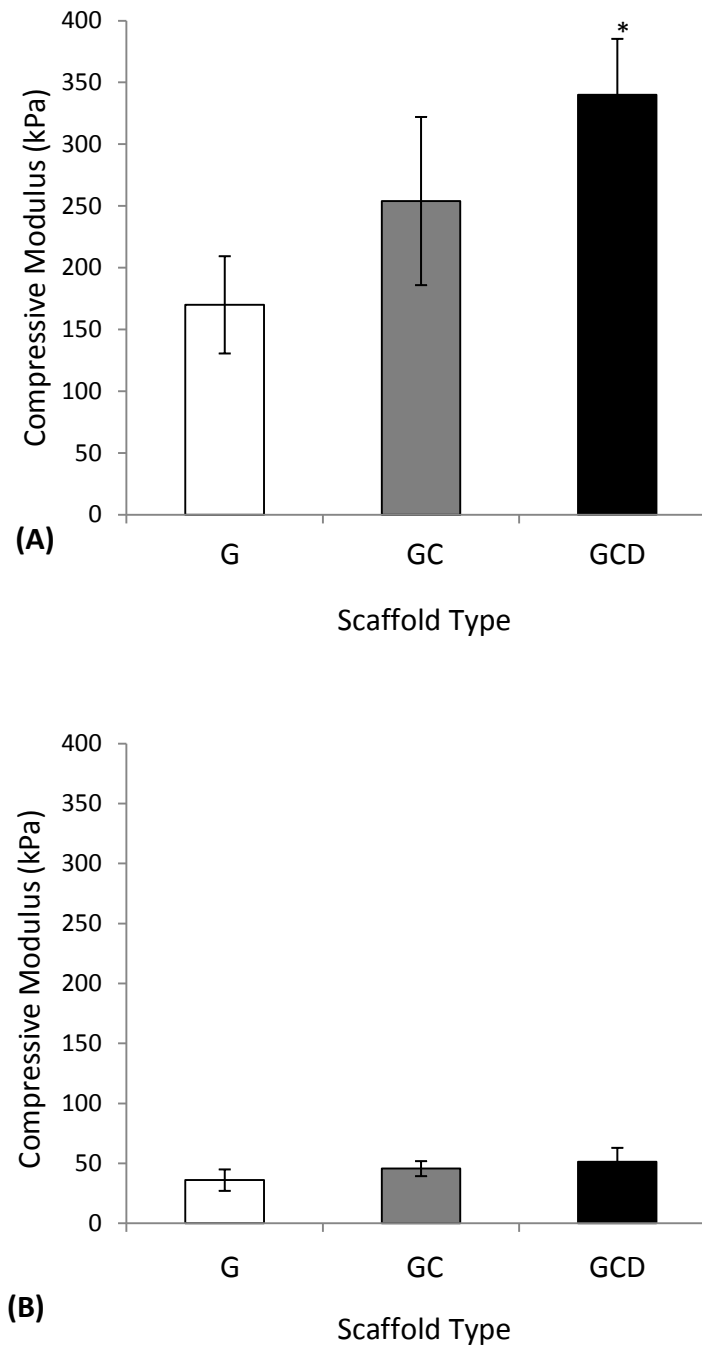


**Figure 4.19** Compressive modulus of G, GC, and GCD scaffolds (A) dry state and (B) wet state, analyzed by a universal testing machine (\* represented statistically significant difference relative to gelatin at  $P < 0.05$ ).

G = gelatin scaffold

GC = gelatin/chitoooligosaccharide scaffold

GCD = gelatin/chitoooligosaccharide/demineralized bone powder scaffold

### **13. Biological characterization of the scaffolds**

In this section, biological characteristics of gelatin scaffold (G), gelatin/COS scaffold (GC), and gelatin/COS/DBP scaffold (GCD), were presented as follows:

#### **13.1 Cell proliferation of PD cells cultured on scaffolds**

In this study, periosteum-derived (PD) cells were seeded and cultured on G, GC, and GCD scaffolds under proliferating medium ( $\alpha$ -MEM, 15% FBS, 100 U/ml penicillin/streptomycin) from 6 hours to 7 days. The number of attached and proliferated cells on scaffolds, analyzed by using DNA quantitative assay, was presented in Figure 4.20.

It was observed that PD cells could attach and proliferate on GC, and GCD scaffolds with the similar extent to those on pure gelatin scaffold. Furthermore, the number of both cells slightly increased during the culture period. Therefore, it could be implied from this investigation that the scaffolds prepared from gelatin, chitooligosaccharide, and demineralized bone powder could support cell activities. Thus, the scaffold was provided prior to the further study on osteogenic differentiation of PD cells.

After 6 hours of cell seeding, it could be noticed that there was no statistically significant difference in the number of cells adhered on all scaffolds. After 3 days of seeding, the significant differences in the number of proliferated cells was not found while they were observed increasing number of PD cells. After 5 days to 7 days of culture, it could be noticed that the number of proliferated cell on the scaffold incorporated with both COS and DBP tended to be slightly higher than the pure gelatin scaffold. However, the number of PD cells in the scaffolds during the culture period from 6 hours to 7 days was not different except at day 5.

Furthermore, the morphology of PD cells cultured on G, GC, and GCD scaffolds under proliferating medium for 7 days were demonstrated in Figure 4.24. The SEM results were noticed that PD cells attached and spreaded on the surface of all scaffolds. No difference in cell morphology was observed among three types of scaffolds. The results on attachment and proliferation of PD cells implied that the blended scaffolds from gelatin, chitooligosaccharide, and demineralized bone powder could obviously enhance the attachment and proliferation of PD cells.

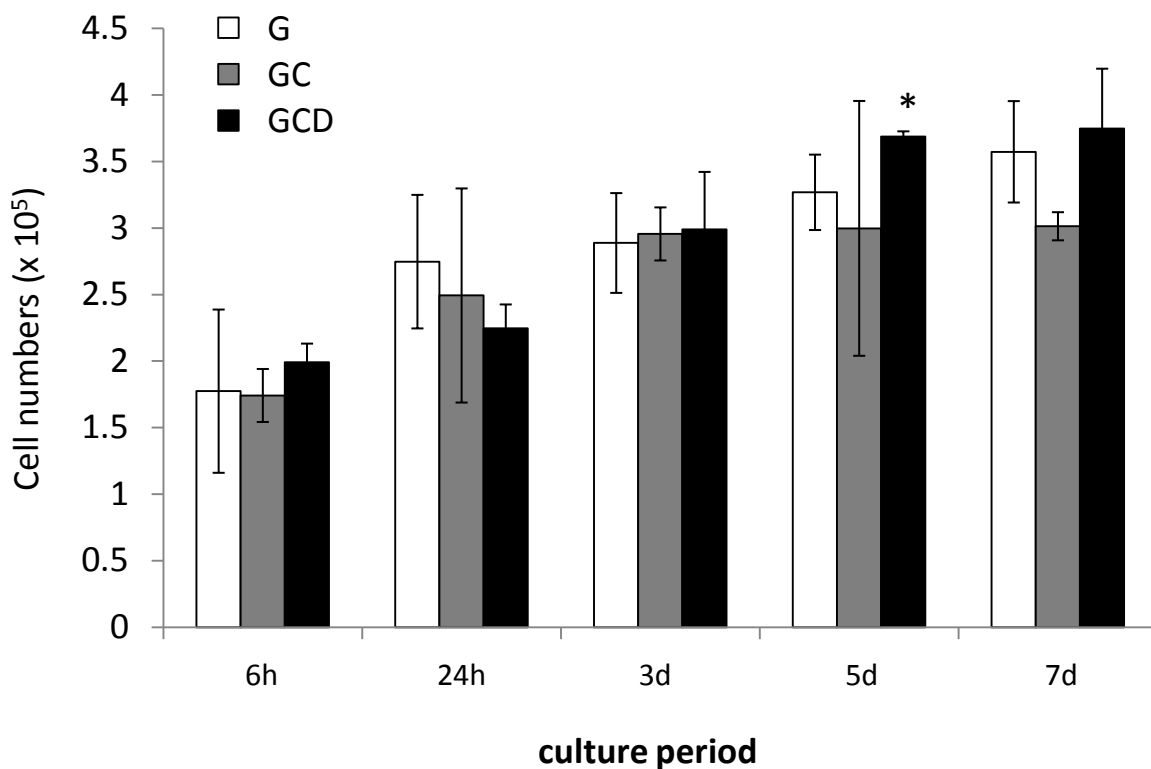


**Figure 4.20** Number of PD cells attached and proliferated on G, GC, and GCD scaffolds from 6 h to 7 days, assessed by DNA quantitative assay (\* represented a significant difference relative to gelatin within same culture period at  $P < 0.05$ ).

G = gelatin scaffold

GC = gelatin/chitoooligosaccharide scaffold

GCD = gelatin/chitoooligosaccharide/demineralized bone powder scaffold

### 13.2 Osteogenic differentiation test

In this section, the PD cells were cultured on the G, GC, and GCD scaffolds under the osteogenic medium for 28 days. The amount of total DNA of PD cells was measured in order to normalize the level of ALP activity and calcium deposition.

The ALP activity of PD cells cultured on the scaffolds under osteogenic medium was shown in Figure 4.21. A remarkable increase in ALP production of PD cells from day 3 to day 7 was observed in all scaffolds. The highest level of ALP activity in all groups of scaffolds was found at day 7. Comparison of ALP level produced by PD cultured cells found that the PD cells cultured in GCD scaffold had significantly higher ALP activity than those of the GC scaffold and G scaffold ( $P < 0.001$ ). ALP activity on all scaffolds were gradually decreased after day 7 until it reached the normal level at day 14.

The calcium deposition of PD cells cultured on G, GC, and GCD scaffolds under osteogenic medium was illustrated in Figure 4.22. The calcium deposition of PD cells cultured scaffolds was found since day 7 after cultivation. Mineralization gradually increased during the entire duration of the culture period. The highest calcium deposited along the culture period was found after 28 days of cultivation. The GCD scaffold exhibited the greatest amount of deposited calcium. The results were associated with the ALP activity data described earlier. Furthermore, the group of scaffolds that presented highest ALP activity also gave the highest calcium content.

Moreover, the morphology of PD cells cultured on G, GC, and GCD scaffolds under osteogenic medium for 28 days was illustrated in Figure 4.25. The results were noticed that the spreading of PD cells at 28 days was wider than those cultured at 7 days. The PD cells attached on GC and GCD scaffolds was found mineralized crystals.

The results supported the previous study that the calcium level analysis of PD cells which were cultured on the combined scaffolds made from gelatin, chitooligosaccharide, and demineralized bone powder could stimulate the highest level of calcium deposition.

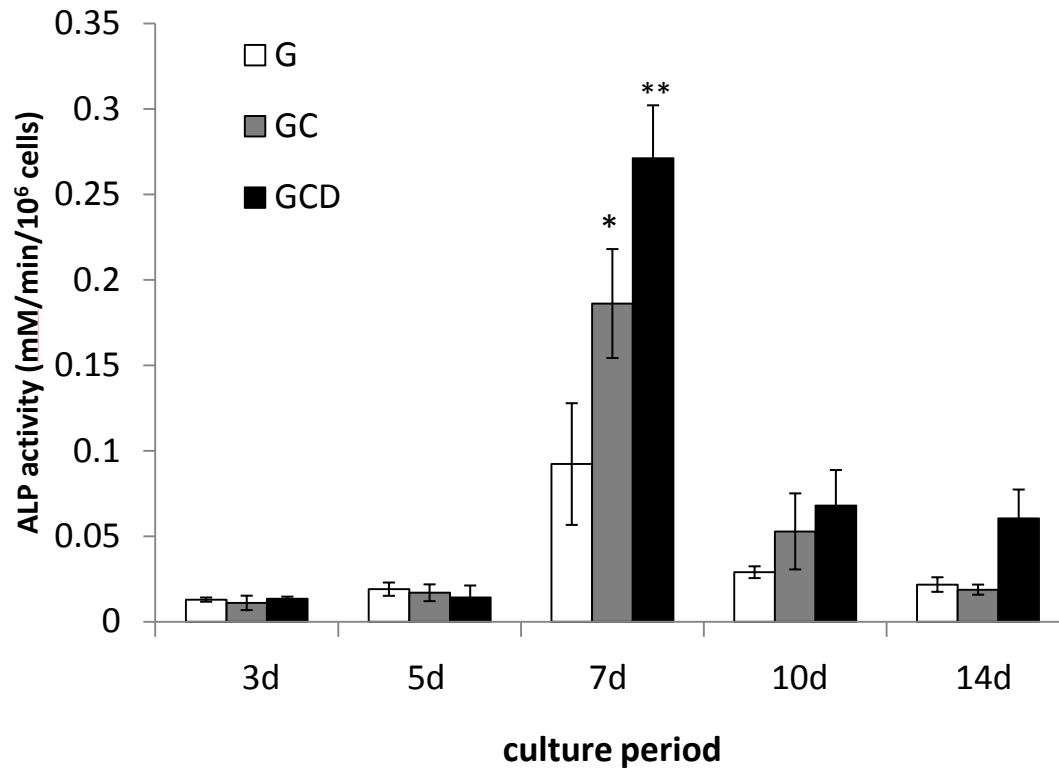


**Figure 4.21** ALP activity of PD cells cultured on G, GC, and GCD scaffolds under osteogenic medium from 3 days to 14 days (\* represented statistically significant difference relative to gelatin within same culture period at  $P < 0.05$ , \*\* represented statistically significant difference relative to gelatin within same culture period at  $P < 0.001$ ).

G = gelatin scaffold

GC = gelatin/chitoooligosaccharide scaffold

GCD = gelatin/chitoooligosaccharide/demineralized bone powder scaffold

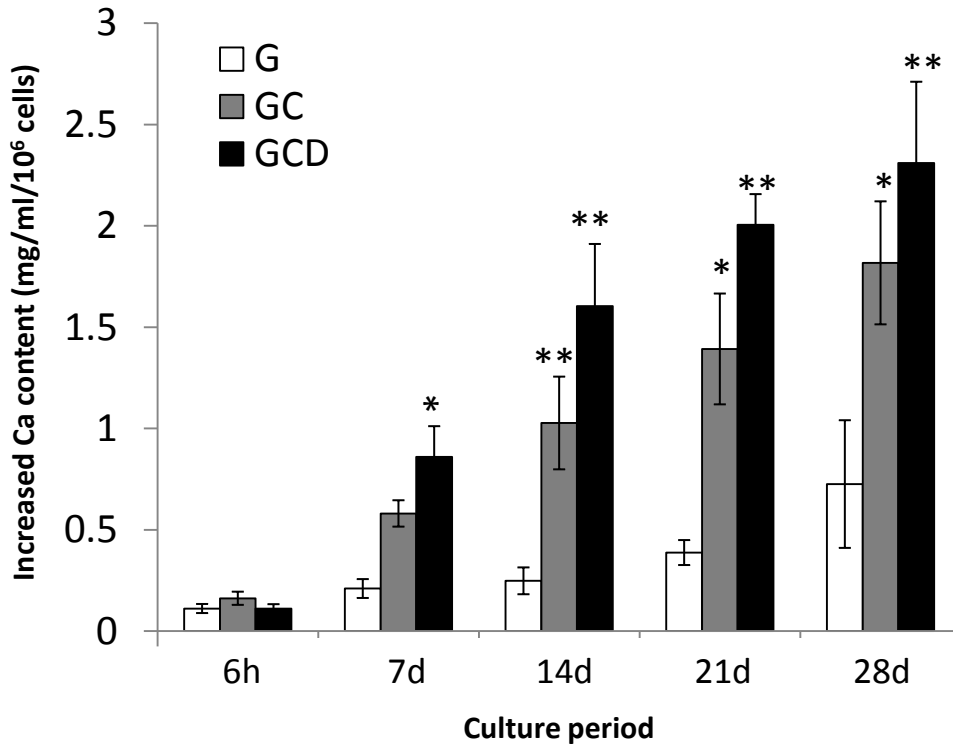


**Figure 4.22** Calcium content of PD cells cultured on G, GC, and GCD scaffolds under osteogenic medium from 6h to 28 days (\* represented statistically significant difference relative to gelatin within same culture period at  $P < 0.05$ , \*\* represented statistically significant difference relative to gelatin within same culture period at  $P < 0.001$ ).

G = gelatin scaffold

GC = gelatin/chitooligosaccharide scaffold

GCD = gelatin/chitooligosaccharide/demineralized bone powder scaffold

For gene expression of PD cells cultured with gelatin, chitoooligosaccharide, and demineralized bone powder scaffolds, total RNA were extracted from the PD cells cultured in different scaffolds together with osteogenic medium for 4 weeks under standard protocol. Then RT-PCR analysis was performed for osterix, runx2, BMP-2, ALP, Col I, and Osteopontin. The GAPDH was used as normalized control gene. The expression level of osteogenic indicator genes for PD cells cultured with G, GC, and GCD scaffolds were illustrated in Figure 4.23. The results showed that the PD cells cultured in different scaffolds had higher expression for osterix, runx2, BMP-2, ALP, Col I, and Osteopontin than that cultured cells without scaffolds (control). Furthermore, the PD cells cultured on GCD scaffolds had obviously expressed of runx2, and Col I when compared with other conditions. The results supported that the combination of biomaterial scaffold, GCD, showed up-regulation of osteogenic gene expression of PD cells. Moreover, the combination of gelatin and chitoooligosaccharide showed higher osteogenic expression than pure gelatin scaffold.

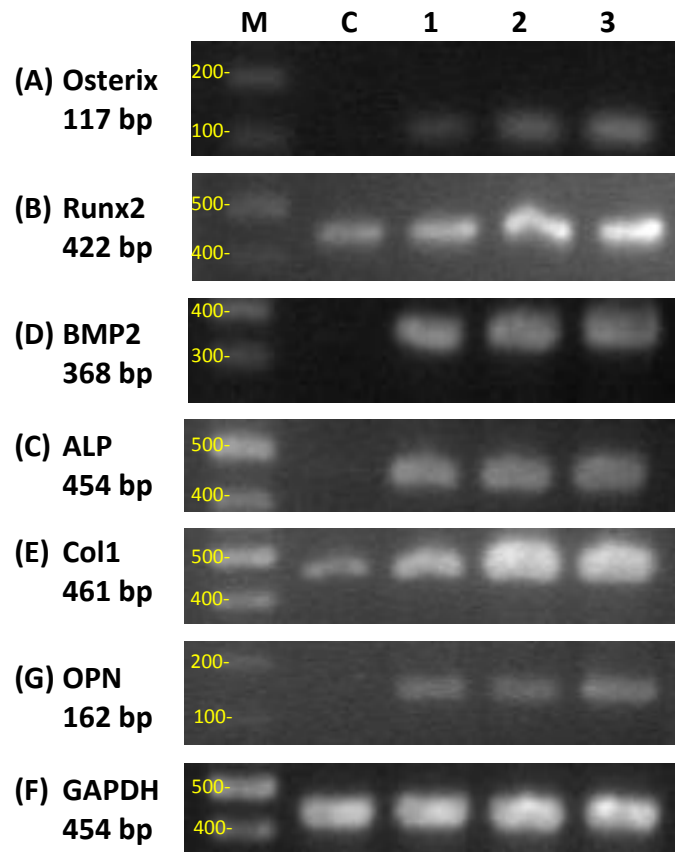


**Figure 4.23** A typical result of gel-electrophoresis of PCR products to evaluate the expression of PD cells cultured with combination of G, GC, and GCD scaffolds. (A) osterix (B) runx2 (C) BMP2 (D) ALP (E) Col1 (F) Osteopontin The amount of total RNA was standardized by the expression level of GAPDH (G). Lane M = DNA markers, lane C = control group, lane 1 = G scaffold, lane 2 = GC scaffold, lane 3 = GCD scaffold

G = gelatin scaffold  
 GC = gelatin/chitooligosaccharide scaffold  
 GCD = gelatin/chitooligosaccharide/demineralized bone powder scaffold



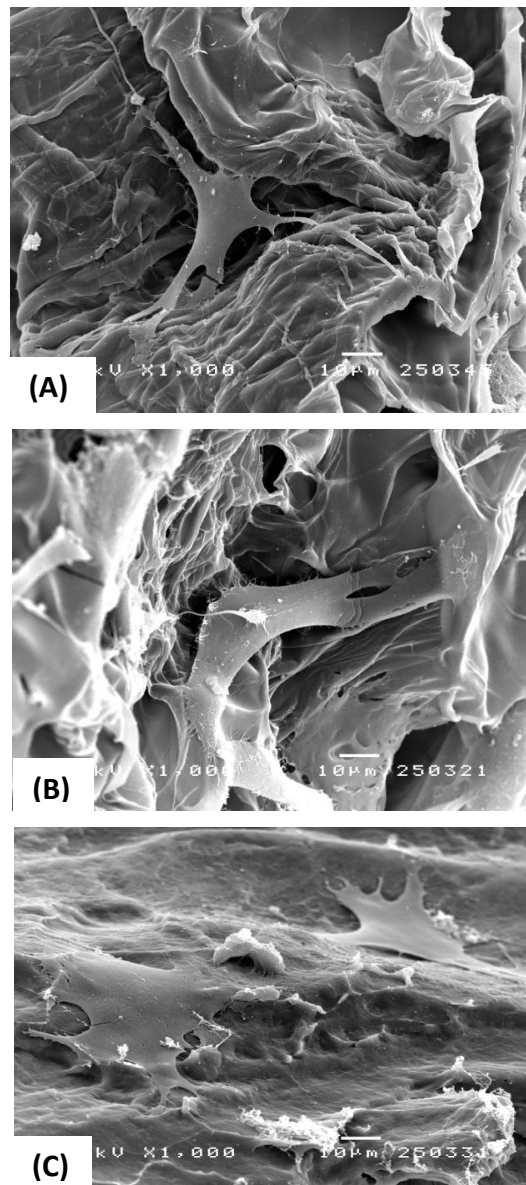


**Figure 4.24** Morphology of periosteum-derived cells cultured under proliferating medium for 7 days on the combined scaffolds from gelatin, chitoooligosaccharide, and demineralized bone powder. (A) G (B) GC (C) GCD scaffold. (scale bar = 10  $\mu\text{m}$ , magnification 1000X)

G = gelatin scaffold

GC = gelatin/chitoooligosaccharide scaffold

GCD = gelatin/chitoooligosaccharide/demineralized bone powder scaffold

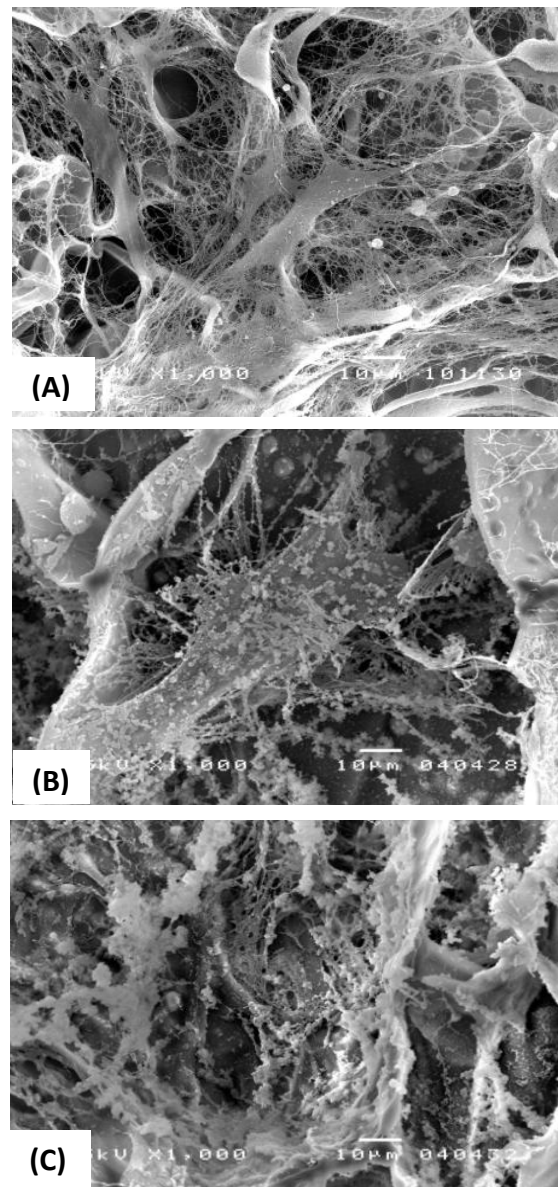


**Figure 4.25** Morphology of periosteum-derived cells cultured under osteogenic medium for 28 days on the combined scaffolds from gelatin, chitoooligosaccharide, and demineralized bone powder. (A) G (B) GC (C) GCD scaffold (scale bar = 10  $\mu\text{m}$ , magnification 1000X)

G = gelatin scaffold

GC = gelatin/chitoooligosaccharide scaffold

GCD = gelatin/chitoooligosaccharide/demineralized bone powder scaffold

Determination of calcium level in PD cells cultured scaffolds was applied in order to assure that PD cells cultured scaffolds had mineralization. The scaffolds cultured PD cells were evaluated the element of cell surface. After 28 days of culture in osteogenic medium, all samples were analyzed by energy dispersive X-ray spectroscopy (EDX) to confirm the production of calcium from PD cells. EDX results on the cell surface were summarized in Table 4.3. Calcium and phosphate contents on cell surface were found in all scaffolds. For the pure gelatin (G) scaffold, the deposited calcium was found approximately 10-13% whereas deposition of calcium was not found in the scaffolds without PD cells. For the gelatin/chitooligosaccharide (GC) scaffold, the calcium deposited was observed approximately 29-34% whereas in the scaffolds without PD cells were deposited calcium only 0-1%. For gelatin/chitooligosaccharide/demineralized bone powder (GCD) scaffold, the deposited calcium were observed approximately 20-44% whereas in the scaffolds without PD cells were deposited calcium only 1-2%. When we focused on relative ratio of calcium to phosphorus (Ca : P), the results showed that for pure collagen scaffold found Ca : P deposit in range 1.84–2.00 whereas the GC scaffold and GCD scaffold were found higher Ca : P deposit approximately 1.47–1.81, 1.66-1.76, respectively (Figure 4.26).

In general, the Ca : P ratio of natural hydroxyapatite is estimately 1.67. It was found that the GCD scaffold provided closest range of Ca : P among the other groups (1.66-1.76). The results suggested that Ca : P ratio of combined scaffold from gelatin/chitooligosaccharide /demineralized bone powder is higher than the other scaffolds. The EDX data associated with the calcium content reported in Figure 4.22.

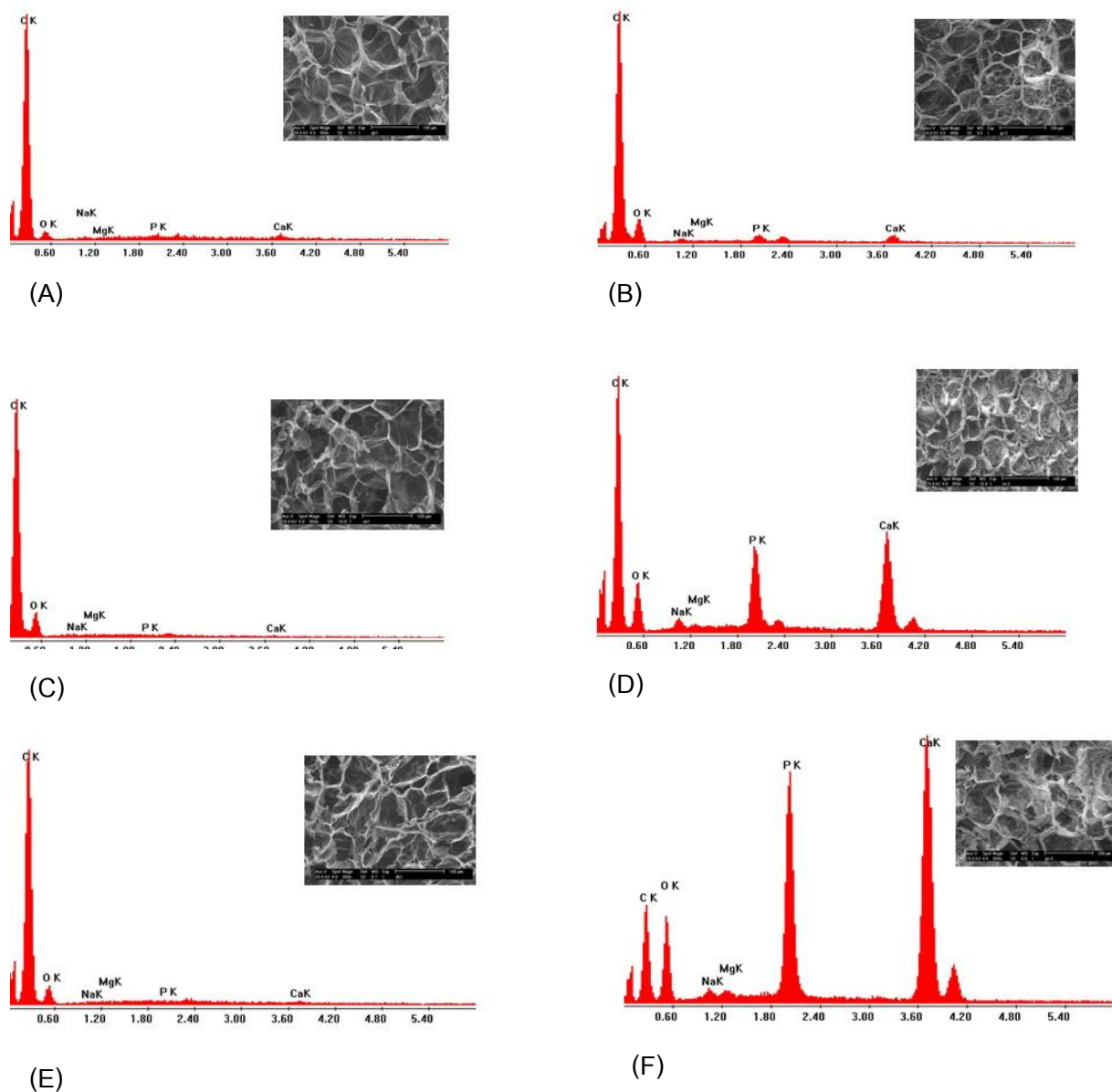


**Figure 4.26** Surface element of PD cells cultured on G, GC, and GCD scaffolds under osteogenic medium for 28 days, analyzed by EDX. (A) G scaffold without cells, (B) G scaffold with PD cells, (C) GC scaffold without cells, (D) GC scaffold with PD cells, (E) GCD scaffold without cells, (F) GCD scaffold with PD cells

G = gelatin scaffold

GC = gelatin/chitooligosaccharide scaffold

GCD = gelatin/chitooligosaccharide/demineralized bone powder scaffold

**Table 4.3** Weight percentage of elemental analyses on PD cells surface after 28 days cultured in osteogenic medium compared with non-cell seeding condition.

(A)

Type of scaffolds	Wt% (without PD cells)					
	O	Na	Mg	Ca	P	Ca : P
G	81-85	9-15	5-18	0	2-4	0
GC	77-88	4-8	3-8	0-1	3-5	0-0.2
GCD	68-83	5-13	7-18	1-2	3-5	0.33-0.4

(B)

Type of scaffolds	Wt% (with PD cells)					
	O	Na	Mg	Ca	P	Ca : P
G	56-61	7-9	1-2	10-13	20-24	1.84-2.00
GC	27-41	5-7	4-7	29-34	16-23	1.47-1.81
GCD	60-75	5-10	3-5	20-44	12-25	1.66-1.76

The results verified that the percentage of increased surface elements of PD cells were presented in Table 4.3. The results demonstrated that they had the content of oxygen, phosphorus and calcium. When focused on the GCD scaffolds, they showed Ca : P ratio closest to Ca : P ratio in theoretical hydroxyapatite (1.67).

#### **14. Summary**

From the study of this part, the results showed that the scaffolds produced from gelatin, chitooligosaccharide, and demineralized bone powder could promote attachment, proliferation, osteogenic differentiation, and bone matrix production of PD cells. Especially, the PD cells cultured in GCD scaffolds exhibited higher osteogenic differentiation than those cultured in G and GC scaffolds. The PD cells cultured in GCD scaffolds showed increasing of the ALP activity, calcium deposition, mineralization, and osteogenic gene expression. Demineralized bone powder which blended in the scaffolds could enhance the osteogenic differentiation of PD cells and be able to utilize for bone regeneration. The developed scaffolds have osteogenic capacity for stimulating new bone formation that can be applied in bone tissue engineering in *in vivo* model.

### **15. Osteogenic differentiation potential of gelatin/chitooligosaccharide/demineralized bone powder scaffolds in animal model**

In this study, the sterilized scaffolds of G, GC, and GCD scaffolds were implanted into the subcutaneous sites of male Wistar rats for 4 weeks and 8 weeks. After post-implantation, each sample were analyzed to detected the increased calcium content and evaluated specific staining for detect new bone osteoid and mineralization. Firstly, the increasing calcium content of scaffold implants was quantified using calcium assay with standard protocol (Figure 4.27). The results showed that the calcium level was increased from 4 weeks to 8 weeks with statistically significant difference ( $P<0.05$ ). Furthermore, the calcium level of the GCD scaffold implant was significantly higher than that of the other groups during the same time ( $P<0.001$ ).

For specific histological staining, the explants were fixed in 10% formalin solution, embedded in paraffin blocks, then sliced and placed on the slide. All slides were stained with hematoxylin and eocin (H&E) in order to evaluate the osteoid formation. H&E staining of explants results were shown in Figure 4.28 for 4 weeks post implantation and Figure 4.29 for 8 weeks post implantation. For 4 weeks analysis, the new bone formation, osteoid, was observed which indicated with black arrows. The ostoid area showed light pink area located near the remnant scaffold fragments (strong red area) which distributed around the slide. For 8 weeks analysis, the osteoid areas were observed greater than 4 weeks after implantation for each condition. Especially for GCD scaffold explants, the H&E stains were showed larger osteoid area and more homogeneity of osteoid area than the other scaffold explants.

Bone histomorphometry was analyzed from H&E results using Image Pro Plus program. The results were represented in Figure 4.30. The results demonstrated that the osteoid area was increased from 4 weeks to 8 weeks with statistically significant difference ( $P<0.05$ ). Furthermore, the GCD scaffold explants showed greater osteoid area than GC scaffold and G scaffold with statistically significant difference ( $P<0.001$ ).

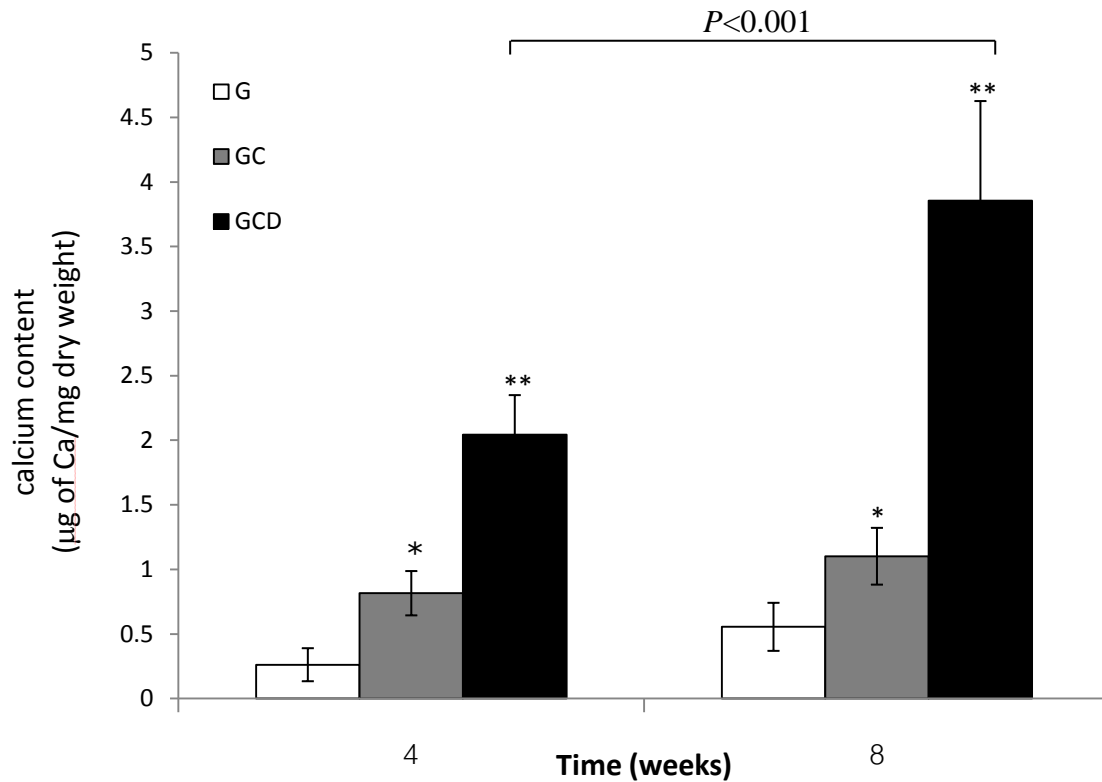


**Figure 4.27** Deposited calcium of scaffolds after implantation in Wistar rats. \* represented a significant difference relative to gelatin within same culture period at  $P<0.05$ , \*\* represented a significant difference relative to gelatin within same culture period at  $P<0.001$ .

G = gelatin scaffold

GC = gelatin/chitooligosaccharide scaffold

GCD = gelatin/chitooligosaccharide/demineralized bone powder scaffold



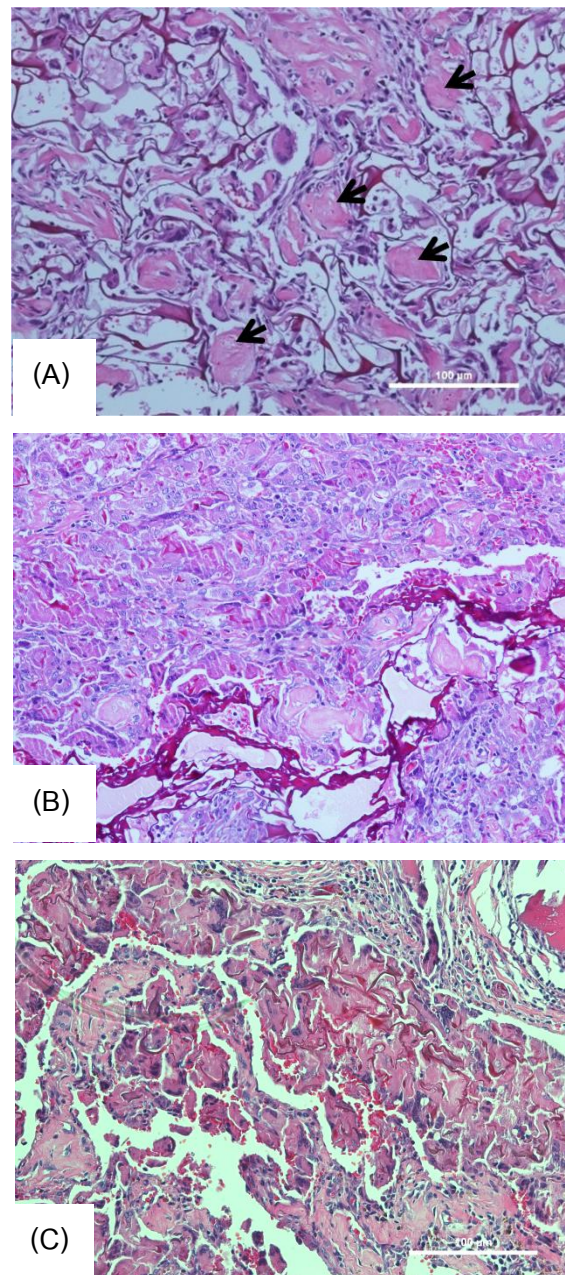


**Figure 4.28** H&E histological sections of subcutaneously implanted G, GC, and GCD scaffolds in Wistar rat at 4 weeks post implantation. (A) G scaffold (B) GC scaffold (C) GCD scaffold: Black arrow = osteoid formation area

G = gelatin scaffold

GC = gelatin/chitooligosaccharide scaffold

GCD = gelatin/chitooligosaccharide/demineralized bone powder scaffold

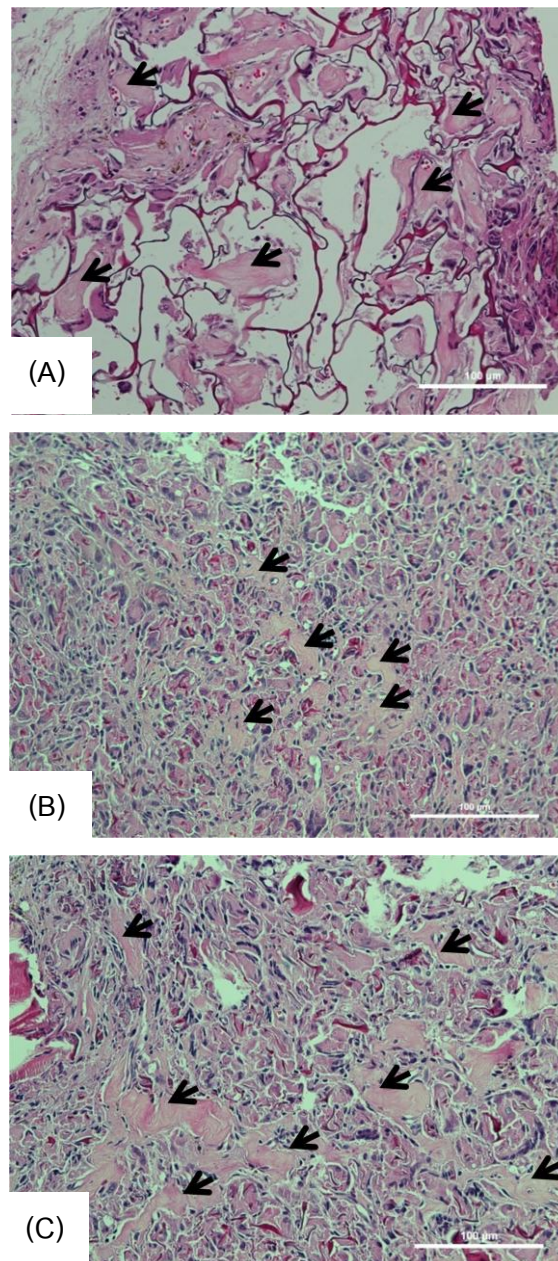


**Figure 4.29** H&E histological sections of subcutaneously implanted G, GC, and GCD scaffolds in Wistar rat at 8 weeks post implantation. (A) G scaffold (B) GC scaffold (C) GCD scaffold: Black arrow = osteoid formation area

G = gelatin scaffold

GC = gelatin/chitooligosaccharide scaffold

GCD = gelatin/chitooligosaccharide/demineralized bone powder scaffold

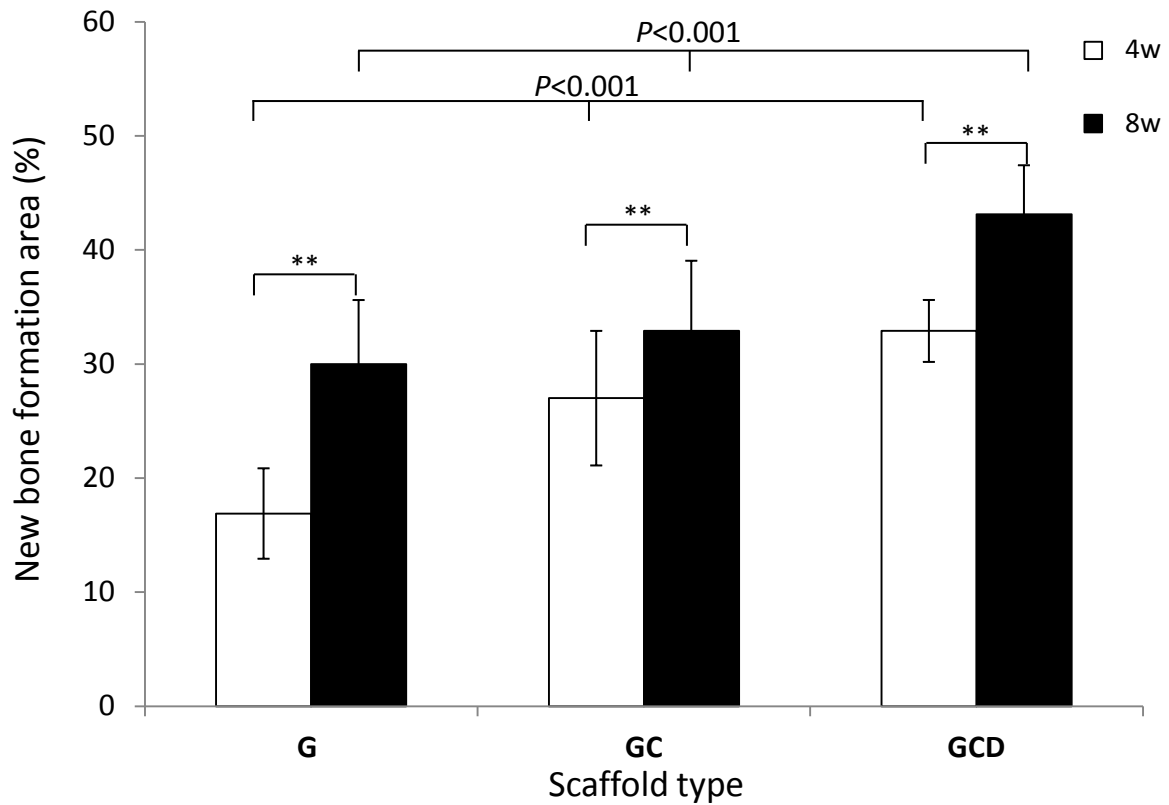


**Figure 4.30** Histomorphometric analysis of H&E sections of subcutaneously implanted G, GC, and GCD scaffolds in Wistar rat after 4 weeks and 8 weeks of implantation. \*\* represented a significant difference during the same period of implantation at  $P < 0.001$ .

G = gelatin scaffold

GC = gelatin/chitooligosaccharide scaffold

GCD = gelatin/chitooligosaccharide/demineralized bone powder scaffold

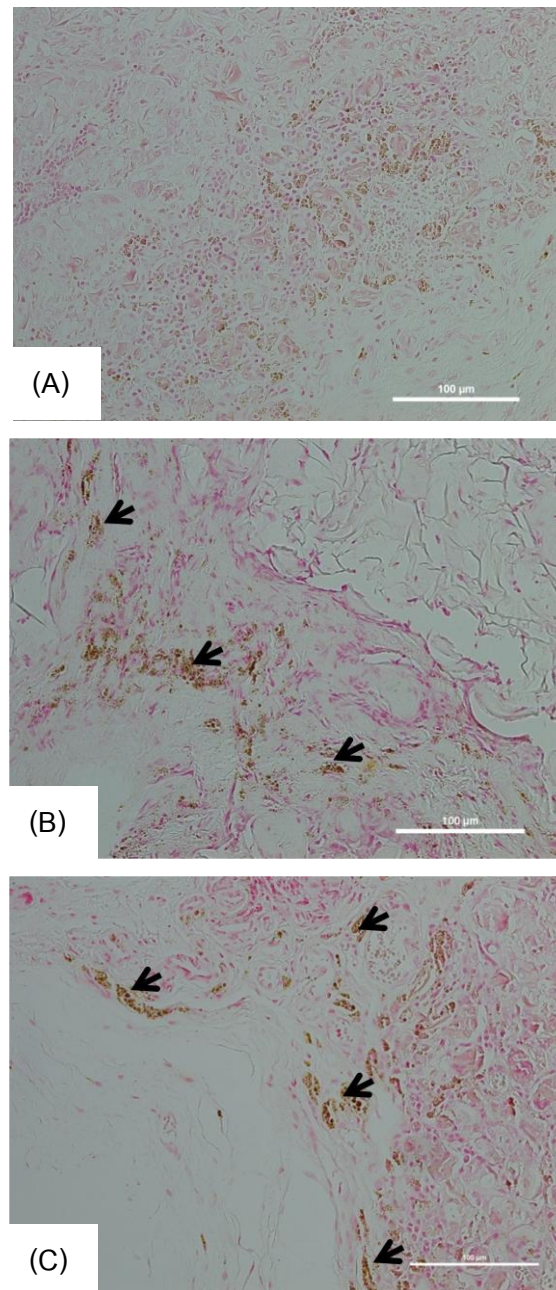


**Figure 4.31** von Kossa histological sections of subcutaneously implanted G, GC, and GCD scaffolds in Wistar rat at 8 weeks post implantation. (A) G scaffold (B) GC scaffold (C) GCD scaffold

G = gelatin scaffold

GC = gelatin/chitooligosaccharide scaffold

GCD = gelatin/chitooligosaccharide/demineralized bone powder scaffold

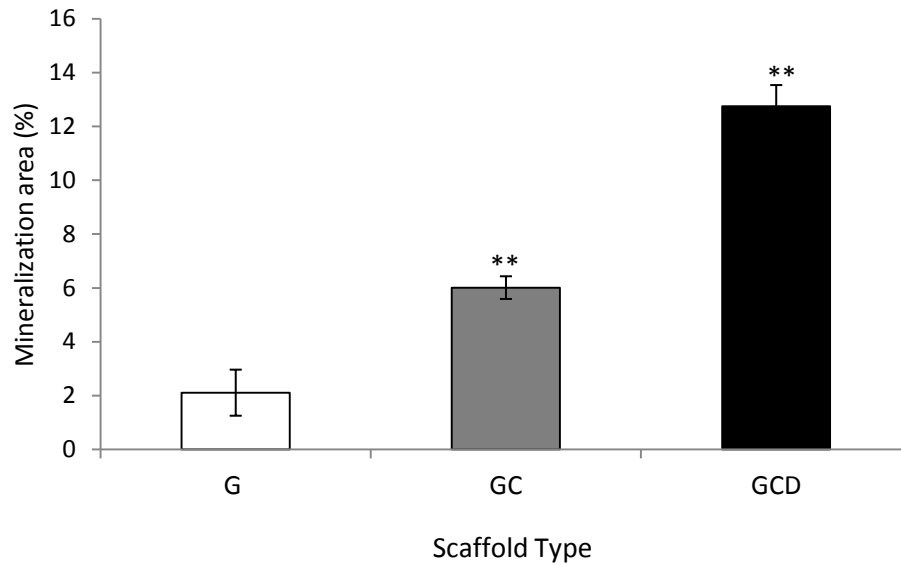


**Figure 4.32** Histomorphometric analysis of von Kossa sections of subcutaneously implanted G, GC, and GCD scaffolds in Wistar rat after 4 weeks and 8 weeks of implantation. \*\* represented a significant difference relative to gelatin within same culture period at  $P < 0.001$ ).

G = gelatin scaffold

GC = gelatin/chitooligosaccharide scaffold

GCD = gelatin/chitooligosaccharide/demineralized bone powder scaffold

To verify the mineralization of the implanted scaffolds, all sample slides were stained with von Kossa in order to evaluate the calcium deposit. H&E staining of explants results were shown in Figure 4.31 for 8 weeks post implantation. In von Kossa staining analysis, the mineralization area was observed as brown color area. The mineralization area was detected and distributed around the slide. Especially in GCD scaffold explants, the mineralization area in GCD scaffold was greater than that in the other scaffold explants.

Mineralization was analyzed from von Kossa results using Image Pro Plus program. These images were measured using Image Pro Plus program. The results were represented in Figure 4.32. The results demonstrated that the mineralization area was increased from the G scaffold explants, GC scaffold explants, to GCD scaffold with statistically significant difference ( $P < 0.001$ ).

## **16. Summary**

This study was summarized that the combined scaffolds of gelatin, chitooligosaccharide, and demineralized bone powder could promote osteogenesis in subcutaneous implantation in the model of male Wistar rats. H&E staining showed that new bone formation at 8 weeks was larger and more homogeneity than 4 weeks post-implantation. Especially GCD scaffolds showed more osteoid than the other scaffolds. It was found that von Kossa staining showed obvious mineralization at 8 weeks post-implantation. Interestingly, GCD scaffolds exhibited more bone matrix than the other scaffolds. These implied that the developed scaffolds had osteoinductive potential for developing new bone formation that can be applied in orthopaedics approach in the future.

# CHAPTER V

## DISCUSSIONS AND CONCLUSIONS

### 1. Discussions

#### Part I: Mesenchymal stem cells for bone tissue engineering

Human mesenchymal stem cells (hMSCs) have been used in research for tissue engineering of bone on scaffolds. Periosteum tissue is one alternative source of human MSCs. The periosteum-derived (PD) cells are commonly applied for many years. The first study about osteogenic function of periosteum was described in 1742. The first report of successful culture periosteum was performed by H.B. Fell in 1932 (Hutmacher and Sittinger, 2003). Periosteum can be described as an osteoprogenitor cell-containing bone envelope, which can be activated to proliferate by trauma and lymphocyte mitogens (Van et al., 1982). Cells located within the periosteum and bone marrow can differentiate into fibroblastic, osteogenic or reticular cells (Kasten et al., 2003; Meyer et al., 2004).

Periosteal-derived mesenchymal precursor cells generate progenitor cells committed to one or more cell lines with an apparent degree of plasticity. Outgrowth cultures of periosteum pieces favor the co-culture of different cell types. Periosteal cells are able to heal a segmental bone defect after implantation and induce osteogenic tissue when seeded into diffusion chambers (Schantz et al., 2002).

To evaluate the phenotype of the expanded periosteal cells, we performed FACS analysis in order to assess multipotent MSCs from various tissue sources such as bone marrow. CD45, a marker of hematopoietic lineage cells was not expressed by MSCs and was not detected in any of the donors tested (Pittenger et al., 1999). The previous study of Roberts (2011) reported the human periosteum-derived cells cultured with calcium phosphate scaffolds. They showed that PD cells displayed classical surface markers used for identification of MSCs including positivity for CD73, CD90 and CD105. Additionally, the population had a low positivity relating to CD34 (hematopoietic progenitor) and was negative for CD45, CD20 and CD14 (Roberts et al., 2011). Moreover, Eyckmans and Luyten (2006) detected expression of CD73, CD105, and CD166 in PD cells. Furthermore, the CD45 (HSC marker) was not found in the PD cells. These data indicated that periosteum contained cells that can be expanded displaying high self-renewal capacity and the phenotype of multipotent

MSCs. Thereafter, the multipotency towards the mesenchymal lineages was assessed (Eyckmans and Luyten, 2006).

In previous research, periosteum has received considerable attention as a grafting material for the repair of bone and joint defects. The findings of bone formation induced by cultured human periosteum-derived cells using a rat model are presented. Schantz (2002) reported that cultured human periosteal cells harvested from calvarial bone in combination with a three dimensional scaffold expressed osteogenic markers and induced new bone formation in the back muscles of nude mice (Schantz et al., 2002).

Furthermore, Musina (2005) have studied human MSCs from many tissue sources including bone marrow, adipose tissue, skin, placenta, and thymus. The morphology of MSCs during isolation and culturing were similar and did not differ by the expression of the main cell surface marker genes including CD10, CD13, CD31, CD44, CD90, and CD105 (Musina et al., 2005).

In our study, we have successfully isolated a universal cell population with mesenchymal stem cell characteristics from human periosteum. We have studied the morphology, immunophenotype, gene expressions of mesenchymal stem cells, and differentiation ability of PD cells. The PD cells isolated from periosteum tissue showed the positive expression of MSC surface markers such as CD29, CD44, CD90 and CD105 but did not express hematopoietic stem cell (HSC) markers such as CD34 and CD45. Moreover, the results revealed that PD cells are superior in terms of the osteogenic, chondrogenic, and adipogenic capacity *in vitro* as shown from the evidences that the PD cells could stimulate the MSC lineages such as osteogenic, chondrogenic, and adipogenic lineages via conditioned culture and upregulated the expression of osteogenic (Runx2, ALP, collagen I), chondrogenic (Sox-9), and adipogenic (LPL, PPAR- $\gamma$ ) genes. The data demonstrated that PD cells could be a new cell source that may be suitable for bone repair.

Moreover, our results are resemble to the study of Gargette et al. (2009) that characterized MSCs from human endometrium. They showed that endometrium-derived cells could differentiate into osteoblasts, chondrocytes, adipocytes, including smooth muscle cells. The RT-PCR analyses confirmed that the endometrium derived cells expressed PTHR1, collagen type II, LPL, and Caldesmon which represent osteogenic, chondrogenic, adipogenic, and myogenic differentiation. Furthermore, the endometrium-derived cells expressed MSCs markers CD29, CD44, CD90, CD105, including CD140B, CD146 but not hematopoietic markers CD31, CD34, CD45 via flow cytometry.



Bone formation was observed in bone defect treated with periosteal cells from cultured medium within 35 days of grafting. As in a previous study of Kanou (2005), the new bone induced from the grafted tissue was detected in the bone defect, this new bone did not completely fill the defect by 35 days post grafting. Some investigators have suggested that the application of bone growth factors is required to enhance osteoblastic differentiation of periosteum-derived cells (Kanou et al., 2005).

The *in vitro* approach with human MSCs such as periosteum-derived cells which act as osteoprogenitors may be a useful model for the assessment of cellular response to new biomaterials prior to their application *in vivo*.

## **Part II: Osteogenic characterization of collagen/demineralized bone powder scaffolds**

The systems of collagen/demineralized bone powder were developed for bone tissue engineering applications. The combined scaffolds of collagen and DBP with various particle sizes were prepared. The fabricated scaffolds at different blending ratios were characterized for physical and biological properties with mesenchymal stem cells. Furthermore, isolated MSCs from human periosteum (PD cells) were cultured in scaffolds in order to compare their osteogenic differentiation potential. The biological properties including osteogenic potential of PD cells cultured on COL and COL/DBP scaffolds were investigated.

In this work, we hypothesized that the DBP with various particle sizes could affect the osteogenic differentiation of MSCs. Small, medium, and large particle sizes of DBP were prepared and collagen was introduced to blend with those at fixed weight blending ratio. To verify cell attachment and cell proliferation behavior, PD cells were seeded and cultured on COL and COL/DBP scaffolds. Over the culture period, the pure COL scaffold tended to promote cell attachment and proliferation better than the COL/DBP scaffolds. The number of cells attached and proliferated on the pure COL scaffold was significantly higher than those on COL/DBP scaffolds.

Demineralized bone powder (DBP), a promising bone graft mainly composed of collagen and bone morphogenetic proteins (BMPs), has been widely used for bone regeneration since Urist's discovery of BMPs in the 1960s (Urist et al., 1965). DBP is considered as the most osteoinductive form as it possesses the maximum surface area for interaction with target cells at the graft site (Lasa Jr et al., 1995).

Furthermore, DBP provides other growth factors such as transforming growth factor-beta (TGF- $\beta$ s), insulin-like growth factors (IGFs), fibroblast growth factors (FGFs), platelet derived growth factor (PDGFs) (Solheim, 1998). In general, TGF- $\beta$  is produced and secreted

by bone cells and is stored in bone matrix (Centrella et al., 1994). Many findings suggested that TGF- $\beta$  is of primary importance in the regulation of bone turnover (Mohan and Baylink, 1991) and plays a significant role in competence for early stages of chondroblastic and osteoblastic differentiation *in vitro* and *in vivo* (Roelen and Dijke, 2003). Because TGF- $\beta$  and BMPs are major osteoinduction and chondroinduction factors in bone. Thus, it is likely that osteoinduction and chondroinduction of DBP involves in TGF- $\beta$ /BMP signaling pathway genes (Centrella, et al., 1994).

The study of Aubin (1995) developed biomaterials derived from demineralized bone powder were evaluated for their ability to support scaffold interactions. Evaluation of several osteogenic markers, ALP activity, calcium deposition, and cell surface mineralization, was verified to examine this phenomenon. ALP has been implicated in a key indicator that increased in enzymatic activity correspond to an increased osteoblastic phenotype *in vitro* (Aubin et al., 1995).

Moreover, Kasten et al. (2003) reported that DBP seemed to be more favorable than hydroxyapatite and  $\beta$ -tricalcium phosphate to support later stages of osteoblast differentiation *in vitro* (Kasten et al., 2003). Mauney et al. (2005) found that mechanical stimulation promotes osteogenic differentiation of hMSCs on partially demineralized bone scaffolds *in vitro* (Mauney, et al., 2005). However, the combination of DBP with biomaterial enhances the osteogenic differentiation of hMSCs. Zhou (2005) suggested that the DBP combined with porous collagen sponge system was cultured with hMSCs to assess DBP stimulation of osteoblastic differentiation. The results showed that DBP combined with collagen activated higher ALP activity in hMSCs than that in pure collagen. Finally, DBP induced hMSCs to express the osteoblast phenotype. These studies showed that the osteoinductive potential can influence the differentiation pathway of hMSCs when stimulated by DBP. These results support the potential to engineer bone *in vitro* by using hMSCs and DBP/collagen sponges (Zhou et al., 2005). Furthermore, they investigated that DBP induced osteogenic differentiation of hMSCs in collagen scaffolds under osteogenic medium. DBP stimulated ALP activity in hMSCs after 3 weeks of cultivation. Moreover, the DBP has affected on osteocyte gene expression in hMSCs such as up-regulated expression of ALP and Osteocalcin.

Previous study of Mauney in 2005 investigated demineralized bone (DB) derived from bovine and fully mineralization bone (FB) in order to compare their ability to support *in vitro* osteogenic differentiation of human bone marrowstromal cell (BMSC). BMSCs were seeded on bone-derived scaffolds and then evaluated osteoblast-related markers, alkaline

phosphatase (ALP) activity and bone sialoprotein (BSP) and osteopontin (OP) mRNA expression. Biochemical analysis of ALP activity demonstrated that, following 7 days of cultivation on DB scaffolds, BMSCs displayed significantly higher activity than cells maintained on the FB scaffolds. Interestingly, after 14 days of cultivation on bone derived scaffolds, BMSCs had significantly increased ALP activity. (Mauney et al., 2005)

Additionally, the previous study revealed that the DBP with the size of 550–710  $\mu\text{m}$  provided maximum osteoinductive potential *in vitro* and *in vivo* bioassays (Zhang et al., 1997). According to Vail (2004), it was suggested that the particle size of equine DBP were related with osteoinduction. The muscular implantation of DBP allograft in horses after 8 weeks reported that the DBP with medium particle size (200-1,000  $\mu\text{m}$ ) were associated with osteoinductive activity and minimal signs of local inflammation whereas the DBP with smaller particle size (40-200  $\mu\text{m}$ ) were found to have greater local inflammatory response (Vail et al., 1994).

The previous studies supported our results that DBP incorporated with collagen scaffolds enhanced the osteogenic differentiation of MSC. Furthermore, our study proved that the particle size of DBP blended in collagen scaffolds affected the level of osteogenic potential as shown by the ALP and calcium quantitative results, including the mineralization on the MSC surface.

The previous *in vitro* studies have demonstrated that other osteoprogenitor cell sources including periosteal cells displayed higher increasing ALP activity following 7 days of cocultivation with partially demineralized bone preparations (8.9% and 2% calcium by weight) in comparison to nondemineralized bone as control, thus leading to the theory that the demineralization process exposes osteogenic factors which are relatively inaccessible prior to this process (Zhang and Wolfenbarger, 1997).

From the report of Zambonin (1995), they studied the effects of different biomaterials, bovine collagen matrix and demineralized bone powder when cultured with human osteoblasts. The study showed that cell viability in the presence of the materials was not different. Collagen matrix showed increasing proliferation of human osteoblasts, whereas demineralized bone powder decreased cell growth, but rather increased osteoblast bone matrix synthesis (Zambonin and Grano, 1995).

### **Part III: Gelatin/chitooligosaccharide/demineralized bone powder scaffolds for bone tissue engineering**

In this part, the systems of gelatin/chitooligosaccharide/demineralized bone powder were developed for bone tissue engineering applications. The combined scaffolds of gelatin, COS, and DBP were prepared. The fabricated scaffolds at different blending ratios were characterized for physical and biological properties with PD cells. Furthermore, isolated MSCs from human periosteum (PD cells) were cultured in scaffolds in order to compare the osteogenic differentiation potential. Behavior of PD cells cultured on G, GC, and GCD scaffolds were elucidated.

The effects of three biomaterials (demineralized bone powder, gelatin, and chitooligosaccharide) on cell proliferation and osteogenic differentiation have been studied in cultured human periosteum-derived (PD cells). The reasons why human cells were selected are biocompatibility and availability. When biomaterials are implanted in human bone tissue, the best way to analyze their effects is to use human cells. The desirable effect is obtained by stimulation of osteoblast behavior including ALP activity, calcium deposition, mineralization, and osteogenic gene expression. According to the characterization performed, our cells had a specific differentiated osteoblastic phenotype. The results indicated that the biomaterial scaffolds fabricated from demineralized bone powder, gelatin, and chitooligosaccharide induced similar effects on cell proliferation whereas the combination of all materials (GCD) displayed significantly higher osteogenic potential than the others (GC, and G scaffolds).

There were many previous successful studies of demineralized bone powder implants in many types of craniomaxillofacial, orthopedic, periodontal, and hand reconstruction procedures (Glowacki, et al., 1981; Rosenthal and Glowacki, 1999; Sonis, et al., 1985). Animal studies showed that the sequential cellular changes in response to implants of demineralized bone materials include chemotaxis and attachment of progenitor cells to the matrix, vascularization, and ultimately osteogenesis and marrow formation (Muthukumaran et al., 1985).

Moreover, the previous study of Honsawek in 2010 revealed that DBP exhibited biocompatibility and osteogenic potential in Wistar rat bioassay. The DBP demonstrated new bone formation in model of intramuscular implantation. Furthermore, the demineralized bone powder blended with porcine small intestinal submucosa (DBP/SIS) as a composite scaffold exhibited high osteoinductivity. The residual of DBP/SIS was surrounded by osteoid-like matrix and newly formed bone (Honsawek et al., 2010).

Furthermore, Zhang (2003) developed composited scaffolds from calcium phosphate-chitosan for use in bone tissue engineering. The results suggested that human osteoblast-like cells (MG63) cultured on the scaffolds showed significantly higher ALP level and osteocalcin production during the 11-day culture period. Calcium phosphate was added to the scaffolds to prevent chitosan from fast degradation that may affect the differentiation of osteoblast cells (Zhang et al., 2003).

Our study of scaffolds fabricated from gelatin, chitooligosaccharide, and demineralized bone powder are consistent with the study of Rattanavaraporn (2010). They investigated the behaviors of rat MSCs on films prepared from gelatin (G) and low-molecular weight chitooligosaccharide (COS) at the weight blending ratios of G/COS 70/30. The MSCs attached and spreaded on the blended G/COS film was larger than those attached on pure gelatin film. The osteogenic differentiation of MSCs cultured on films was evaluated via ALP activity and calcium quantitation assays. This study proved that attachment, proliferation and osteogenic differentiation of MSCs strongly depended on molecular mass of chitosan and the ratio of their blends with gelatin (Rattanavaraporn et al., 2010). These findings supported our study that the combination of gelatin/chitooligosaccharide scaffolds cultured with PD cells could enhance osteogenic differentiation better than pure gelatin scaffolds. Moreover, after DBP was mixed into G/COS, the combined scaffold of gelatin/COS/DBP displayed higher osteoinductive potential than gelatin/COS scaffolds and pure gelatin scaffolds.

## 2. Conclusions

The aim of this research was to investigate the biological characteristics of MSCs isolated from human periosteum and to determine cell surface markers using flow cytometry. MSC surface markers were detected in PD cells but HSC surface markers were not detected. Moreover, the MSCs can remarkably differentiate into osteogenic, chondrogenic, and adipogenic lineages depending on different conditioned media. After that, we studied the influences of particle size of demineralized bone powder (DBP) in combination with collagen scaffolds. The DBP was classified into 3 ranges of particle sizes: 75 to 125 microns, 125 to 250 microns, and 250 to 500 microns. The results showed that MSCs could attach and proliferate on collagen/demineralized bone powder scaffolds better than those on pure collagen scaffolds. Moreover, DBP with the size of 250 to 500 microns blended with collagen scaffolds had excellent osteoblastic differentiation when compared to scaffolds having smaller DBP. It was discovered that COL/DBP scaffolds promoted osteoblastic differentiation. The DBP in the range of 250 to 500 microns was further blended with gelatin and chitooligosaccharide (GCD) for the fabrication of novel scaffolds compared with gelatin/chitooligosaccharide (GC) scaffolds, and pure gelatin (G) scaffolds. The results suggested that GCD scaffolds promoted osteoblastic differentiation better than the other scaffolds. For *in vivo* study, the combination of G, C, and DBP blended scaffolds were implanted in subcutaneous of male Wistar rats. After two-week implantation, there were new collagen and new osteoid formation. After eight-week implantation, more new bone formation was observed. For the potential of biocompatibility and osteoinductivity, this study showed that GCD scaffolds exhibited remarkably higher osteogenic differentiation potential than the other scaffolds.

In conclusion, the new combined scaffolds of materials from gelatin/chitooligosaccharide/demineralized bone powder showed high osteoinductive potential for bone tissue engineering. In term of cells, it could be concluded that mesenchymal stem cells derived from human periosteum had high potential to differentiate into mature bone cells in order to be alternative model for bone tissue engineering application.

### **3. Recommendations**

This study has compared the osteogenic capacities of human periosteum-derived mesenchymal stem cells on the scaffolds from gelatin, chitooligosaccharide, and demineralized bone powder. Remarkable results were found in the combined scaffolds of gelatin, chitooligosaccharide, and demineralized bone powder compared to the gelatin blended chitooligosaccharide and pure gelatin scaffolds. Therefore, for further investigation, the developed scaffolds should be further studied in *in vivo* using critical size bone defect model.

## References

- [1] Andrades, J. A., Santamaria, J. A., Nimni, M. E. and Becerra, J. (2001). Selection and amplification of a bone marrow cell population and its induction to the chondro-osteogenic lineage by rhOP-1: an in vitro and in vivo study. **International Journal of Developmental Biology**.45, 4 :689-693.
- [2] Anthony, A. and Lanza, R. (2001). **Methods of Tissue Engineering**. San Diego: Elsevier Science.
- [3] Arpornmaeklong, P., Pripatnanont, P. and Suwatwirote, N. (2008). Properties of chitosan–collagen sponges and osteogenic differentiation of rat-bone-marrow stromal cells. **International Journal of Oral and Maxillofacial Surgery**. 37, 4 :357-366.
- [4] Arpornmaeklong, P., Suwatwirote, N., Pripatnanont, P. and Oungbho, K. (2007). Growth and differentiation of mouse osteoblasts on chitosan–collagen sponges. **International Journal of Oral and Maxillofacial Surgery**. 36, 4: 328-337.
- [5] Aubin, J., Liu, F., Malaval, L. and Gupta, A. (1995). Osteoblast and chondroblast differentiation. **Bone**. 17, 2: S77-S83.
- [6] Barron, V. and Pandit, A. (2003). Combinatorial approaches in tissue engineering: progenitor cells, scaffolds, and growth factors. **Tissue engineering**: 1-21.
- [7] Bayat, M., Momen-Heravi, F., Marjani, M. and Motahhary, P. (2010). A comparison of bone reconstruction following application of bone matrix gelatin and autogenous bone grafts to alveolar defects: an animal study. **Journal of Cranio-Maxillofacial Surgery**. 38, 4: 288-292.
- [8] Bernas, T. and Dobrucki, J. (2002). Mitochondrial and nonmitochondrial reduction of MTT: Interaction of MTT with TMRE, JC-1, and NAO mitochondrial fluorescent probes. **Cytometry**. 47,4 236-242.
- [9] Bruder, S. P. and Fox, B. S. (1999). Tissue Engineering of Bone: Cell Based Strategies. **Clinical Orthopaedics and Related Research**.367: S68-S83.



- [10] Cao, Y., Croll, T. I., Lees, J. G., Tuch, B. E. and Cooper-White, J. J. (2005). Scaffolds, Stem Cells, and Tissue Engineering: A Potent Combination!. **Australian Journal of Chemistry** .58,10: 691-703.
- [11] Centrella, M., Horowitz, M. C., Wozney, J. M. and McCarthy, T. L. (1994). Transforming growth factor- $\beta$  gene family members and bone. **Endocrine reviews**. 15, 1: 27-39.
- [12] Chang, K. L., Tai, M. C. and Cheng, F. H. (2001). Kinetics and products of the degradation of chitosan by hydrogen peroxide. **Journal of Agricultural and Food Chemistry**. 49, 10: 4845-4851.
- [13] Chen, Q., Roether, J. and Boccaccini, A. (2008). Tissue engineering scaffolds from bioactive glass and composite materials. **Topics in Tissue Engineering**. 4: 1-27.
- [14] Drury, J. L. and Mooney, D. J. (2003). Hydrogels for tissue engineering: scaffold design variables and applications. **Biomaterials**. 24, 24: 4337-4351.
- [15] Einhorn, T. A. (2003). Clinical applications of recombinant human BMPs: early experience and future development. **Journal of Bone and Joint Surgery**. 85-A, Suppl 3: 82-88.
- [16] Eyckmans, J. and Luyten, F. P. (2006). Species specificity of ectopic bone formation using periosteum-derived mesenchymal progenitor cells. **Tissue Engineering**. 12, 8: 2203-2213.
- [17] Friess, W. (1998). Collagen-biomaterial for drug delivery. **European Journal of Pharmaceutics and Biopharmaceutics**. 45, 2: 113-136.
- [18] Frost, H. and Sullivan, E. (2008). Bone Grafts and Bone Substitutes. **Orthopedic Network News: 4**. Retrieved from OrthopedicNetworkNews.com
- [19] Frost, R. L. and Bahfenne, S. (2009). Raman and mid-IR spectroscopic study of the magnesium carbonate minerals—brugnatellite and coalingite. **Journal of Raman Spectroscopy** 40, 4: 360-365.

- [20] Glowacki, J., Murray, J. E., Kaban, L. B., Folkman, J. and Mulliken, J. B. (1981). Application of the biological principle of induced osteogenesis for craniofacial defects. **The Lancet**. 317, 8227: 959-962.
- [21] Greenwald, A. S., Boden, S. D., Goldberg, V. M., Khan, Y., Laurencin, C. T. and Rosier, R. N. (2001). Bone-graft substitutes: facts, fictions, and applications. **Journal of Bone and Joint Surgery**. 83-A, Suppl 2: 98-103.
- [22] Hattori S, Oxford C, Reddi AH (2007) Identification of superficial zone articular chondrocyte stem/progenitor cells. **Biochemical and Biophysical Research Communications**. 358: 99–103.
- [23] Hutmacher, D. W. (2001). Scaffold design and fabrication technologies for engineering tissues state of the art and future perspectives. **Journal of Biomaterials Science, Polymer Edition**. 12, 1: 107-124.
- [24] Hutmacher, D. W. and Sittinger, M. (2003). Periosteal cells in bone tissue engineering. **Tissue Engineering**. 9, 4: 45-64.
- [25] Hofmann, S., Hagenmüller, H., Koch, A. M., Müller, R., Vunjak-Novakovic, G., Kaplan, D. L., et al. (2007). Control of in vitro tissue-engineered bone-like structures using human mesenchymal stem cells and porous silk scaffolds. **Biomaterials**. 28, 6: 1152-1162.
- [26] Honsawek, S., Bumrungrpanichthaworn, P., Thanakit, V., Kunrangseesomboonc, V., Muchmeec, S., Ratprasertc, S., et al. (2010). Osteoinductive potential of small intestinal submucosa/demineralized bone matrix as composite scaffolds for bone tissue engineering. **Asian Biomedicine**. 4, 6: 913-922.
- [27] Huang, Y., Onyeri, S., Siewe, M., Moshfeghian, A. and Madihally, S. V. (2005). In vitro characterization of chitosan–gelatin scaffolds for tissue engineering. **Biomaterials**. 26, 36: 7616-7627.
- [28] Jimi, E., Hirata, S., Shin, M., Yamazaki, M. and Fukushima, H. (2010). Molecular mechanisms of BMP-induced bone formation: Cross-talk between BMP and NF- $\kappa$ B signaling pathways in osteoblastogenesis. **Japanese Dental Science Review**. 46, 1: 33-42.

- [29] Jo, C. H., Kim, O. S., Park, E. Y., Kim, B. J., Lee, J. H., Kang, S. B., et al. (2008). Fetal mesenchymal stem cells derived from human umbilical cord sustain primitive characteristics during extensive expansion. **Cell and Tissue Research**. 334,3: 423-433.
- [30] Jung, U.-W., Kim, S.-K., Kim, C.-S., Cho, K.-S., Kim, C.-K. and Choi, S.-H. (2007). Effect of chitosan with absorbable collagen sponge carrier on bone regeneration in rat calvarial defect model. **Current Applied Physics**. 7, Supplement 1: e68-e70.
- [31] Kasten, P., Luginbühl, R., Van Griensven, M., Barkhausen, T., Krettek, C., Böhner, M., et al. (2003). Comparison of human bone marrow stromal cells seeded on calcium-deficient hydroxyapatite,  $\beta$ -tricalcium phosphate and demineralized bone matrix. **Biomaterials**.24,15: 2593-2603.
- [32] Kanou, M., Ueno, T., Kagawa, T., Fujii, T., Sakata, Y., Ishida, N., et al. (2005). Osteogenic potential of primed periosteum graft in the rat calvarial model. **Annals of plastic surgery**. 54,1: 71.
- [33] Keaveny, T. M., Wachtel, E. F. and Kopperdahl, D. L. (1999). Mechanical behavior of human trabecular bone after overloading. **Journal of orthopaedic research**. 17,3 :346-353.
- [34] Kohles, S., Vernino, A., Clagett, J., Yang, J., Severson, S. and Holt, R. (2000). A morphometric evaluation of allograft matrix combinations in the treatment of osseous defects in a baboon model. **Calcified Tissue International**. 67,2: 156-162.
- [35] Komori, T. (2006). Regulation of osteoblast differentiation by transcription factors. **Journal of cellular biochemistry**.99,5: 1233-1239.
- [36] Krampera, M., Pizzolo, G., Aprili, G. and Franchini, M. (2006). Mesenchymal stem cells for bone, cartilage, tendon and skeletal muscle repair. **Bone**. 39, 4: 678-683.
- [37] Lasa Jr, C., Hollinger, J., Drohan, W. and MacPhee, M. (1995). Delivery of demineralized bone powder by fibrin sealant. **Plastic and Reconstructive Surgery**. 96, 6: 1409.
- [38] Lanza, R. P. and Vacanti, J. (2007). **Principles of tissue engineering**. Academic Press.

- [39] Li, J., Pan, J., Zhang, L. and Yu, Y. (2003). Culture of hepatocytes on fructose-modified chitosan scaffolds. **Biomaterials**. 24,13: 2317-2322.
- [40] Mauney, J. R., Jaquiéry, C., Volloch, V., Heberer, M., Martin, I. and Kaplan, D. L. (2005). *In vitro* and *in vivo* evaluation of differentially demineralized cancellous bone scaffolds combined with human bone marrow stromal cells for tissue engineering. **Biomaterials**. 26,16: 3173-3185.
- [41] Madihally, S. V. and Matthew, H. W. T. (1999). Porous chitosan scaffolds for tissue engineering. **Biomaterials**. 20,12: 1133-1142.
- [42] Maniopoulos, C., Sodek, J. and Melcher, A. (1988). Bone formation *in vitro* by stromal cells obtained from bone marrow of young adult rats. **Cell and Tissue Research**. 254, 2: 317-330.
- [43] Marolt, D., Augst, A., Freed, L. E., Vepari, C., Fajardo, R., Patel, N., et al. (2006). Bone and cartilage tissue constructs grown using human bone marrow stromal cells, silk scaffolds and rotating bioreactors. **Biomaterials**. 27, 36: 6138-6149.
- [44] Mauney, J., Sjostrom, S., Blumberg, J., Horan, R., O'leary, J., Vunjak-Novakovic, G., et al. (2004). Mechanical stimulation promotes osteogenic differentiation of human bone marrow stromal cells on 3-D partially demineralized bone scaffolds *in vitro*. **Calcified Tissue International**. 74, 5: 458-468.
- [45] Mayer H, Bertram H, Lindenmaier W, Korff T, Weber H, et al. (2005) Vascular endothelial growth factor (VEGF-A) expression in human mesenchymal stem cells: autocrine and paracrine role on osteoblastic and endothelial differentiation. **Journal of Cellular Biochemistry**. 95: 827–839.
- [46] Meyer, U., Joos, U. and Wiesmann, H. (2004). Biological and biophysical principles in extracorporeal bone tissue engineering: Part I. **International Journal of Oral and Maxillofacial Surgery**. 33, 4: 325-332.
- [47] Mistry, A. S. and Mikos, A. G. (2005). Tissue engineering strategies for bone regeneration. **Regenerative Medicine II**. Springer Berlin/ Heidelberg.

- [48] Mizuno, S. and Glowacki, J. (1996). Three-dimensional composite of demineralized bone powder and collagen for *in vitro* analysis of chondroinduction of human dermal fibroblasts. **Biomaterials**. 17, 18: 1819-1825.
- [49] Mohan, S. and Baylink, D. J. (1991). Bone growth factors. **Clinical Orthopaedics and Related Research**. Feb, 263: 30-48.
- [50] Murugan, R. and Ramakrishna, S. (2005). Development of nanocomposites for bone grafting. **Composites Science and Technology**. 65, 15: 2385-2406.
- [51] Musina, R. A., Bekchanova, E. S. and Sukhikh, G. T. (2005). Comparison of Mesenchymal Stem Cells Obtained from Different Human Tissues. **Bulletin of Experimental Biology and Medicine**. 139, 4: 504-509.
- [52] Muthukumar, N. and Reddi, A. (1985). Bone matrix-induced local bone induction. **Clinical Orthopaedics and Related Research**. 200, Nov: 159-164.
- [53] Nedović, V. and Willaert, R. (2005). **Applications of cell immobilisation biotechnology**. Springer Verlag.
- [54] O'Brien, F. J., Harley, B. A., Yannas, I. V. and Gibson, L. (2004). Influence of freezing rate on pore structure in freeze-dried collagen-GAG scaffolds. **Biomaterials**. 25, 6: 1077-1086.
- [55] O'Brien, F. J., Harley, B., Yannas, I. V. and Gibson, L. J. (2005). The effect of pore size on cell adhesion in collagen-GAG scaffolds. **Biomaterials**. 26, 4: 433-441.
- [56] Ohara, N., Hayashi, Y., Yamada, S., Kim, S. K., Matsunaga, T., Yanagiguchi, K., et al. (2004). Early gene expression analyzed by cDNA microarray and RT-PCR in osteoblasts cultured with water-soluble and low molecular chitooligosaccharide. **Biomaterials**. 25, 10: 1749-1754.
- [57] Park, D. J., Choi, B. H., Zhu, S. J., Huh, J. Y., Kim, B. Y. and Lee, S. H. (2005). Injectable bone using chitosan-alginate gel/mesenchymal stem cells/BMP-2 composites. **Journal of Cranio-Maxillofacial Surgery**. 33, 1: 50-54.

- [58] Peng, L., Cheng, X. R., Wang, J. W., Xu, D. X. and Wang, G. (2006). Preparation and evaluation of porous chitosan/collagen scaffolds for periodontal tissue engineering. **Journal of Bioactive and Compatible Polymers**. 21,3: 207-220.
- [59] Peter, M., Ganesh, N., Selvamurugan, N., Nair, S., Furuike, T., Tamura, H., et al. (2010). Preparation and characterization of chitosan-gelatin/nanohydroxyapatite composite scaffolds for tissue engineering applications. **Carbohydrate Polymers**. 80, 3: 687-694.
- [60] Piattelli, A., Scarano, A., Corigliano, M. and Piattelli, M. (1996). Comparison of bone regeneration with the use of mineralized and demineralized freeze-dried bone allografts: a histological and histochemical study in man. **Biomaterials**. 17, 11: 1127-1131.
- [61] Pittenger, M. F., Mackay, A. M., Beck, S. C., Jaiswal, R. K., Douglas, R., Mosca, J. D., et al. (1999). Multilineage potential of adult human mesenchymal stem cells. **Science**. 284, 5411: 143-147.
- [62] Quirk, R. A., Chan, W. C., Davies, M. C., Tendler, S. J. B. and Shakesheff, K. M. (2001). Poly (L-lysine)-GRGDS as a biomimetic surface modifier for poly (lactic acid). **Biomaterials**. 22,8: 865-872.
- [63] Ratanavaraporn, J., Damrongsakkul, S., Sanchavanakit, N., Banaprasert, T. and Kanokpanont, S. (2006). Comparison of Gelatin and Collagen Scaffolds for Fibroblast Cell Culture. **Journal of Metals, Materials and Minerals**. 16,1: 31-36.
- [64] Ratanavaraporn, J., Kanokpanont, S., Tabata, Y. and Damrongsakkul, S. (2009). Growth and osteogenic differentiation of adipose-derived and bone marrow-derived stem cells on chitosan and chitooligosaccharide films. **Carbohydrate Polymers**. 78, 4: 873-878.
- [65] Rebelatto CK, Aguiar AM, Moretao MP, Senegaglia AC, Hansen P, et al. (2008) Dissimilar differentiation of mesenchymal stem cells from bone marrow, umbilical cord blood, and adipose tissue. **Experimental Biology and Medicine**. 233: 901–913.

- [66] Roberts, S. J., Geris, L., Kerckhofs, G., Desmet, E., Schrooten, J. and Luyten, F. P. (2011). The combined bone forming capacity of human periosteal derived cells and calcium phosphates. **Biomaterials**. 32,19: 4393–4405.
- [67] Roelen, B. A. J. and Dijke, P. (2003). Controlling mesenchymal stem cell differentiation by TGF $\beta$  family members. **Journal of Orthopaedic Science**. 8,5: 740-748.
- [68] Rosenthal, R. K., Folkman, J. and Glowacki, J. (1999). Demineralized bone implants for nonunion fractures, bone cysts, and fibrous lesions. **Clinical Orthopaedics and Related Research**, 364 (Jul): 61-69.
- [69] Sampath, T. and Reddi, A. (1981). Dissociative extraction and reconstitution of extracellular matrix components involved in local bone differentiation. **Proceedings of the National Academy of Sciences**. 78, 12: 7599-7603.
- [70] Sampath, T. and Reddi, A. (1983). Homology of bone-inductive proteins from human, monkey, bovine, and rat extracellular matrix. **Proceedings of the National Academy of Sciences**. 80, 21: 6591–6595.
- [71] Schantz, J. T., Hutmacher, D. W., Chim, H., Ng, K. W., Lim, T. C. and Teoh, S. H. (2002). Induction of ectopic bone formation by using human periosteal cells in combination with a novel scaffold technology. **Cell Transplantation**. 11,2: 125-138.
- [72] She, Z., Zhang, B., Jin, C., Feng, Q. and Xu, Y. (2008). Preparation and in vitro degradation of porous three-dimensional silk fibroin/chitosan scaffold. **Polymer Degradation and Stability**. 93,7: 1316-1322.
- [73] Solheim, E. (1998). Osteoinduction by demineralised bone. **International Orthopaedics**. 22, 5: 335-342.
- [74] Sonis, S., Williams, R., Jeffcoat, M., Black, R. and Shklar, G. (1985). Healing of spontaneous periodontal defects in dogs treated with xenogeneic demineralized bone. **Journal of Periodontology**. 56,8: 470-9.
- [75] Song, E., Yeon Kim, S., Chun, T., Byun, H. J. and Lee, Y. M. (2006). Collagen scaffolds derived from a marine source and their biocompatibility. **Biomaterials**. 27,15: 2951-2961.

- [76] Šoptrajanov, B., Stefov, V., Kuzmanovski, I. and Jovanovski, G. (1999). Fourier transform infrared and Raman spectra of manganese hydrogenphosphate trihydrate. **Journal of Molecular Structure**. 482–483, 0: 103-107.
- [77] Tabata, Y. and Ikada, Y. (1998). Protein release from gelatin matrices. **Advanced Drug Delivery Reviews**. 31, 3: 287-301.
- [78] Tabata, Y. (2003). Tissue regeneration based on growth factor release. **Tissue Engineering**. 9, 4: 5-15.
- [79] Takahashi, Y., Yamamoto, M. and Tabata, Y. (2005a). Enhanced osteoinduction by controlled release of bone morphogenetic protein-2 from biodegradable sponge composed of gelatin and  $\beta$ -tricalcium phosphate. **Biomaterials**. 26, 23: 4856-4865.
- [80] Takahashi, Y., Yamamoto, M. and Tabata, Y. (2005b). Osteogenic differentiation of mesenchymal stem cells in biodegradable sponges composed of gelatin and  $\beta$ -tricalcium phosphate. **Biomaterials**. 26,17: 3587-3596.
- [81] Tangsadthakun, C., Kanokpanont, S., Sanchavanakit, N., Pichyangkura, R., Banaprasert, T., Tabata, Y., et al. (2007). The influence of molecular weight of chitosan on the physical and biological properties of collagen/chitosan scaffolds. **Journal of Biomaterials Science, Polymer Edition**. 18, 2: 147-163.
- [82] Tarek, M. N. and Domard, A. (1995). Collagen and its interaction with chitosan: II. Influence of the physicochemical characteristics of collagen. **Biomaterials**. 16, 11: 865-871.
- [83] Urist, M. R. (1965). Bone: formation by autoinduction. **Science**. 150,3698: 893-899.
- [84] Urist, M. R. and Dawson, E. (1981). Intertransverse process fusion with the aid of chemosterilized autolyzed antigen-extracted allogeneic (AAA) bone. **Clinical Orthopaedics and Related Research**. 154: 366–372.
- [85] Urist, M. R. and Dowell, T. A. (1968). Inductive substratum for osteogenesis in pellets of particulate bone matrix. **Clinical Orthopaedics and Related Research**. 61, Nov-Dec: 61-78.



- [86] Urist, M. R., Silverman, B. F., Büring, K., Dubuc, F. L. and Rosenberg, J. M. (1967). The Bone Induction Principle. **Clinical Orthopaedics and Related Research**. 53, Jul-Aug: 243-283.
- [87] Vail, T. B., Trotter, G. W. and Powers, B. E. (1994). Equine Demineralized Bone Matrix: Relationship Between Particle Size and Osteoinduction. **Veterinary Surgery** 23, 5: 386-395.
- [88] Van, P. T., Vignery, A. and Baron, R. (1982). Cellular kinetics of the bone remodeling sequence in the rat. **The Anatomical Record**.202,4: 445-451.
- [89] Wahl, D. and Czernuszka, J. (2006). Collagen-hydroxyapatite composites for hard tissue repair. **European Cells & Materials Journal**. 11, 43-56.
- [90] Walsh, W. and Christiansen, D. (1995). Demineralized bone matrix as a template for mineral-organic composites. **Biomaterials**.16,18: 1363-1371.
- [91] Wang, M. L., Tuli, R., Manner, P. A., Sharkey, P. F., Hall, D. J. and Tuan, R. S. (2003). Direct and indirect induction of apoptosis in human mesenchymal stem cells in response to titanium particles. **Journal of Orthopaedic Research**. 21,4: 697-707.
- [92] Xianmiao, C., Yubao, L., Yi, Z., Li, Z., Jidong, L. and Huanan, W. (2009). Properties and in vitro biological evaluation of nano-hydroxyapatite/chitosan membranes for bone guided regeneration. **Materials Science and Engineering: C**. 29,1: 29-35.
- [93] Yaszemski, M. J., Payne, R. G., Hayes, W. C., Langer, R. and Mikos, A. G. (1996). Evolution of bone transplantation: molecular, cellular and tissue strategies to engineer human bone. **Biomaterials**. 17, 2: 175-185.
- [94] Zambonin, G. and Grano, M. (1995). Biomaterials in orthopaedic surgery: effects of different hydroxyapatites and demineralized bone matrix on proliferation rate and bone matrix synthesis by human osteoblasts. **Biomaterials**. 16, 5: 397-402.
- [95] Zhang, M., Powers Jr, R. M. and Wolfenbarger Jr, L. (1997). Effect (s) of the demineralization process on the osteoinductivity of demineralized bone matrix. **Journal of Periodontology**. 68,11: 1085-1092.

- [96] Zhang, Y., Ni, M., Zhang, M. and Ratner, B. (2003). Calcium phosphate-chitosan composite scaffolds for bone tissue engineering. **Tissue Engineering**. 9, 2 (Apr): 337-345.
- [97] Zhao, F., Yin, Y., Lu, W. W., Leong, J. C., Zhang, W., Zhang, J., et al. (2002). Preparation and histological evaluation of biomimetic three-dimensional hydroxyapatite/chitosan-gelatin network composite scaffolds. **Biomaterials**. 23,15: 3227-3234.
- [98] Zhao, F., Grayson, W. L., Ma, T., Bunnell, B. and Lu, W. W. (2006). Effects of hydroxyapatite in 3-D chitosan-gelatin polymer network on human mesenchymal stem cell construct development. **Biomaterials**. 27,9: 1859-1867.
- [99] Zhou, S., Yates, K. E., Eid, K. and Glowacki, J. (2005). Demineralized bone promotes chondrocyte or osteoblast differentiation of human marrow stromal cells cultured in collagen sponges. **Cell and Tissue Banking**. 6,1: 33-44.

## **APPENDICES**

## APPENDIX A

### PCR primer sequences

PCR primer	Sequence	Annealing temperature (°C)	Product size (bp)	References
ALP	Sense 5'-TGG AGC TTC AGA AGC TCA ACA CCA-3' Antisense 5'-ATC TCG TTG TCT GAG TAC CAG TCC-3'	60	453	(Pittenger, et al., 1999)
BMP-2	Sense 5'-GAA TCC AAG CCA AAC ACA AAC AG-3' Antisense 5'-ATC TCG TTG TCT GAG TAC CAG TCC-3'	55	368	(Mayer, et al., 2005)
Col I	Sense 5'-TAA CCA CTG CTC CAC TCT GG-3' Antisense 5'-GGA CAC AAT GGA TTG CAA GC-3'	60	461	(Jo, et al., 2008)
GAPDH	Sense 5'-ACC ACA GTC CAT GCC ATC AC-3' Antisense 5'-TCC ACC ACC CTG TTG CTG TA-3'	60	454	(Wang, et al., 2003)
LPL	Sense 5'-GAG ATT TCT CTG TAT GGC ACC-3' Antisense 5'-CTG CAA ATG AGA CAC TTT CTC-3'	55	277	(Rebelatto, et al., 2008)
OPN	Sense 5'-GAG ATT TCT CTG TAT GGC ACC-3' Antisense 5'-CTG CAA ATG AGA CAC TTT CTC-3'	52	162	(Mayer, et al., 2005)
Osterix	Sense 5'-CAA GCT GTA TGG CAA GGC TTC-3' Antisense 5'-AGC TCA TCC GAA CGA GTG AAC-3'	55	117	(Mayer, et al., 2005)
PPAR- $\gamma$	Sense 5'-GCT GTT ATG GGT GAA ACT CTG-3' Antisense 5'-ATA AGG TGG AGA TGC CTC-3'	60	351	(Rebelatto, et al., 2008)
RUNX2	Sense 5'-TAT GGC ACT TCG TCA GGA TCC-3' Antisense 5'-GCG TCA CCA TTC TGG-3'	55	422	(Mayer, et al., 2005)
Sox-9	Sense 5'-ATC TGA AGA AGG AGA GCG AG-3' Antisense 5'-TCA GAA GTC TCC AGA GCT TG-3'	54	264	(Hattori S, et al., 2007)

## APPENDIX B

### Standard curve for MTT assay

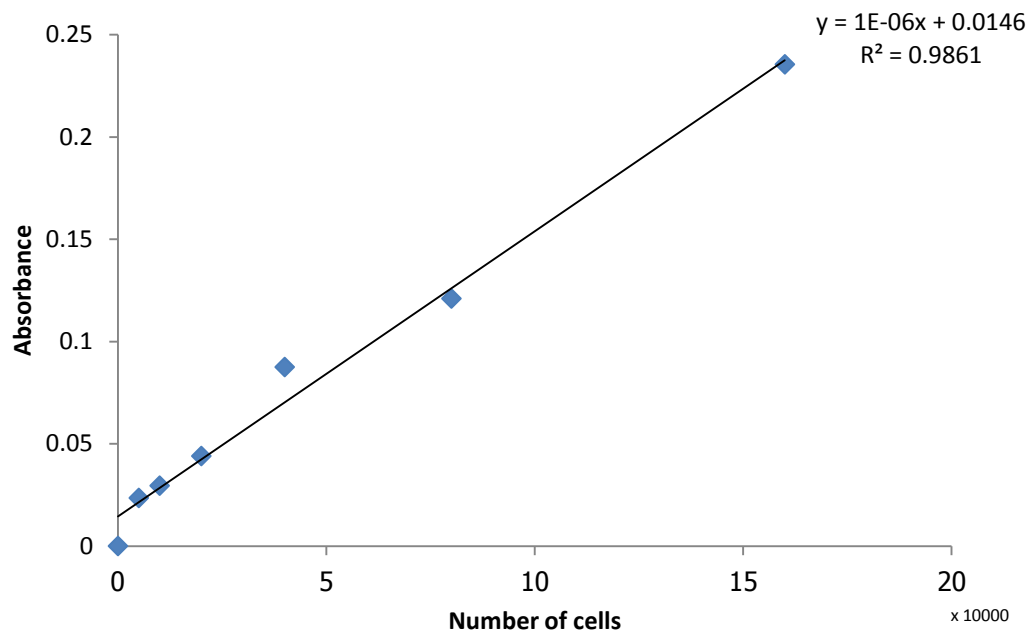


**Figure B** Standard curve of cell number for MTT assay

## APPENDIX C

### Standard curve for DNA assay

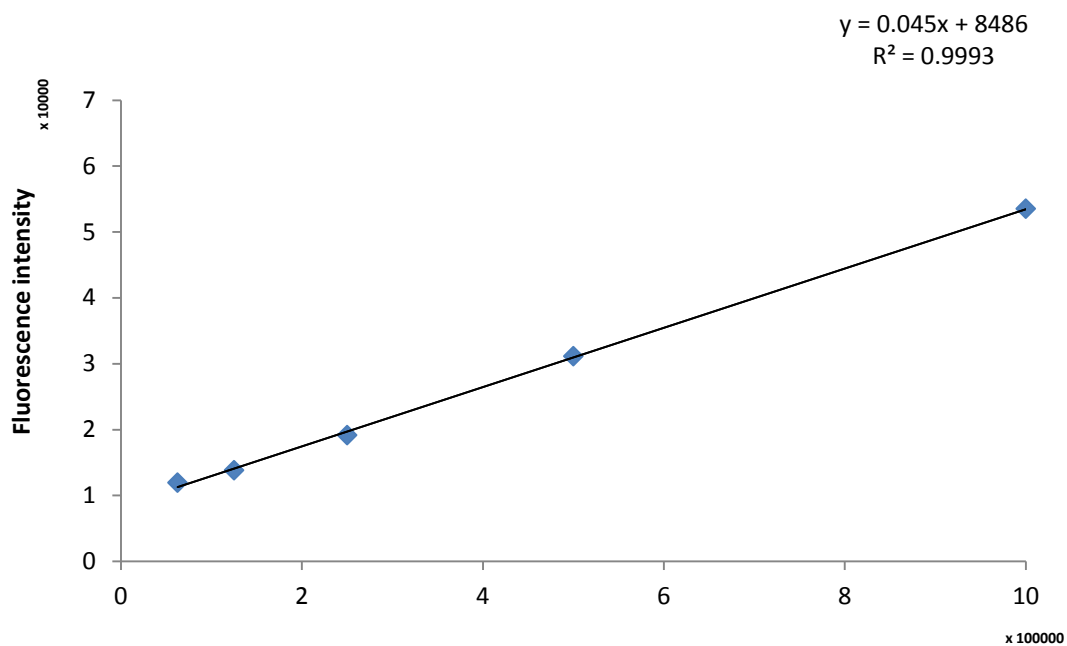


**Figure C** Standard curve of cell number for DNA assay

## APPENDIX D

### Standard curve for *p*-nitrophenyl phosphate assay

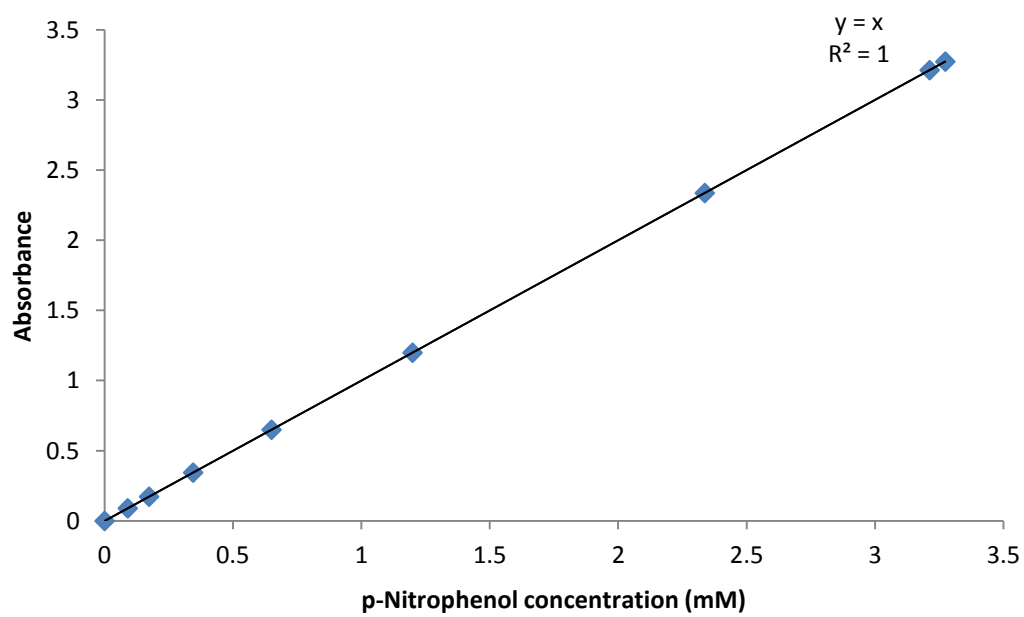


**Figure D** Nitrophenol standard curve for *p*-nitrophenyl phosphate assay (ALP)

## APPENDIX E

### Standard curve for O-cresolphthalein assay

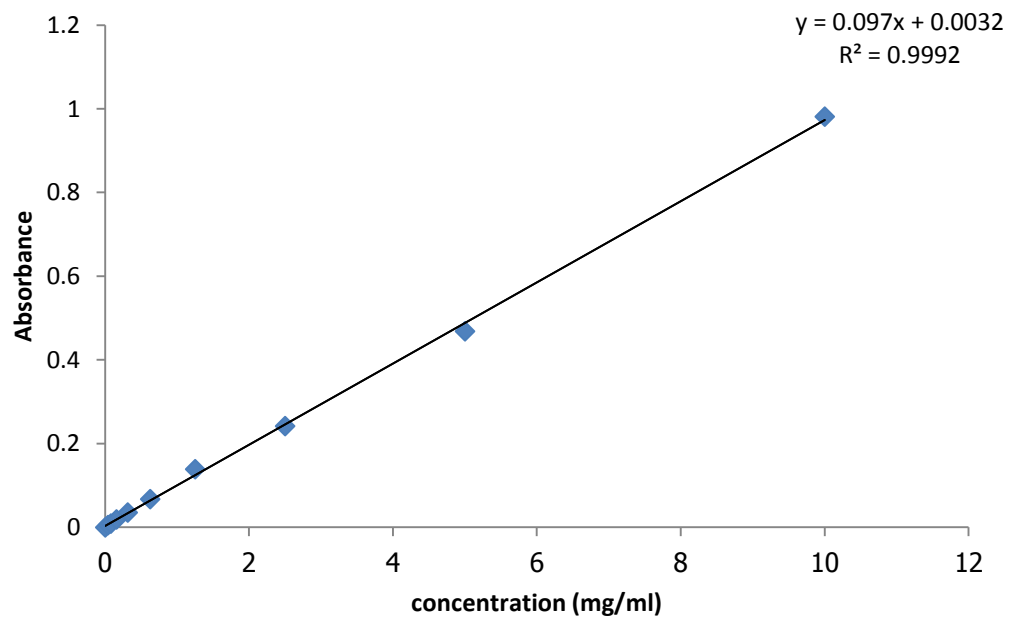


**Figure E** Calcium standard curve for O-cresolphthalein assay



## BIOGRAPHY

Mr. Thakoon Thitiset was born in Bangkok, Thailand on January 8, 1982. He graduated at the high school level in 2000 from Assumption College Thonburi. In 2005, he was received Bachelor Degree with major of Clinical Psychology from Faculty of Social Science, Kasetsart University. In 2007, he acquired Master Degree with major of Medical Biochemistry from Faculty of Medicine, Chulalongkorn University. Field of his Master's thesis is stem cell & bone biochemistry. After graduation, he pursued his graduate study to doctoral degree in the field of Biomedical Engineering at Faculty of Engineering, Chulalongkorn University and continued his dissertation on bone tissue engineering. During Ph.D. study, he was appointed as BME Chula representative for the 6<sup>th</sup> International Student Forum in order to share his research with international Ph.D. students at Graduate University of the Chinese Academy of Science (GUCAS), Beijing, People's Republic of China in September 25 - 29, 2010. Furthermore, he was selected as a participant of Japan Asia Young Scientist and Engineer Study Visit (JAYSES2011) project in order to join seminar and workshop about frontier engineering and technology together with Tokyo Institute of Technology students in August 21-30, 2011, which was organized in Thailand. During study, he work as teacher assistant (T.A.) of Biomedical Engineering program for 1 year at the Faculty of Engineering, Chulalongkorn University.

Some part of his reseach was accepted for oral presentation as follows:

- The Commission on Higher Education Congress III: University Staff Development Consortium” (CHE-UDSC Congress III), Pattaya, Chonburi, Thailand, September 4-6, 2010 (excellent oral presentation award).

- The Joint Conference in Medical Sciences 2011: Chula-Rama-Siriraj (JCMS2011), Impact Arena Muang Thong Thani, Bangkok, Thailand, June 14 – 16, 2011 (good oral presentation award).